H Compound Absorbers

Sound absorbers, except simple porous layers, are compound absorbers, i.e. they consist of elements in special arrangements, such as air volumes, foils (either limp or elastic, tight or porous), membranes, plates (either stiff or elastic, tight or porous) mostly with perforations ("necks") in the shape of e.g. slits or circular holes, porous absorber layers, etc. The aim mostly is to evaluate the input admittance G of such absorbers, or impedance $Z = 1/G$, because it is this quantity with which absorbers enter into acoustical computations.

Many compound absorbers, in turn, are arrays of elementary absorbers, such as arrays of Helmholtz resonators, and they have an inhomogeneous surface, e.g. the neck areas of Helmholtz resonators and the hard plate between the necks. One must distinguish what the input admittance stands for, either the neck area or the whole array. If the lateral dimensions of an array element are small compared to the wavelength λ_0 (typically $< \lambda_0/4$), the performance of an absorber in most applications can be equivalently described by an average admittance (or "homogenised" admittance), which is the average of the local admittances in an array. Otherwise the array must be treated as a periodic structure with the admittance profile along the surface explicitly taken into account.

A further distinction concerns the radiation impedance $Z_r = Z_r' + j \cdot Z_r''$ of the absorber, or more distinctly the radiation resistance Z_r', whether or not it is included in the absorber impedance Z. This distinction comes from the general equivalent network of a source and an absorber.

The network consists of a pressure source, with P_i the sound pressure of the incident wave and the internal source impedance Z_r, and the absorber with input impedance Z_e.

For a plane wave with polar angle Θ of incidence the radiation resistance is

$$Z_r' = Z_0 / \cos \Theta .$$

It does not contain information about the absorber. The radiation reactance, however, contains the oscillating mass of necks and therefore influences the tuning of resonators.

Thus it makes sense to attribute Z_r' to the source and Z_r'' to the absorber.

It should be noted that this attribution is a matter of convention, and therefore one must examine absorber formulas for the convention being used.

It will be indicated, at the end of some sections in this chapter about absorber elements, how the absorber element is introduced into the equivalent chain network of a multilayer absorber. Most technical sound absorbers can be described with such an equivalent network (*Sect. C.5*). Some sections below will mainly give chains of equations which lead to the finally desired input admittance G or input impedance Z by iterated insertion.

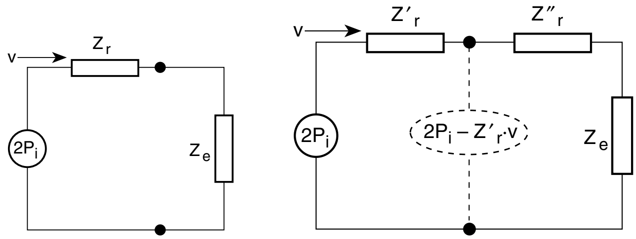

Possible attributions of the radiation impedance $Z_r = Z'_r + jZr''$ to the absorber input impedance Z_e.

H.1 Absorber of Flat Capillaries

► *See also:* Mechel, Vol. II, Ch. 10 (1995)

See *Sect. J.1* for sound in flat capillaries.

A plane sound wave is incident on a layer of thickness d (with hard backing) consisting of thin plates with mutual distance 2h. The arrangement has a surface porosity σ.

The plates first are assumed to be normal to the back wall.

Viscous and thermal losses are considered in the capillaries between the plates.

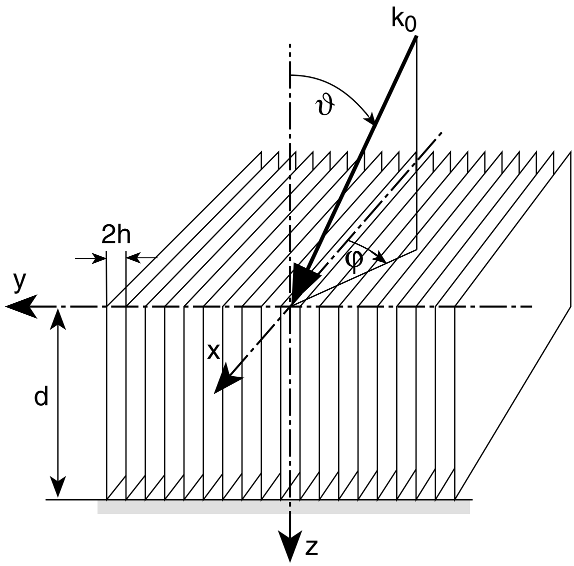

With reflection factor r on the front side and transmission factor t from outside to inside of the capillaries:

Sound wave in front of the absorber:

$$p = p_e + p_r = A \cdot e^{-j(k_x x + k_y y)} (e^{-jk_z z} + r\, e^{+jk_z z})$$
$$k_x = k_0 \sin\vartheta\, \cos\varphi \quad ; \quad k_y = k_0 \sin\vartheta\, \sin\varphi \quad ; \quad k_z = k_0 \cos\vartheta. \tag{1}$$

Sound wave inside the capillaries:

$$p_a = A \cdot t \cdot e^{-\Gamma_{ax} x} \cdot \cosh(\Gamma_{az}(z-d)) \cdot e^{-jk_y y}$$

$$(\Delta - \Gamma_a^2) p_a = 0 \quad ; \quad \Gamma_{ax}^2 + \Gamma_{az}^2 = \Gamma_a^2$$

$$\Gamma_{ax} = jk_x = jk_0 \sin\vartheta\, \cos\varphi \quad ; \quad \frac{\Gamma_{az}}{k_0} = \sqrt{\left(\frac{\Gamma_a}{k_0}\right)^2 - \sin^2\vartheta\, \cos^2\varphi} \tag{2}$$

$$v_{az} = \frac{-1}{\Gamma_a Z_a} \frac{\partial p_a}{\partial z} \quad ; \quad v_{ax} \neq 0 \quad ; \quad v_{ay} = 0,$$

where Γ_a is the propagation constant in a flat capillary, $Z_a = Z_i/\sigma$, and Z_i is the wave impedance in a flat capillary (*Sect. J.1*).

Input impedance:

$$\frac{Z}{Z_0} = \frac{Z_a}{Z_0} \frac{\Gamma_a/k_0}{\Gamma_{az}/k_0} \coth(k_0 d \cdot \Gamma_{az}/k_0)$$

$$\xrightarrow[k_0 d \ll 1]{} \frac{1}{k_0 d} \frac{Z_a/Z_0 \cdot \Gamma_a/k_0}{(\Gamma_a/k_0)^2 - \sin^2\vartheta\, \cos^2\varphi} = \begin{cases} \dfrac{1}{k_0 d} \dfrac{Z_a/Z_0}{\Gamma_a/k_0} & ; \quad \vartheta = 0 \text{ or } \varphi = \pm\pi/2 \\[2ex] \dfrac{1}{k_0 d} \dfrac{Z_a/Z_0 \cdot \Gamma_a/k_0}{(\Gamma_a/k_0)^2 - \sin^2\vartheta} & ; \quad \varphi = 0 \end{cases} \tag{3}$$

$$\xrightarrow[k_0 d \gg 1]{} \frac{Z_a/Z_0 \cdot \Gamma_a/k_0}{\sqrt{(\Gamma_a/k_0)^2 - \sin^2\vartheta\, \cos^2\varphi}} = \begin{cases} Z_a/Z_0 & ; \quad \vartheta = 0 \text{ or } \varphi = \pm\pi/2 \\[2ex] \dfrac{Z_a/Z_0 \cdot \Gamma_a/k_0}{\sqrt{(\Gamma_a/k_0)^2 - \sin^2\vartheta}} & ; \quad \varphi = 0 \end{cases} .$$

Reflection factor r and absorption coefficient α as usual:

$$r = \frac{\cos\vartheta \dfrac{Z}{Z_0} - 1}{\cos\vartheta \dfrac{Z}{Z_0} + 1} \quad ; \quad \alpha(\vartheta, \varphi) = 1 - |r|^2$$

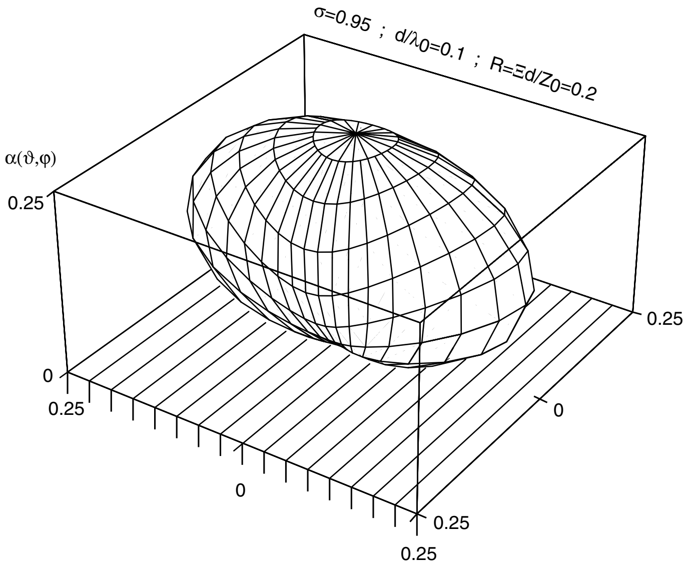

Absorption coefficient $\alpha(\vartheta, \varphi)$ as function of direction of sound incidence.
The lamellae distance 2h is given by the normalised flow resistance R of the arrangement

Next, the lamellae are assumed to be inclined with ϑ_0.

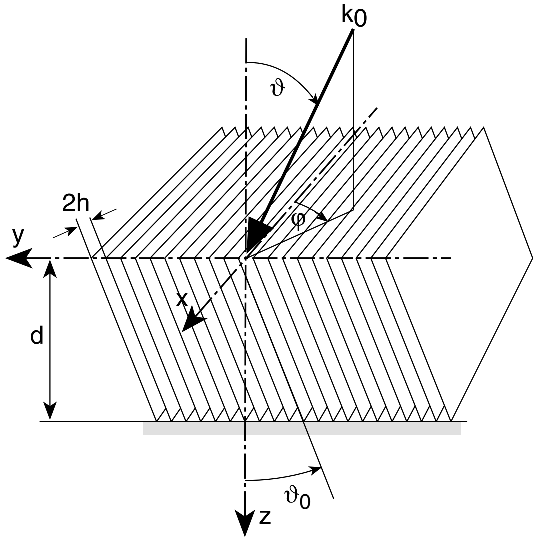

The effective depth changes to

$d_{eff} = d/\cos\vartheta_0$;

the outside wave impedance changes to

$Z_0 = Z_0/\cos\vartheta_0$.

Thus

$$\frac{Z(\vartheta_0 = 0,\ d)}{Z_0} \to \frac{1}{\cos\vartheta_0}\,\frac{Z(\vartheta_0 = 0,\ d_{eff})}{Z_0} \tag{4}$$

and

$$r = \frac{Z/Z_0 - 1}{Z/Z_0 + 1} \to \frac{\dfrac{Z(0,\,d_{eff})}{Z_0}\,\dfrac{\cos\vartheta}{\cos\vartheta_0} - 1}{\dfrac{Z(0,\,d_{eff})}{Z_0}\,\dfrac{\cos\vartheta}{\cos\vartheta_0} + 1}. \tag{5}$$

The inclination of the lamellae (indicated in the next diagram) has no immediate influence on the sound absorption $\alpha(\vartheta, \varphi)$ as a function of angles of incidence.

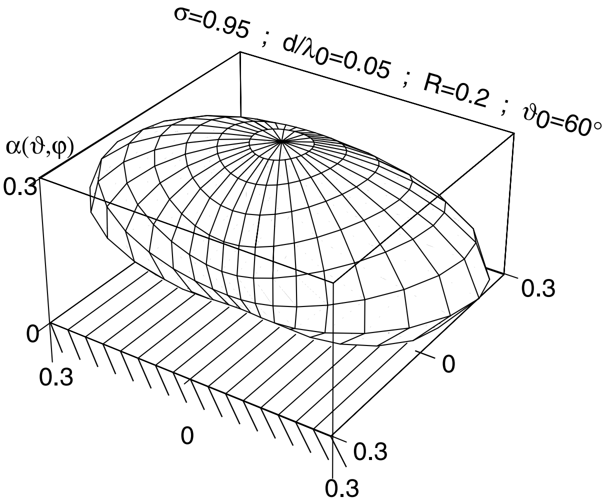

Absorption coefficient $\alpha(\vartheta, \varphi)$ as function of direction of sound incidence, with inclined lamellae. The lamellae distance 2h is given by the normalised flow resistance R of the arrangement

H.2 Plate with Narrow Slits

► *See also:* Mechel, Vol. II, Ch. 18 (1995)

"Narrow" slits means only plane waves are considered in the neck channels (in contrast to "wide" slits in the next section, where higher modes are assumed in the necks), but they are still wide enough so that viscous and thermal losses in the necks may be neglected.

Consider an array of parallel slits with width a and mutual distance L in a (rigid) plate with thickness d.

Excitation is by a plane wave with normal incidence and amplitude A_e.

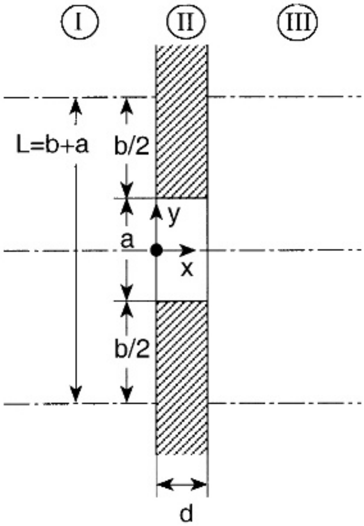

There are three sound zones I, II, III.

Field formulation in zone II:

$$\begin{aligned} p_{II}(x,y) &= Be^{-jk_0x} + Ce^{jk_0x} \\ v_{IIx}(x,y) &= \frac{1}{Z_0}\left[Be^{-jk_0x} - Ce^{jk_0x}\right] \\ v_{IIy}(x,y) &= 0 \end{aligned} \qquad (1)$$

Field in zone I in front of the plate:

$$\begin{aligned} p_I(x,y) &= A_e e^{-jk_0x} + A_0 e^{jk_0x} + 2\sum_{n>0} A_n\, e^{\gamma_n x}\cos(\eta_n y) \\ v_{Ix}(x,y) &= \frac{1}{Z_0}\left[A_e e^{-jk_0x} - A_0 e^{jk_0x} + 2j\sum_{n>0} A_n\,\frac{\gamma_n}{k_0}\, e^{\gamma_n x}\cos(\eta_n y)\right] \\ v_{Iy}(x,y) &= -\frac{2j}{Z_0}\sum_{n>0} A_n\,\frac{\eta_n}{k_0}\, e^{\gamma_n x}\sin(\eta_n y) \end{aligned} \qquad (2)$$

Field in zone III behind the plate:

$$\begin{aligned} p_{III}(x,y) &= D_0 e^{-jk_0x} + 2\sum_{n>0} D_n\, e^{-\gamma_n x}\cos(\eta_n y) \\ v_{IIIx}(x,y) &= \frac{1}{Z_0}\left[D_0 e^{-jk_0x} - 2j\sum_{n>0} D_n\,\frac{\gamma_n}{k_0}\, e^{-\gamma_n x}\cos(\eta_n y)\right] \\ v_{IIIy}(x,y) &= -\frac{2j}{Z_0}\sum_{n>0} D_n\,\frac{\eta_n}{k_0}\, e^{-\gamma_n x}\sin(\eta_n y) \end{aligned} \qquad (3)$$

Wave numbers and propagation constants:

$$\eta_0 = 0 \quad ; \quad \eta_n = \frac{2\pi n}{L} = k_0 \cdot n\frac{\lambda_0}{L} \quad ; \quad n = 1, 2, \ldots$$
$$\gamma_0 = jk_0 \; ; \quad \gamma_n = \sqrt{\eta_n^2 - k_0^2} = k_0\sqrt{\left(n\frac{\lambda_0}{L}\right)^2 - 1} \quad ; \quad n = 1, 2, \ldots \tag{4}$$

From particle velocity boundary conditions:

$$A_0 = A_e - \frac{a}{L} \cdot (B - C)$$
$$A_n = -j\frac{a}{L}\frac{k_0}{\gamma_n}\,si_n \cdot (B - C) \tag{5}$$
$$D_n = j\frac{a}{L}\frac{k_0}{\gamma_n}\,si_n\, e^{\gamma_n d} \cdot (B\, e^{-jk_0 d} - C\, e^{+jk_0 d}) \quad ; \quad n = 0,\ 1,\ 2, \ldots$$

with $si_n = \dfrac{\sin(n\pi a/L)}{n\pi a/L}$; $\quad si_0 = 1.$

From matching average sound pressures in the slit orifices:

$$\frac{B}{A_e} = \frac{(1+S)\, e^{+jk_0 d}}{2S\, \cos(k_0 d) + j(1+S^2)\, \sin(k_0 d)}$$
$$\frac{C}{A_e} = \frac{-(1-S)\, e^{-jk_0 d}}{2S\, \cos(k_0 d) + j(1+S^2)\, \sin(k_0 d)} \tag{6}$$

$$\frac{B-C}{A_e} = 2\frac{\cos(k_0 d) + jS\, \sin(k_0 d)}{2S\, \cos(k_0 d) + j(1+S^2)\, \sin(k_0 d)}$$
$$\frac{B\, e^{-jk_0 d} - C\, e^{+jk_0 d}}{A_e} = \frac{2}{2S\, \cos(k_0 d) + j(1+S^2)\, \sin(k_0 d)} \tag{7}$$

with the abbreviation $\quad S = \dfrac{a}{L}\left[1 + 2j\sum_{i>0}\dfrac{k_0}{\gamma_i}\, s_i^2\right].$ (8)

Front side orifice impedance Z_{sf}:

$$\frac{Z_{sf}}{Z_0} = \frac{< p_{II}(0,y) >}{Z_0 < v_{IIx}(0,y) >} = \frac{B+C}{B-C} = \frac{S + j\, \tan(k_0 d)}{1 + j\, S \cdot \tan(k_0 d)}; \tag{9}$$

the last expression has the typical form of a (normalised) impedance (here S) which is transformed by a transmission line of length d.

Back side orifice impedance Z_{sb}:

$$\frac{Z_{sb}}{Z_0} = \frac{< p_{II}(d,y) >}{Z_0 < v_{IIx}(d,y) >} = \frac{Be^{-jk_0 d} + Ce^{+jk_0 d}}{Be^{-jk_0 d} - Ce^{+jk_0 d}} = S, \tag{10}$$

$$\frac{Z_{sb}}{Z_0} = \frac{a}{L}\left[1 + 2j\sum_{n>0}\frac{1}{\sqrt{\left(n\,\frac{\lambda_0}{L}\right)^2 - 1}}\left(\frac{\sin(n\pi\; a/L)}{n\pi\; a/L}\right)^2\right]. \tag{11}$$

The first term in the brackets represents the radiation resistance.

If one subtracts in the front side orifice the sound pressure of the equivalent source $2P_i = 2A_e$, then:

$$\frac{< p_{II}(0,y) - 2A_e >}{Z_0 < v_{IIx}(0,y) >} = \frac{B + C - 2A_e}{B - C} = -S, \tag{12}$$

i.e. the orifice impedances on both sides are symmetrical.

End correction of the orifice:

$$\frac{\Delta\ell}{a} = \frac{Z''_{sb}}{k_0 a\; Z_0} = \frac{1}{k_0 a}S'' \approx \frac{1}{\pi}\sum_{n=1}^{\infty}\frac{S_n^2}{n} = \frac{a}{L}\cdot\sum_{n=1}^{\infty}\frac{\sin^2(n\pi a/L)}{(n\pi a/L)^3}. \tag{13}$$

If the summation is approximated by an integration

$$\frac{\Delta\ell}{a} \approx \frac{1}{\pi}\;\ln\left[\frac{1}{2}\tan\left(\frac{\pi}{4}\,\frac{a}{L}\right) + \frac{1}{2}\cot\left(\frac{\pi}{4}\,\frac{a}{L}\right)\right] \tag{14}$$

and from a numerical regression

$$\begin{aligned} x &= \lg(a/L) \\ \frac{\Delta\ell}{a} &= -0.395\,450\cdot x + 0.346\,161\cdot x^2 + 0.141\,928\cdot x^3 + 0.0200\,128\cdot x^4. \end{aligned} \tag{15}$$

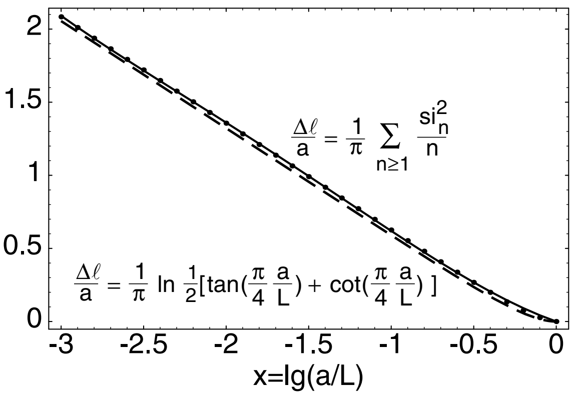

End correction of a slit in an array; points: summation; solid line: regression; dashed line: integration

H.3 Plate with Wide Slits

▸ *See also:* Mechel, Vol. II, Ch. 18 (1995)

See *Sect. H.2* for the arrangement, co-ordinates and field zones.

In contrast to *Sect. H.2*, higher modes are assumed in the neck channels. The field formulations in the three zones are as follows.

Zone I:

$$\begin{aligned} p_I(x,y) &= A_e e^{-jk_0x} + \sum_{n\ge 0} \delta_n A_n\, e^{\gamma_n x} \cos(\eta_n y)\,, \\ Z_0 v_{Ix}(x,y) &= A_e e^{-jk_0x} + j\sum_{n\ge 0} \delta_n A_n \frac{\gamma_n}{k_0}\, e^{\gamma_n x}\cos(\eta_n y)\,, \\ Z_0 v_{Iy}(x,y) &= -2j\sum_{n>0} A_n \frac{\eta_n}{k_0}\, e^{\gamma_n x}\sin(\eta_n y)\,. \end{aligned} \tag{1}$$

Zone II:

$$\begin{aligned} p_{II}(x,y) &= \sum_{n\ge 0} [B_n e^{-j\kappa_n x} + C_n e^{j\kappa_n x}]\ \cos(\varepsilon_n y)\,, \\ Z_0 v_{IIx}(x,y) &= \sum_{n\ge 0} \frac{\kappa_n}{k_0} [B_n e^{-j\kappa_n x} - C_n e^{j\kappa_n x}]\ \cos(\varepsilon_n y)\,, \\ Z_0 v_{IIy}(x,y) &= -j\sum_{n\ge 0} \frac{\varepsilon_n}{k_0} [B_n e^{-j\kappa_n x} + C_n e^{j\kappa_n x}]\ \sin(\varepsilon_n y)\,. \end{aligned} \tag{2}$$

Zone III:

$$\begin{aligned} p_{III}(x,y) &= \sum_{n\ge 0} \delta_n D_n\, e^{-\gamma_n x}\cos(\eta_n y)\,, \\ Z_0 v_{IIIx}(x,y) &= -j\sum_{n\ge 0} \delta_n D_n \frac{\gamma_n}{k_0}\, e^{-\gamma_n x}\cos(\eta_n y)\,, \\ Z_0 v_{IIIy}(x,y) &= -2j\sum_{n>0} D_n \frac{\eta_n}{k_0}\, e^{-\gamma_n x}\sin(\eta_n y) \end{aligned} \tag{3}$$

$$\text{with}\quad \delta_n = \begin{cases} 1\,;\ n=0 \\ 2\,;\ n>0 \end{cases} \quad ; \quad \delta_{mn} = \begin{cases} 1\,;\ m=n \\ 0\,;\ m\ne n \end{cases} \tag{4}$$

and lateral wave numbers

$$\eta_0 = 0 \quad ; \quad \eta_n = \frac{2\pi n}{L} = k_0\cdot n\frac{\lambda_0}{L} \quad ; \quad \varepsilon_0 = 0 \quad ; \quad \varepsilon_n = \frac{2\pi n}{a} = k_0\cdot n\frac{\lambda_0}{a} \tag{5}$$

as well as axial propagation constants

$$\begin{aligned} &\gamma_0 = jk_0\,;\ \ \gamma_n = \sqrt{\eta_n^2 - k_0^2} = k_0\sqrt{\left(n\frac{\lambda_0}{L}\right)^2 - 1} \ \ ;\ \ \mathrm{Re}\{\gamma_n\}\ge 0 \quad \text{or} \quad \mathrm{Im}\{\gamma_n\}\ge 0\,, \\ &\kappa_0 = k_0\,;\ \ \kappa_n = \sqrt{k_0^2 - \varepsilon_n^2} = k_0\sqrt{1-\left(n\frac{\lambda_0}{a}\right)^2} \ \ ;\ \ \mathrm{Im}\{\kappa_n\}\le 0 \quad \text{or} \quad \mathrm{Re}\{\kappa_n\}\ge 0\,. \end{aligned} \tag{6}$$

Mode coupling coefficients in the orifice planes are as follows:

$$\begin{aligned} s_{m,n} &= \frac{1}{a}\int_{-a/2}^{+a/2} \cos(\eta_m y)\ \cos(\varepsilon_n y)\ dy \quad ; \quad m = 0,\ 1,\ 2, \ldots \\ &= \frac{1}{2}\left[\frac{\sin((\eta_m - \varepsilon_n)\ a/2)}{(\eta_m - \varepsilon_n)\ a/2} + \frac{\sin((\eta_m + \varepsilon_n)\ a/2)}{(\eta_m + \varepsilon_n)\ a/2}\right] \\ &= (-1)^n \frac{m\pi\ a/L}{(m\pi\ a/L)^2 - (n\pi)^2}\ \sin(m\pi\ a/L) \\ &= \frac{(-1)^n}{\pi}\ \frac{m\frac{a}{L}\cdot\sin\left(m\pi\frac{a}{L}\right)}{\left(m\frac{a}{L}\right)^2 - n^2} \quad ; \quad m\frac{a}{L} \neq n \neq 0, \end{aligned} \tag{7}$$

and the special cases are:

$$s_{m,n} = \frac{1}{2}\ \text{for}\ m\frac{a}{L} = n \neq 0 \quad ; \quad s_{0,0} = 1 \quad ; \quad s_{m,0} = \frac{\sin(m\pi\ a/L)}{m\pi\ a/L} \quad ; \quad s_{0,n>0} = 0. \tag{8}$$

Boundary conditions for the particle velocities at the zone limits give ($m = 0, 1, 2, \ldots$):

$$\begin{aligned} A_m &= -j\frac{k_0}{\gamma_m}\left[-\delta_{0,m}A_e + \frac{a}{L}\sum_{n\geq 0}\frac{\kappa_n}{k_0}\ s_{m,n}\cdot(B_n - C_n)\right], \\ D_m\ e^{-\gamma_m d} &= j\frac{a}{L}\frac{k_0}{\gamma_m}\sum_{n\geq 0}\frac{\kappa_n}{k_0}\ s_{m,n}\cdot(B_n e^{-j\kappa_n d} - C_n e^{+j\kappa_n d})\ . \end{aligned} \tag{9}$$

The boundary conditions for the sound pressure yield ($m = 0, 1, 2, \ldots$):

$$\begin{aligned} \frac{1}{\delta_m}\ (B_m + C_m) &= \delta_{0,m}A_e + \sum_{n\geq 0}\delta_n\ s_{n,m}\cdot A_n\ , \\ \frac{1}{\delta_m}\ (B_m e^{-j\kappa_m d} + C_m e^{+j\kappa_m d}) &= \sum_{n\geq 0}\delta_n\ e^{-\gamma_n d}\ s_{n,m}\cdot D_n. \end{aligned} \tag{10}$$

Instead of solving these systems for A_m, B_m, C_m, D_m the auxiliary quantities X_n, Y_n are introduced:

$$X_{n\pm} := B_n \pm C_n \quad ; \quad Y_{n\pm} := B_n e^{-j\kappa_n d} \pm C_n e^{+j\kappa_n d} \tag{11}$$

with intrinsic relations:

$$\begin{aligned} X_{n+} &= X_{n-}\cdot\frac{1 + e^{-2j\kappa_n d}}{1 - e^{-2j\kappa_n d}} - 2Y_{n-}\cdot\frac{e^{-j\kappa_n d}}{1 - e^{-2j\kappa_n d}}\ , \\ Y_{n+} &= 2X_{n-}\cdot\frac{e^{-j\kappa_n d}}{1 - e^{-2j\kappa_n d}} - Y_{n-}\cdot\frac{1 + e^{-2j\kappa_n d}}{1 - e^{-2j\kappa_n d}}. \end{aligned} \tag{12}$$

The B_n, C_n follow from:

$$\begin{aligned} B_n &= \frac{1}{2}(X_{n+} + X_{n-}) = \frac{1}{2}(Y_{n+} + Y_{n-})e^{+j\kappa_n d}\ , \\ C_n &= \frac{1}{2}(X_{n+} - X_{n-}) = \frac{1}{2}(Y_{n+} - Y_{n-})e^{-j\kappa_n d}. \end{aligned} \tag{13}$$

A coupled system of equations for X_{n-}, Y_{n-} is obtained with the form

$$\begin{aligned}
&\sum_{n\geq 0} a_{mn}\cdot X_{n-} + c_m\cdot Y_{m-} = b_m\cdot A_e \qquad ; \quad m=0,\ 1,\ 2,\ldots\ ,\\
&c_m\cdot X_{m-} + \sum_{n\geq 0} a_{mn}\cdot Y_{n-} = 0 \qquad ; \quad m=0,\ 1,\ 2,\ldots
\end{aligned} \tag{14}$$

and the coefficients

$$\begin{aligned}
a_{m,n} &= j\,\frac{a}{L}\,\frac{\kappa_n}{k_0}\,S_{m,n} + \frac{\delta_{m,n}}{\delta_m}\,\frac{1+e^{-2j\kappa_m d}}{1-e^{-2j\kappa_m d}}\ ,\\
c_m &= -\frac{2}{\delta_m}\,\frac{e^{-j\kappa_m d}}{1-e^{-2j\kappa_m d}} \qquad ; \quad b_m = \delta_{0,m} + s_{0,m} = 2\delta_{0,m}
\end{aligned} \tag{15}$$

with the abbreviations

$$\begin{aligned}
S_{m,n} &= \sum_{i\geq 0} \delta_i \frac{k_0}{\gamma_i}\, s_{i,m}\cdot s_{i,n} = -j\ \delta_{0m}\delta_{0n} + 2\cdot\sum_{i>0}\frac{k_0}{\gamma_i}\, s_{i,m}\cdot s_{i,n}\ ;\\
&\quad m,n = 0,\ 1,\ 2,\ldots
\end{aligned} \tag{16}$$

The normalised backside orifice impedance is:

$$\begin{aligned}
\frac{Z_{sb}}{Z_0} &= \frac{<p_{II}(d,y)>}{Z_0\ <v_{IIx}(d,y)>} = \frac{Y_{0+}}{Y_{0-}}\\
&= j\,\frac{a}{L}\left[\sum_{i\geq 0}\delta_i\,\frac{k_0}{\gamma_i}\,s_{i0}^2 + \sum_{n>0}\frac{\kappa_n}{k_0}\,\frac{Y_{n-}}{Y_{0-}}\cdot\sum_{i\geq 0}\delta_i\frac{k_0}{\gamma_i}\,s_{i0}\,s_{in}\right].
\end{aligned} \tag{17}$$

The first term in the brackets is just the orifice impedance of a neck with only plane waves in it; thus the second term is a correction term for the influence of higher modes in the neck.

The normalised front side orifice impedance is:

$$\begin{aligned}
\frac{Z_{sf}}{Z_0} &= \frac{<p_{II}(0,y)>}{Z_0\ <v_{IIx}(0,y)>} = \frac{X_{0+}}{X_{0-}}\\
&= \frac{2A_e}{B_0 - C_0} - j\,\frac{a}{L}\left[\sum_{i\geq 0}\delta_i\,\frac{k_0}{\gamma_i}\,s_{i0}^2 + \sum_{n>0}\frac{\kappa_n}{k_0}\,\frac{X_{n-}}{X_{0-}}\cdot\sum_{i\geq 0}\delta_i\frac{k_0}{\gamma_i}\,s_{i0}\,s_{in}\right].
\end{aligned} \tag{18}$$

After subtraction of the sound pressure of the equivalent source (the first term in the last expression) the orifice impedances on both sides remain symmetrical.

The slit impedances above were defined with the average sound pressure and axial particle velocity. The slit radiation impedances, which are defined with the radiated power (Sect. F.1) are:

$$
\begin{aligned}
\frac{Z_{rb}}{Z_0} &= \frac{\int_a p_{II}(d,y)\cdot Z_0 v_{IIx}^*(d,y)\,dy}{Z_0^2 \int_a v_{IIx}(d,y)\cdot v_{IIx}^*(d,y)\,dy} = \frac{\sum\limits_{n\geq 0} \frac{1}{\delta_n}\frac{\kappa_n^*}{k_0}\, Y_{n+}Y_{n-}^*}{\sum\limits_{n\geq 0} \frac{1}{\delta_n}\left|\frac{\kappa_n}{k_0}\right|^2 |Y_{n-}|^2}, \\
\frac{Z_{rf}}{Z_0} &= \frac{\int_a p_{II}(0,y)\cdot Z_0 v_{IIx}^*(0,y)\,dy}{Z_0^2 \int_a v_{IIx}(0,y)\cdot v_{IIx}^*(0,y)\,dy} = \frac{\sum\limits_{n\geq 0} \frac{1}{\delta_n}\frac{\kappa_n^*}{k_0}\, X_{n+}X_{n-}^*}{\sum\limits_{n\geq 0} \frac{1}{\delta_n}\left|\frac{\kappa_n}{k_0}\right|^2 |X_{n-}|^2}.
\end{aligned}
\tag{19}
$$

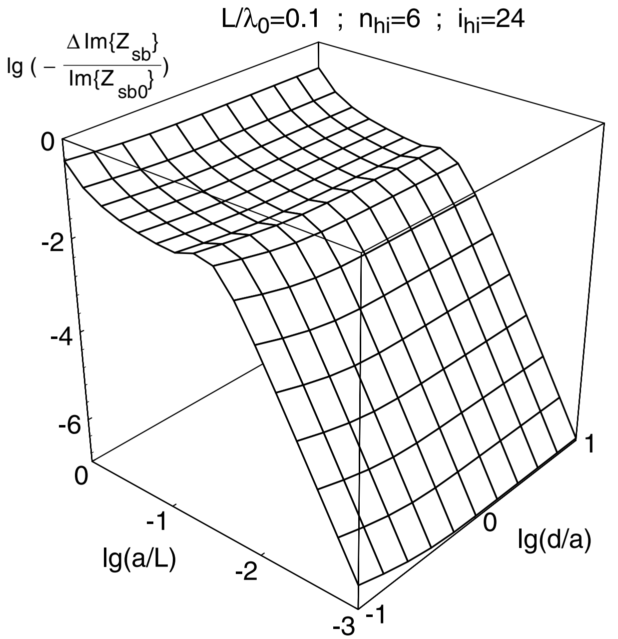

Relative change of the imaginary part of the neck orifice impedance Z_{sb} due to higher modes in the neck, as compared to the impedance Z_{sb0} with only plane waves in the neck

The relative change of the orifice reactance Z''_{sb} (and therefore also for the end correction) due to higher modes as compared with the orifice reactance Z''_{sb0} with only plane waves in the neck (*Sect. H.2*) is:

$$Z''_{sb} = Z''_{sb0} \cdot \left(1 + \frac{\Delta Z''_{sb}}{Z''_{sb0}}\right) = Z''_{sb0} \cdot (1 - 10^{F(x,y)}) \; ,$$

$$F(x, y) = \lg(-\frac{\Delta Z''_{sb}}{Z''_{sb0}}) = f(x) \cdot (1 + g(y)) \; ; \qquad (20)$$

$$x = \lg(a/L) \quad ; \quad y = \lg(d/a)$$

with functions f(x) and g(y) in the ranges $-3 \leq x < 0$ and $1 \leq y \leq 1$:

$$f(x) = -1.739\,68 + 1.484\,35\,(x + 1.5) - 1.842\,30\,(x + 1.5)^2$$
$$+0.292\,538\,(x + 1.5)^3 + 0.428\,402\,(x + 1.5)^4 \; ,$$

$$g(y) = H(-y) \cdot \left[0.00\,259\,355\,y - 0.0758\,181\,y^2 \right. \qquad (21)$$
$$\left. +0.330\,845\,y^3 + 0.226\,933\,y^4\right] \quad ; \quad H(-y) = \begin{cases} 1\,; & y \leq 0 \\ 0\,; & y > 0 \end{cases} \; .$$

The influence of higher modes is small if $a/L < 0.25$, and only if $d/a \ll 1$ does the plate thickness becomes sensible.

H.4 Dissipationless Slit Resonator

▸ *See also:* Mechel, Vol. II, Ch. 18 (1995)

Parallel slits in a neck plate and air volumes V behind them form an array of slit resonators.

Excitation is by a plane wave with normal incidence and amplitude A_e.

First, higher modes will be assumed in the necks, then the special case of only plane waves in the neck will be treated.

The field formulations *with higher modes* remain as in *Sect. H.3*, except in the volumes in zone III:

$$p_{III}(x, y) = \sum_{n\geq 0} \delta_n D_n \; \cosh(\gamma_n(x - d - t)) \; \cos(\eta_n y) \; ,$$

$$Z_0 v_{IIIx}(x, y) = j \sum_{n\geq 0} \delta_n D_n \, \frac{\gamma_n}{k_0} \; \sinh(\gamma_n(x - d - t)) \; \cos(\eta_n y) \; , \qquad (1)$$

$$Z_0 v_{IIIy}(x, y) = -2j \sum_{n>0} D_n \, \frac{\eta_n}{k_0} \; \cosh(\gamma_n(x - d - t)) \; \sin(\eta_n y)$$

(with wave numbers and propagation constants from *Sect. H.3*).

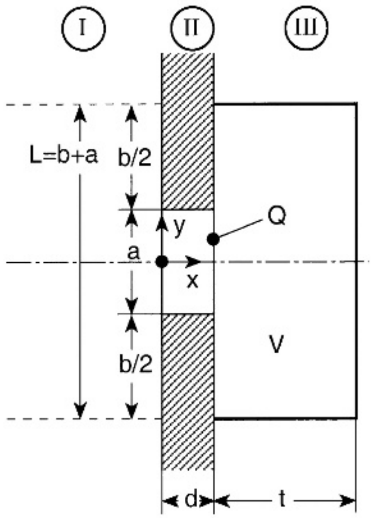

The boundary conditions give for the auxiliary quantities $X_{n\pm}, Y_{n\pm}$:

$$X_{n\pm} := B_n \pm C_n \quad ; \quad Y_{n\pm} := B_n e^{-j\kappa_n d} \pm C_n e^{+j\kappa_n d} ,$$

$$B_n = \frac{1}{2}(X_{n+} + X_{n-}) = \frac{1}{2}(Y_{n+} + Y_{n-})e^{+j\kappa_n d} ,$$

$$C_n = \frac{1}{2}(X_{n+} - X_{n-}) = \frac{1}{2}(Y_{n+} - Y_{n-})e^{-j\kappa_n d} , \tag{2}$$

$$X_{n+} = X_{n-} \cdot \frac{1 + e^{-2j\kappa_n d}}{1 - e^{-2j\kappa_n d}} - 2Y_{n-} \cdot \frac{e^{-j\kappa_n d}}{1 - e^{-2j\kappa_n d}} ,$$

$$Y_{n+} = 2X_{n-} \cdot \frac{e^{-j\kappa_n d}}{1 - e^{-2j\kappa_n d}} - Y_{n-} \cdot \frac{1 + e^{-2j\kappa_n d}}{1 - e^{-2j\kappa_n d}} .$$

a coupled system of linear equations:

$$\sum_{n\geq 0} a_{mn} \cdot X_{n-} + c_m \cdot Y_{m-} = b_m \cdot A_e \quad ; \quad m = 0,\ 1, \dots ,$$
$$c_m \cdot X_{m-} + \sum_{n\geq 0} d_{mn} \cdot Y_{n-} = 0 \quad ; \quad m = 0,\ 1, \dots \tag{3}$$

with coefficients

$$a_{m,n} = j\,\frac{a}{L}\,\frac{\kappa_n}{k_0}\,S_{m,n} + \frac{\delta_{m,n}}{\delta_m}\,\frac{1 + e^{-2j\kappa_m d}}{1 - e^{-2j\kappa_m d}} ,$$

$$d_{m,n} = j\,\frac{a}{L}\,\frac{\kappa_n}{k_0}\,T_{m,n} + \frac{\delta_{m,n}}{\delta_m}\,\frac{1 + e^{-2j\kappa_m d}}{1 - e^{-2j\kappa_m d}} , \tag{4}$$

$$c_m = -\frac{2}{\delta_m}\,\frac{e^{-j\kappa_m d}}{1 - e^{-2j\kappa_m d}} \quad ; \quad b_m = \delta_{0,m} + s_{0,m} = 2\delta_{0,m} ,$$

wherein the $S_{m,n}$ are defined as in Sect. H.3, as well as the $s_{m,n}$, and

$$T_{m,n} = \sum_{i\geq 0} \delta_i \frac{k_0}{\gamma_i} \frac{si_{i,m} \cdot si_{i,n}}{\tanh(\gamma_n t)} \quad ; \quad m, n = 0,\ 1,\ 2, \ldots . \tag{5}$$

The amplitudes A_m, D_m are given by:

$$\begin{aligned} A_m &= -j \frac{k_0}{\gamma_m} \left[-\delta_{0,m} A_e + \frac{a}{L} \sum_{n\geq 0} \frac{\kappa_n}{k_0}\, s_{m,n} \cdot X_{n-} \right] \\ D_m &= j \frac{a}{L} \frac{k_0}{\gamma_m \cdot \sinh(\gamma_m t)} \sum_{n\geq 0} \frac{\kappa_n}{k_0}\, s_{m,n} \cdot Y_{n-}. \end{aligned} \tag{6}$$

The back side orifice impedance Z_{sb} is:

$$\begin{aligned} \frac{Z_{sb}}{Z_0} &= j \frac{a}{L} \left[T_{0,0} + \sum_{n>0} \frac{\kappa_n}{k_0} \frac{Y_{n-}}{Y_{0-}}\, T_{0,n} \right] = -j \frac{a/L}{\tan(k_0 t)} \\ &+ j \frac{a}{L} \left[2 \sum_{i>0} \frac{k_0}{\gamma_i} \frac{s_{i,0}^2}{\tanh(\gamma_i t)} + \sum_{n>0} \frac{\kappa_n}{k_0} \frac{Y_{n-}}{Y_{0-}} \sum_{i\geq 0} \delta_i \frac{k_0}{\gamma_i} \frac{s_{i,0} s_{i,n}}{\tanh(\gamma_i t)} \right]. \end{aligned} \tag{7}$$

The last term in the first line is the spring reactance of the resonator volume when it is driven by a piston of width a. Therefore the first term in the second line is the mass reactance of the back side orifice.

With *only plane waves* in the neck (i.e. narrow necks and/or low frequencies) substitute

$$B_0 = B; \quad C_0 = C; \quad B_{n>0} = C_{n>0} = 0 \tag{8}$$

to get for the back side orifice impedance Z_{sb}:

$$\frac{Z_{sb}}{Z_0} = j \frac{a}{L} T_{0,0} = -j \frac{a/L}{\tan(k_0 t)} + j\, 2 \frac{a}{L} \sum_{i>0} \frac{k_0}{\gamma_i} \frac{s_{i,0}^2}{\tanh(\gamma_i t)}. \tag{9}$$

The front side orifice impedance Z_{sf} has the form of the impedance of a free plate (see Sect. H.2; see there for S):

$$\frac{Z_{sf}}{Z_0} = \frac{< p_{II}(0,y) >}{Z_0 < v_{IIx}(0,y) >} = \frac{B+C}{B-C} = \frac{2\, A_e}{B-C} - S = \frac{Z_{sb}/Z_0 + j\, \tan(k_0 d)}{1 + j\, (Z_{sb}/Z_0)\, \tan(k_0 d)}. \tag{10}$$

The back side end correction $\Delta\ell_b/a$ can be defined from the back side neck reactance Z''_{sb} by:

$$\frac{\Delta\ell_b}{a} = \frac{1}{k_0 a} \left(\frac{Z''_{sb}}{Z_0} + j \frac{a/L}{\tan(k_0 t)} \right). \tag{11}$$

The influence of the shape parameter t/L is of interest.

The back side end correction sensibly differs from the end correction of a free plate (i.e. from the front side end correction) only for rather small values of t/L; then it is larger than the front side end correction.

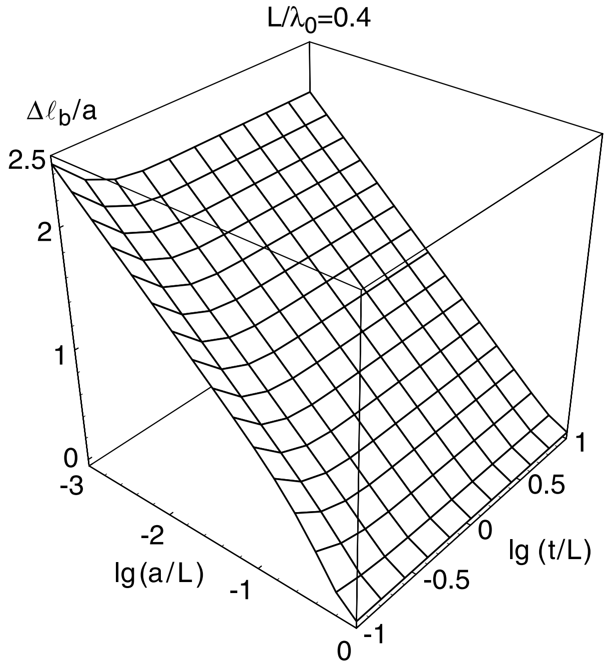

Influence of the shape parameter t/L on the end correction $\Delta\ell_b/a$ of the back side neck orifice (towards the resonator volume)

For slit resonators *with higher modes* in the neck the back orifice end correction is (in the range $-1 \le y, z \le 0$):

$$\frac{\Delta\ell_b}{a} \approx \frac{\Delta\ell}{a}(x) \cdot [1 + f(y\,;\,z_0, x_0)] \cdot [1 + g(z\,;\,y_0, x_0)]\,;$$

$$x = \lg\frac{a}{L} \quad ; \quad y = \lg\frac{d}{a} \quad ; \quad z = \lg\frac{t}{L},$$

$$f(y\,;\,z_0, x_0) \approx g(z\,;\,y_0, x_0) \approx 0 \qquad \text{for} \quad y \ge y_0 \quad ; \quad z \ge z_0\,;$$

$$x_0 = -1 \quad ; \quad y_0 = z_0 = 0,3 \approx \lg(2), \tag{12}$$

$$f(y\,;\,z_0, x_0) = 0.001\,448\,29 \cdot y + 0.002\,555\,10 \cdot y^2 + 0.034\,305\,10 \cdot y^3 + 0.015\,682\,99 \cdot y^4,$$

$$g(z\,;\,y_0, x_0) = -0.000\,932\,290 \cdot z - 0.007\,672\,04 \cdot z^2 - 0.019\,259\,72 \cdot z^3 - 0.018\,048\,39 \cdot z^4,$$

where $\Delta\ell/a$ is the end correction for a free slit in an array.

H.5 Resonance Frequencies and Radiation Loss of Slit Resonators

▸ *See also:* Mechel, Vol. II, Ch. 18 (1995)

The slit resonator is a special form of a Helmholtz resonator. Let V be the volume of the resonator, Q the cross-section area of the neck, then the resilience F, the oscillating mass M and the angular resonance frequency ω_0 of the resonator usually are given as (ρ_0 = density of air; c_0 = sound velocity):

$$\begin{aligned} F &= \frac{V}{Q^2 \rho_0 c_0^2} \quad ; \quad M = \rho_0 Q\,(d + \Delta\ell + \Delta\ell_b)\,, \\ \omega_0 &= \frac{1}{\sqrt{F \cdot M}} = c_0 \sqrt{\frac{Q}{V \cdot (d + \Delta\ell + \Delta\ell_b)}} \approx c_0 \sqrt{\frac{Q}{V \cdot (d + 2\Delta\ell)}} . \end{aligned} \tag{1}$$

This formula is known to return seriously false results for some parameter combinations.

If the resonance condition is defined by zero reactance of the front side orifice impedance Z_{sf}, then it is (for slit resonators with only plane waves in the neck):

$$\begin{aligned} &\mathrm{Im}\left\{\frac{Z_{sv}}{Z_0} + S\right\} = \mathrm{Im}\left\{\frac{S + T + j\,(1 + ST)\ \tan(k_0 d)}{1 + jT\tan(k_0 d)}\right\} \overset{!}{=} 0\,, \\ &S = \frac{a}{L}\left[1 + 2j\sum_{n>0}\frac{k_0}{\gamma_n}\, s_n^2\right] \quad ; \quad s_n = \frac{\sin(n\pi a/L)}{n\pi a/L} \ ; \quad s_0 = 1\,, \\ &T = j\frac{a}{L}\sum_{n\geq 0}\frac{k_0}{\gamma_n}\,\frac{s_n^2}{\tanh(\gamma_n t)} = j\frac{a}{L}\left[-\frac{a/L}{\tan(k_0 t)} + 2\sum_{n>0}\frac{k_0}{\gamma_n}\,\frac{s_n^2}{\tanh(\gamma_n t)}\right]. \end{aligned} \tag{2}$$

Because of the periodicity of $\tan(k_0 d)$ one must further demand that the zero value be crossed with positive slopes (in order to avoid anti-resonances), i.e. transition from spring to mass-type reactance with increasing frequency. The resonance condition then is:

$$k_0 a\left(\frac{\Delta\ell}{a} + \frac{\Delta\ell_b}{a}\right) - \frac{a/L}{\tan(k_0 t)} + \left[1 - (k_0 a)^2 \cdot \frac{\Delta\ell}{a}\,\frac{\Delta\ell_b}{a} + \frac{a}{L}\,\frac{\Delta\ell}{a}\,\frac{k_0 a}{\tan(k_0 t)}\right] \cdot \tan(k_0 d) = 0. \tag{3}$$

For low frequencies with $\tan(k_0 d) \approx k_0 d$, $\tan(k_0 t) \approx k_0 t$:

$$\left(2\pi\frac{a}{\lambda_0}\right)^2 \left[\frac{t}{a}\left(\frac{d}{a} + 2\frac{\Delta\ell}{a}\right) + \frac{a}{L}\,\frac{d}{a}\,\frac{\Delta\ell}{a}\right] - \left(2\pi\frac{a}{\lambda_0}\right)^4 \frac{d}{a}\left(\frac{\Delta\ell}{a}\right)^2 - \frac{a}{L} = 0, \tag{4}$$

and neglecting further the term with $(a/\lambda_0)^4$, the lowest resonance is approximately:

$$\frac{L}{\lambda_0} \approx \frac{1}{2\pi\sqrt{\frac{t}{L}\left(\frac{d}{a} + 2\frac{\Delta\ell}{a}\right) + \left(\frac{a}{L}\right)^2 \frac{d}{a}\,\frac{\Delta\ell}{a}}}. \tag{5}$$

A better approximation is obtained with a continued fraction expansion of tan z:

$$\frac{L}{\lambda_0} \approx \frac{1}{2\pi\sqrt{\frac{t}{L}\left(\frac{d}{a}+2\frac{\Delta\ell}{a}+\frac{1}{3}\frac{t}{L}\right)}}, \tag{6}$$

or with volume V, volume cross-section area Q_V, neck cross-section area Q:

$$\omega_0 \approx c_0\sqrt{\frac{Q}{V\cdot(d+\Delta\ell+\Delta\ell_b+\frac{1}{3}QV/Q_V^2)}}. \tag{7}$$

This form of the resonance formula may be compared with the traditional formula (1). A resonance formula for the lowest resonance with a higher precision is:

$$\frac{L}{\lambda_0} \approx \frac{L/t}{2\pi}\sqrt{\frac{v-\sqrt{v^2-4uw}}{2u}}$$
$$u=\frac{(a/L)^2}{t/L}\,\frac{\Delta\ell}{a}\left(1+\frac{\Delta\ell/a}{t/L}\right) \;;\; v=1+\frac{1}{3}\,\frac{t/L}{d/a}+\frac{\Delta\ell}{a}\left(\frac{2}{d/a}+3\frac{(a/L)^2}{t/L}\right) \;;\; w=\frac{t/L}{d/a}. \tag{8}$$

A slit resonator in an array has a *radiation loss* corresponding to its back radiation (reflection). Its radiation loss factor η is given by:

$$\eta = \frac{R}{\omega_0 M} = R\cdot\omega_0 F = \frac{R}{\sqrt{\frac{M}{F}}}, \tag{9}$$

or with approximations for the circuit elements at resonance:

$$R=\rho_0 c_0\,\frac{a^2}{L} \;;\; F=\frac{Lt}{a^2\rho_0 c_0^2} \;;\; M=\rho_0 a^2\left(\frac{d}{a}+2\frac{\Delta l}{a}+\frac{1}{3}\frac{t}{L}\right),$$
$$\eta=\frac{R}{\sqrt{M/F}}=\sqrt{\frac{t/L}{d/a+2\Delta l/a+\frac{1}{3}\,t/L}}. \tag{10}$$

H.6 Slit Array with Viscous and Thermal Losses

► *See also:* Mechel Vol. II, Ch. 19 (1995)

The object is an array of slits in a free plate with thickness d; the width of the slits is a, and their mutual distance L.

The sketch shows the combination with a resonator volume V; it further shows zones of the sound field, field quantities for which boundary conditions exist, and mode amplitudes as well as mode wave numbers of the field formulations.

A plane sound wave with amplitude A_e is incident normally on the plate.

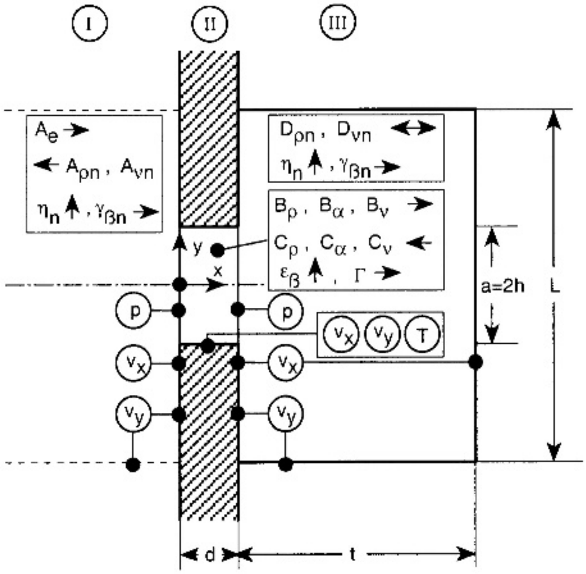

A simplification is applied: the thermal wave component is neglected in the reflected field in zone I and in the transmitted field in zone III (however, viscous waves are considered in these zones). The full triple of density wave ($\beta = \rho$), viscous wave ($\beta = \nu$), and thermal wave ($\beta = \alpha$) is applied in the necks. These waves satisfy the wave equations (see sections about sound in capillaries in Ch. J, "Duct Acoustics"):

$$(\Delta + k_\beta^2)\,\Phi_\beta = 0 \quad , \quad \beta = \rho, \alpha \quad ; \quad (\Delta + k_\nu^2)\,\vec{\Psi} = 0 \; ,$$
$$k_\nu^2 = -j\,\frac{\omega}{\nu} \quad ; \quad k_\alpha^2 \approx k_{\alpha 0}^2 = -j\,\kappa\frac{\omega}{\alpha} = \kappa\;\mathrm{Pr}\cdot k_\nu^2 \quad ; \quad k_\rho^2 \approx k_0^2 = \frac{\omega}{c_0}. \tag{1}$$

The particle velocity $\vec{v}$, the sound pressure p and the oscillating (absolute) temperature are:

$$\vec{v} = -\mathrm{grad}(\Phi_\rho + \Phi_\alpha) + \mathrm{rot}\vec{\Psi} \; ,$$
$$\frac{p}{P_0} = \Pi_\rho \cdot \Phi_\rho + \Pi_\alpha \cdot \Phi_\alpha \; , \tag{2}$$
$$\frac{T}{T_0} = \Theta_\rho \cdot \Phi_\rho + \Theta_\alpha \cdot \Phi_\alpha$$

with scalar potential functions Φ_β ; $\beta = \rho, \alpha$; and a vector potential $\vec{\Psi}$. See the sections about capillaries for the coefficients Π_β, Θ_β.

ρ_0	=	density;
c_0	=	adiabatic sound velocity;
κ	=	adiabatic exponent;
ν	=	kinematic viscosity;
η	=	dynamic viscosity;
α	=	temperature conductivity;
Pr	=	Prandtl number;
P_0, T_0	=	athmospheric pressure and temperature

Particle velocity components for boundary conditions are:

$$v_x = -\frac{\partial(\Phi_\rho + \Phi_\alpha)}{\partial x} + \frac{\partial \Psi_z}{\partial y} \quad ; \quad v_y = -\frac{\partial(\Phi_\rho + \Phi_\alpha)}{\partial y} - \frac{\partial \Psi_z}{\partial x}. \tag{3}$$

Numerical coefficients:

$$\delta_n = \begin{cases} 1 \ ; \ n = 0 \\ 2 \ ; \ n > 0 \end{cases} \quad ; \quad \delta_{m,n} = \begin{cases} 1 \ ; \ m = n \\ 0 \ ; \ m \neq n \end{cases} . \tag{4}$$

Incident plane wave (formulated as a potential function): $\Phi_e = A_e \cdot e^{-jk_\rho x}$. (5)

Field potential formulations:

$$\text{in } Zone\ I: \quad \begin{aligned} \Phi_I(x,y) &= A_e \cdot e^{-jk_\rho x} + \sum_{n\geq 0} \delta_n\, A_{\rho n} \cdot e^{+\gamma_{\rho n} x} \cdot \cos(\eta_n y) \ , \\ \Psi_I(x,y) &= \sum_{n\geq 0} \delta_n\, A_{\nu n} \cdot e^{+\gamma_{\nu n} x} \cdot \sin(\eta_n y) \quad ; \quad A_{\nu 0} = 0 \ . \end{aligned} \tag{6}$$

$$\text{in } Zone\ II: \quad \begin{aligned} \Phi_{II}(x,y) &= \sum_{\beta=\rho,\alpha} [B_\beta \cdot e^{-\Gamma x} + C_\beta \cdot e^{+\Gamma x}] \cdot \cos(\varepsilon_\beta y) \ , \\ \Psi_{II}(x,y) &= [B_\nu \cdot e^{-\Gamma x} + C_\nu \cdot e^{+\Gamma x}] \cdot \sin(\varepsilon_\nu y) \ . \end{aligned} \tag{7}$$

$$\text{in } Zone\ III: \quad \begin{aligned} \Phi_{III}(x,y) &= \sum_{n\geq 0} \delta_n\, D_{\rho n} \cdot e^{-\gamma_{\rho n} x} \cdot \cos(\eta_n y) \ , \\ \Psi_{III}(x,y) &= \sum_{n\geq 0} \delta_n\, D_{\nu n} \cdot e^{-\gamma_{\nu n} x} \cdot \sin(\eta_n y) \quad ; \quad D_{\nu 0} = 0 \ . \end{aligned} \tag{8}$$

with wave numbers and propagation constants:

$$\begin{aligned} &\eta_n = n\,\frac{2\pi}{L} \ ; \ n = 0,\ 1,\ 2\ldots \ ; \ \gamma_{\beta n}^2 = \eta_n^2 - k_\beta^2 \ ; \ \beta = \rho,\ \alpha \ ; \ \gamma_{\beta 0} = jk_\beta \ , \\ &\varepsilon_\beta^2 = \Gamma^2 + k_\beta^2 \ ; \ \beta = \rho,\ \alpha,\ \nu \end{aligned} \tag{9}$$

and Γ the known solution (see sections about capillaries) of the characteristic equation

$$(\Gamma h)^2 \left(\frac{\Theta_\rho}{\Theta_\alpha} - 1\right) \frac{\tan(\varepsilon_\nu h)}{\varepsilon_\nu h} + \varepsilon_\rho h \cdot \tan(\varepsilon_\rho h) - \frac{\Theta_\rho}{\Theta_\alpha}\, \varepsilon_\alpha h \cdot \tan(\varepsilon_\alpha h) = 0. \tag{10}$$

Relations between amplitudes:

$$B_\alpha = -\frac{\Theta_\rho}{\Theta_\alpha}\, \frac{\cos(\varepsilon_\rho h)}{\cos(\varepsilon_\alpha h)}\, B_\rho \quad ; \quad B_\nu = -\frac{\Gamma}{\varepsilon_\nu}\, \frac{\cos(\varepsilon_\rho h)}{\cos(\varepsilon_\nu h)} \left(1 - \frac{\Theta_\rho}{\Theta_\alpha}\right) B_\rho; \tag{11}$$

$$C_\alpha = -\frac{\Theta_\rho}{\Theta_\alpha}\,\frac{\cos(\varepsilon_\rho h)}{\cos(\varepsilon_\alpha h)}\,C_\rho \quad ; \quad C_\nu = +\frac{\Gamma}{\varepsilon_\nu}\,\frac{\cos(\varepsilon_\rho h)}{\cos(\varepsilon_\nu h)}\left(1-\frac{\Theta_\rho}{\Theta_\alpha}\right)C_\rho . \tag{12}$$

So only B_ρ, C_ρ must be determined in the set of B_β, C_β.

Mode-coupling coefficients:

$$s_n = \frac{1}{a}\int_{-h}^{+h}\cos(\eta_n y)\,dy = \frac{\sin(\eta_n h)}{\eta_n h} = \frac{\sin(n\pi\,a/L)}{n\pi\,a/L} \quad ; \quad s_0 = 1$$

$$\begin{aligned} S_{\beta n} &= \frac{1}{a}\int_{-a/2}^{+a/2}\cos(\varepsilon_\beta y)\cdot\cos(\eta_n y)\,dy = \frac{1}{2}\left[\frac{\sin(\varepsilon_\beta-\eta_n)h}{(\varepsilon_\beta-\eta_n)h}+\frac{\sin(\varepsilon_\beta+\eta_n)h}{(\varepsilon_\beta+\eta_n)h}\right] \\ &= \frac{\eta_n h\cdot\sin(\eta_n h)\cdot\cos(\varepsilon_\beta h)-\varepsilon_\beta h\cdot\cos(\eta_n h)\cdot\sin(\varepsilon_\beta h)}{(\eta_n^2-\varepsilon_\beta^2)h^2} \end{aligned} \tag{13}$$

$$\begin{aligned} R_{\beta n} &= \frac{1}{a}\int_{-a/2}^{+a/2}\sin(\varepsilon_\beta y)\cdot\sin(\eta_n y)\,dy = \frac{1}{2}\left[\frac{\sin(\varepsilon_\beta-\eta_n)h}{(\varepsilon_\beta-\eta_n)h}-\frac{\sin(\varepsilon_\beta+\eta_n)h}{(\varepsilon_\beta+\eta_n)h}\right] \\ &= \frac{\varepsilon_\beta h\cdot\sin(\eta_n h)\cdot\cos(\varepsilon_\beta h)-\eta_n h\cdot\cos(\eta_n h)\cdot\sin(\varepsilon_\beta h)}{(\eta_n^2-\varepsilon_\beta^2)h^2} \end{aligned}$$

with special cases:

$$\begin{aligned} &S_{\beta n} = \frac{\sin(\varepsilon_\beta h)}{\varepsilon_\beta h}\ ;\ n=0\ ;\ S_{\beta n}=\frac{1}{2}\left(1+\frac{\sin(\eta_n a)}{\eta_n a}\right)\ ;\ \eta_n=\varepsilon_\beta\ ;\ S_{\beta n}=1\ ;\ n=\varepsilon_\beta=0 \\ &R_{\beta n} = 0\ ;\left\{\begin{array}{l} n\ \ =0 \\ \varepsilon_\beta=0 \end{array}\right. \quad ;\ R_{\beta n}=\frac{1}{2}\left(1-\frac{\sin(\eta_n a)}{\eta_n a}\right)\ ;\ \eta_n=\varepsilon_\beta . \end{aligned} \tag{14}$$

The auxiliary quantities $\quad X_\pm = B_\rho \pm C_\rho \quad ; \quad Y_\pm = B_\rho e^{-\Gamma d} \pm C_\rho e^{+\Gamma d}$ (15)

with intrinsic relations

$$\begin{aligned} X_+ &= X_-\cdot\frac{1+e^{-2\Gamma d}}{1-e^{-2\Gamma d}} - 2Y_-\cdot\frac{e^{-\Gamma d}}{1-e^{-2\Gamma d}}\,, \\ Y_+ &= 2X_-\cdot\frac{e^{-\Gamma d}}{1-e^{-2\Gamma d}} - Y_-\cdot\frac{1+e^{-2\Gamma d}}{1-e^{-2\Gamma d}} \end{aligned} \tag{16}$$

from which follow

$$\begin{aligned} B_\rho &= \frac{1}{2}(X_+ + X_-) = \frac{1}{2}(Y_+ + Y_-)\,e^{+\Gamma d}\,, \\ C_\rho &= \frac{1}{2}(X_+ - X_-) = \frac{1}{2}(Y_+ - Y_-)\,e^{-\Gamma d} \end{aligned} \tag{17}$$

are solutions of the following coupled system of equations:

$$\begin{aligned}
&X_- \cdot \left[\frac{1+e^{-2\Gamma d}}{1-e^{-2\Gamma d}} \left(1 - U\sum_{n\geq 0} \delta_n\, s_n V_n\right) - U\sum_{n\geq 0} \delta_n\, s_n W_n \right] \\
&- Y_- \cdot 2\frac{e^{-\Gamma d}}{1-e^{-2\Gamma d}} \left(1 - U\sum_{n\geq 0} \delta_n\, s_n V_n\right) = 2U \cdot A_e, \\
&X_- \cdot 2\frac{e^{-\Gamma d}}{1-e^{-2\Gamma d}} \left(1 - U\sum_{n\geq 0} \delta_n\, s_n V_n\right) - Y_- \cdot \left[\frac{1+e^{-2\Gamma d}}{1-e^{-2\Gamma d}} \left(1 - U\sum_{n\geq 0} \delta_n\, s_n V_n\right) \right. \\
&\left. - U\sum_{n\geq 0} \delta_n\, s_n W_n \right] = 0.
\end{aligned} \tag{18}$$

The other mode amplitudes follow from:

$$\begin{aligned}
A_{\rho n} &= \delta_{0,n} \cdot A_e + V_n \cdot X_+ + W_n \cdot Y_- \\
D_{\rho n} e^{-\gamma_{\rho n} d} &= V_n \cdot Y_+ - W_n \cdot Y_-
\end{aligned} \tag{19}$$

with the coefficients

$$\begin{aligned}
U \;&= \left[S_{\rho 0} - S_{\alpha 0} \frac{\Pi_\alpha}{\Pi_\rho} \frac{\Theta_\rho}{\Theta_\alpha} \frac{\cos(\varepsilon_\rho h)}{\cos(\varepsilon_\alpha h)} \right]^{-1}, \\
V_n \;&= \frac{a}{L} \frac{\eta_n}{\eta_n^2 - \gamma_{\rho n}\gamma_{\nu n}} \left[\varepsilon_\rho R_{\rho n} - \varepsilon_\alpha R_{\alpha n} \frac{\Theta_\rho}{\Theta_\alpha} \frac{\cos(\varepsilon_\rho h)}{\cos(\varepsilon_\alpha h)} \right. \\
&\quad \left. - \frac{\Gamma^2}{\varepsilon_\nu} R_{\nu n} \left(1 - \frac{\Theta_\rho}{\Theta_\alpha}\right) \frac{\cos(\varepsilon_\rho h)}{\cos(\varepsilon_\nu h)} \right], \\
W_n &= \frac{a}{L} \frac{\gamma_{\nu n}\Gamma}{\eta_n^2 - \gamma_{\rho n}\gamma_{\nu n}} \left[S_{\rho n} - S_{\alpha n} \frac{\Theta_\rho}{\Theta_\alpha} \frac{\cos(\varepsilon_\rho h)}{\cos(\varepsilon_\alpha h)} - S_{\nu n} \left(1 - \frac{\Theta_\rho}{\Theta_\alpha}\right) \frac{\cos(\varepsilon_\rho h)}{\cos(\varepsilon_\nu h)} \right].
\end{aligned} \tag{20}$$

Introducing the abbreviations

$$\begin{aligned}
e_n &= S_{\rho n} - S_{\alpha n} \frac{\Theta_\rho}{\Theta_\alpha} \frac{\cos(\varepsilon_\rho h)}{\cos(\varepsilon_\alpha h)} - S_{\nu n} \left(1 - \frac{\Theta_\rho}{\Theta_\alpha}\right) \frac{\cos(\varepsilon_\rho h)}{\cos(\varepsilon_\nu h)}, \\
d_n &= \varepsilon_\rho R_{\rho n} - \varepsilon_\alpha R_{\alpha n} \frac{\Theta_\rho}{\Theta_\alpha} \frac{\cos(\varepsilon_\rho h)}{\cos(\varepsilon_\alpha h)} - \frac{\Gamma^2}{\varepsilon_\nu} R_{\nu n} \left(1 - \frac{\Theta_\rho}{\Theta_\alpha}\right) \frac{\cos(\varepsilon_\rho h)}{\cos(\varepsilon_\nu h)}; \quad d_0 = 0,
\end{aligned} \tag{21}$$

the coefficients can be written as

$$V_n = \frac{a}{L} \frac{\eta_n}{\eta_n^2 - \gamma_{\rho n}\gamma_{\nu n}}\, d_n \quad ; \quad W_n = \frac{a}{L} \frac{\gamma_{\nu n}\Gamma}{\eta_n^2 - \gamma_{\rho n}\gamma_{\nu n}}\, e_n. \tag{22}$$

The back side slit impedance Z_{sb} then is:

$$\frac{Z_{sb}}{Z_0} = -j\, \frac{k_\rho^2}{k_0 \Gamma} \frac{1 - k_\rho^2/k_{\alpha 0}^2}{1 - \kappa\, k_\rho^2/k_{\alpha 0}^2} \frac{1}{U\, e_0} \frac{U \sum_{n\geq 0} \delta_n\, s_n\, W_n}{1 - U \sum_{n\geq 0} \delta_n\, s_n\, V_n} \tag{23}$$

and the front side slit impedance Z_{sf}:

$$\frac{Z_{sf}}{Z_0} = +j\,\frac{k_\rho^2}{k_0\Gamma}\,\frac{1-k_\rho^2/k_{\alpha0}^2}{1-\kappa\,k_\rho^2/k_{\alpha0}^2}\,\frac{1}{U\,e_0}\,\frac{\tanh(\Gamma d)\cdot\left[1-U\sum\limits_{n\geq0}\delta_n\,s_n\,V_n\right]-U\sum\limits_{n\geq0}\delta_n\,s_n\,W_n}{\left[1-U\sum\limits_{n\geq0}\delta_n\,s_n\,V_n\right]-\tanh(\Gamma d)\cdot U\sum\limits_{n\geq0}\delta_n\,s_n\,W_n}. \tag{24}$$

Using the approximations, which are possible for $|\varepsilon_\rho h| \ll 1$; $|\Gamma h|^2 \ll |k_\beta h|^2$; $\beta = \alpha\,,\nu$:

$$\begin{aligned} S_{\rho0} &= \frac{\sin(\varepsilon_\rho h)}{\varepsilon_\rho h} \approx 1\,, \\ S_{\beta0}\,\frac{\cos(\varepsilon_\rho h)}{\cos(\varepsilon_\beta h)} &\approx S_{\rho0}\,\frac{\tan(\varepsilon_\beta h)}{(\varepsilon_\beta h)} \xrightarrow[|\varepsilon_\beta h|\gg1]{} S_{\rho0}\,\frac{1-j}{\sqrt{2}\,|k_\beta h|} \approx \frac{1-j}{\sqrt{2}\,|k_\beta h|}\,, \end{aligned} \tag{25}$$

$$U \approx \frac{1}{S_{\rho0}}\;;\; W_0 \approx -\frac{a}{L}\,\frac{\Gamma}{\gamma_{\rho0}}\,e_0 = -\frac{a}{L}\,\frac{\Gamma}{jk_0}\,e_0\;;\; e_0 \approx S_{\rho0}\left[1-\frac{1-j}{\sqrt{2}\,|k_\beta h|}\right] \approx 1-\frac{1-j}{\sqrt{2}\,|k_\beta h|} \tag{26}$$

one gets:

$$\frac{Z_{sb}}{Z_0} \approx \frac{a}{L} - \frac{jk_0}{\Gamma}\,\frac{\sqrt{2}\,|k_\nu h|}{\sqrt{2}\,|k_\nu h|-(1-j)}\,\frac{2\sum\limits_{n>0} s_n\,W_n}{1-2\sum\limits_{n>0} s_n\,V_n}. \tag{27}$$

The first term is the normalised radiation resistance; in the second term the first two fractions have about unit value for not too narrow slits. The end correction can be evaluated from:

$$\frac{\Delta\ell}{a} = \frac{\mathrm{Im}\{Z_{sb}\}}{Z_0\,k_0 a}. \tag{28}$$

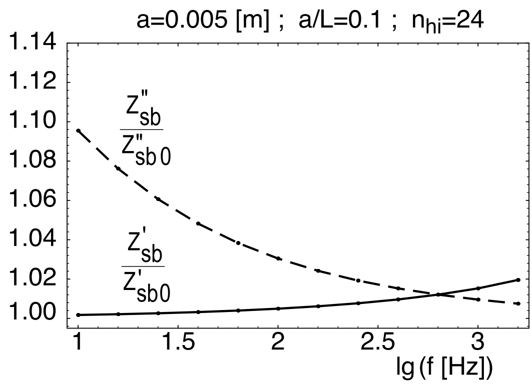

Ratios of the components of the slit impedance Z_{sb} with losses to these of the slit impedance Z_{sb0} without losses

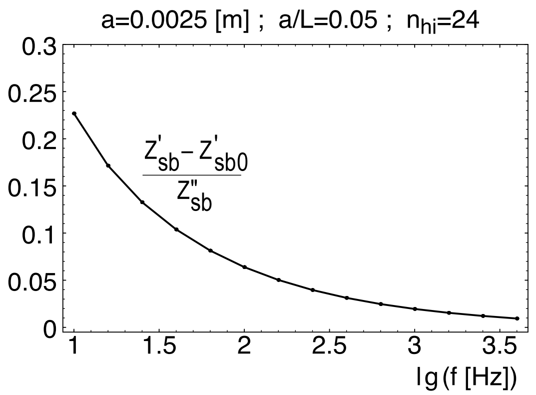

Loss factor of the oscillating mass of a slit when viscous and thermal losses in the neck are taken into account

The components of the slit impedance $Z_{sb} = Z'_{sb} + j \cdot Z''_{sb}$ can approximately be evaluated from those of the slit impedance $Z_{sb0} = Z'_{sb0} + j \cdot Z''_{sb0}$ without losses by:

$$\frac{Z'_{sb}}{Z_0} = \frac{Z'_{sb0}}{Z_0} \cdot \left(1 + \frac{10^{F'(x)}}{\sqrt{a[m]} \cdot \sqrt[3]{a/L}}\right) \quad ; \quad x = \lg \frac{f[Hz]a[m]}{(a/L)^{3/2}} \; ,$$

$$\frac{Z''_{sb}}{Z_0} = \frac{Z''_{sb0}}{Z_0} \cdot \left(1 + \frac{10^{F''(x)}}{\sqrt{a[m]} \cdot \sqrt[3]{a/L}}\right) \quad ; \tag{29}$$

$$F'(x) = -4.641\,06 \;\; + 0.435\,993\,x + 0.0142\,851\,x^2 + 0.000\,461\,347\,x^3 \; ,$$

$$F''(x) = -2.266\,65 - 0.492\,331\,x - 0.000\,719\,182\,x^2 - 0.001\,0208\,x^3 .$$

H.7 Slit Resonator with Viscous and Thermal Losses

► *See also:* Mechel, Vol. II, Ch. 19 (1995)

See the scheme drawing in *Sect. H.6*.

The field formulations remain as in *Sect. H.6*, except the field in the

Zone III:
$$\begin{aligned} \Phi_{III}(x,y) &= \sum_{n \geq 0} \delta_n \, D_{\rho n} \cdot \cosh(\gamma_{\rho n}(x-d-t)) \cdot \cos(\eta_n y) \\ \Psi_{III}(x,y) &= \sum_{n \geq 0} \delta_n \, D_{\nu n} \cdot \sinh(\gamma_{\nu n}(x-d-t)) \cdot \sin(\eta_n y) \quad ; \quad D_{\nu 0} = 0. \end{aligned} \tag{1}$$

The system of equations for the auxiliary quantities X_-, Y_- (see H.6) is:

$$\begin{aligned}
&X_- \cdot \left[\frac{1+e^{-2\Gamma d}}{1-e^{-2\Gamma d}} \left(1 - U \sum_{n\geq 0} \delta_n\, s_n V_n\right) - U \sum_{n\geq 0} \delta_n\, s_n W_n \right] \\
&- Y_- \cdot 2\frac{e^{-\Gamma d}}{1-e^{-2\Gamma d}} \left(1 - U \sum_{n\geq 0} \delta_n\, s_n V_n\right) = 2U \cdot A_e, \\
&X_- \cdot 2\frac{e^{-\Gamma d}}{1-e^{-2\Gamma d}} \left(1 - U \sum_{n\geq 0} \delta_n\, s_n V'_n\right) - Y_- \cdot \left[\frac{1+e^{-2\Gamma d}}{1-e^{-2\Gamma d}} \left(1 - U \sum_{n\geq 0} \delta_n\, s_n V'_n\right) \right. \\
&\left. - U \sum_{n\geq 0} \delta_n\, s_n W'_n \right] = 0
\end{aligned} \tag{2}$$

with the new coefficients

$$\begin{aligned}
V'_n &= \frac{a}{L} \frac{\eta_n}{\eta_n^2 - \gamma_{\rho n}\gamma_{\nu n} \cdot \tanh(\gamma_{\rho n} t)/\tanh(\gamma_{\nu n} t)}\, d_n \quad ; \quad V'_0 = 0\,, \\
W'_n &= \frac{a}{L} \frac{\Gamma\, \gamma_{\nu n}/\tanh(\gamma_{\nu n} t)}{\eta_n^2 - \gamma_{\rho n}\gamma_{\nu n} \cdot \tanh(\gamma_{\rho n} t)/\tanh(\gamma_{\nu n} t)}\, e_n
\end{aligned} \tag{3}$$

and all other terms as in H.6.

The back and front orifice impedances Z_{sb}, Z_{sf} become:

$$\begin{aligned}
\frac{Z_{sb}}{Z_0} &= -j\, \frac{k_\rho^2}{k_0\Gamma} \frac{1-k_\rho^2/k_{\alpha 0}^2}{1-\kappa\, k_\rho^2/k_{\alpha 0}^2} \frac{1}{U\, e_0} \frac{U \sum_{n\geq 0} \delta_n\, s_n\, W'_n}{1 - U \sum_{n\geq 0} \delta_n\, s_n\, V'_n} \\
\frac{Z_{sf}}{Z_0} &= +j\, \frac{k_\rho^2}{k_0\Gamma} \frac{1-k_\rho^2/k_{\alpha 0}^2}{1-\kappa\, k_\rho^2/k_{\alpha 0}^2} \frac{1}{U\, e_0} \frac{\tanh(\Gamma d) \cdot \left[1 - U \sum_{n\geq 0} \delta_n\, s_n\, V'_n\right] - U \sum_{n\geq 0} \delta_n\, s_n\, W'_n}{\left[1 - U \sum_{n\geq 0} \delta_n\, s_n\, V'_n\right] - \tanh(\Gamma d) \cdot U \sum_{n\geq 0} \delta_n\, s_n\, W'_n}.
\end{aligned} \tag{4}$$

Compared with the results of Sect. H.6 only the substitutions $V_n \to V'_n, W_n \to W'_n$ take place, which correspond to the substitutions $\gamma_{\rho n} \to \gamma_{\rho n} \cdot \tanh(\gamma_{\rho n} t)$, $\gamma_{\nu n} \to \gamma_{\nu n}/\tanh(\gamma_{\nu n} t)$.*)

Let Z''_{sM} be the mass reactance part of the back orifice impedance Z_{sb} with losses, and let Z''_{sb0} be the mass reactance part of the *free slit plate without losses* (Sect. H.2), then the relative change of the reactance can be evaluated with:

$$x = \lg(f[\mathrm{Hz}]) \quad ; \quad y = \lg(a[\mathrm{m}]) \quad ; \quad z = \lg(a/L) \quad ; \quad u = \lg(t/L) \tag{5}$$

*) See Preface to the 2nd edition.

from

$$\begin{aligned}
&\lg\left(\frac{Z''_{sM}}{Z''_{sb0}}-1\right) = \\
&-2.240408 \\
&-0.1580984\cdot x+0.00688292\cdot x^2+0.0225970\cdot x^3 \\
&-0.7868117\cdot y+0.3117230\cdot y^2+0.0739239\cdot y^3 \\
&+0.7621584\cdot z+0.4961154\cdot z^2+0.1579759\cdot z^3 \\
&-1.113747\cdot u+1.609799\cdot u^2-2.026946\cdot u^3 \\
&+0.2694603\cdot x\cdot y+0.1078516\cdot x\cdot y^2+0.0741470\cdot x^2\cdot y \\
&+0.1401039\cdot x\cdot z+0.00720527\cdot x\cdot z^2-0.0424421\cdot x^2\cdot z \\
&+0.0937094\cdot u\cdot x-0.0519085\cdot u\cdot x^2+0.7279337\cdot u^2\cdot x \\
&-0.1959382\cdot y\cdot z-0.00180315\cdot y^2\cdot z-0.0587445\cdot y\cdot z^2 \\
&-1.014977\cdot u\cdot y-0.1716795\cdot u\cdot y^2+1.373450\cdot u^2\cdot y \\
&+0.1977607\cdot u\cdot z-0.1665151\cdot u^2\cdot z+0.0690112\cdot u\cdot z^2.
\end{aligned} \tag{6}$$

The loss factor η can be evaluated with:

$$x=\lg(a[m]) \quad ; \quad y=\lg(a/L) \quad ; \quad z=\lg(t/L) \quad ; \quad u=\lg(d/a) \tag{7}$$

in the range

$$0.0025\le a\le 0.02[m];\quad 0.025\le a/L\le 0.4;\quad 0.25\le t/L\le 2.0;\quad 0.25\le d/a\le 4.0$$

from

$$\begin{aligned}
&\lg(\eta) = \\
&-3.42990 \\
&-0.567811\cdot x-0.405786\cdot y+0.395143\cdot z \\
&+0.0811464\cdot z^2-0.0337095\cdot u+0.0871987\cdot u^2 \\
&+0.0168052\cdot u\cdot x+0.0184409\cdot u^2\cdot x-0.225751\cdot u\cdot y \\
&+0.0404207\cdot u^2\cdot y-0.143725\cdot u\cdot z-0.0130437\cdot u^2\cdot z \\
&-0.132369\cdot u\cdot z^2-0.114934\cdot x\cdot y-0.0195440\cdot x\cdot z \\
&-0.000512528\cdot x\cdot z^2+0.0682123\cdot y\cdot z+0.0335370\cdot y\cdot z^2 \\
&+0.0534482\cdot u\cdot x\cdot y+0.0314014\cdot u^2\cdot x\cdot y-0.00696663\cdot u\cdot x\cdot z \\
&+0.0156990\cdot u^2\cdot x\cdot z-0.0805588\cdot u\cdot y\cdot z-0.00456461\cdot u^2\cdot y\cdot z \\
&-0.0409866\cdot x\cdot y\cdot z+0.0150972\cdot u\cdot x\cdot y\cdot z+0.0183208\cdot u^2\cdot x\cdot y\cdot z \\
&+0.597378\cdot u^2\cdot z^2-0.0122410\cdot u\cdot x\cdot z^2+0.00565404\cdot u^2\cdot x\cdot z^2 \\
&-0.0586390\cdot u\cdot y\cdot z^2+0.454270\cdot u^2\cdot y\cdot z^2-0.00757341\cdot x\cdot y\cdot z^2 \\
&-0.000668200\cdot u\cdot x\cdot y\cdot z^2+0.00446479\cdot u^2\cdot x\cdot y\cdot z^2.
\end{aligned} \tag{8}$$

A regression for the lowest resonance frequency f_0[Hz] is with the same variables and range:

$$\begin{aligned}
&\lg(f_0[\mathrm{Hz}]) = \\
&1.624303 - 0.321020 \cdot u - 0.128558 \cdot u^2 \\
&- 1.046357 \cdot x + 0.0110806 \cdot u \cdot x + 0.0100787 \cdot u^2 \cdot x \\
&+ 1.041716 \cdot y - 0.0927421 \cdot u \cdot y + 0.00399800 \cdot u^2 \cdot y \\
&- 0.0841638 \cdot x \cdot y + 0.0258718 \cdot u \cdot x \cdot y + 0.0178172 \cdot u^2 \cdot x \cdot y \\
&- 0.623277 \cdot z + 0.136128 \cdot u \cdot z - 0.0220866 \cdot u^2 \cdot z \\
&- 0.0107052 \cdot x \cdot z - 0.00112857 \cdot u \cdot x \cdot z - 0.000679359 \cdot u^2 \cdot x \cdot z \\
&- 0.057692 \cdot y \cdot z + 0.0667389 \cdot u \cdot y \cdot z - 0.0262524 \cdot u^2 \cdot y \cdot z \\
&- 0.0204744 \cdot x \cdot y \cdot z - 0.00198288 \cdot u \cdot x \cdot y \cdot z + 0.00124123 \cdot u^2 \cdot x \cdot y \cdot z \\
&- 0.0806259 \cdot z^2 + 0.083414 \cdot u \cdot z^2 + 0.00318264 \cdot u^2 \cdot z^2 \\
&+ 0.00264497 \cdot x \cdot z^2 - 0.00150123 \cdot u \cdot x \cdot z^2 - 0.00265546 \cdot u^2 \cdot x \cdot z^2 \\
&- 0.0218893 \cdot y \cdot z^2 + 0.0362045 \cdot u \cdot y \cdot z^2 - 0.00795119 \cdot u^2 \cdot y \cdot z^2 \\
&+ 0.00570269 \cdot x \cdot y \cdot z^2 - 0.00580403 \cdot u \cdot x \cdot y \cdot z^2 - 0.00346127 \cdot u^2 \cdot x \cdot y \cdot z^2.
\end{aligned} \tag{9}$$

H.8 Free Plate with an Array of Circular Holes, with Losses

▸ *See also:* Mechel, Vol. II, Ch. 21 (1995)

The object is a (rigid) plate with thickness d, containing circular holes with diameter 2a in a hexagonal arrangement.

A plane wave with normal incidence has the amplitude A_e.

The sketch shows the arrangement with a symmetry cell behind each hole. In this section the length of the cell is $t = \infty$. The radius b of the cell is fixed so that the cells cover all the backside area of the plate (so also square arrays can be treated with this model).

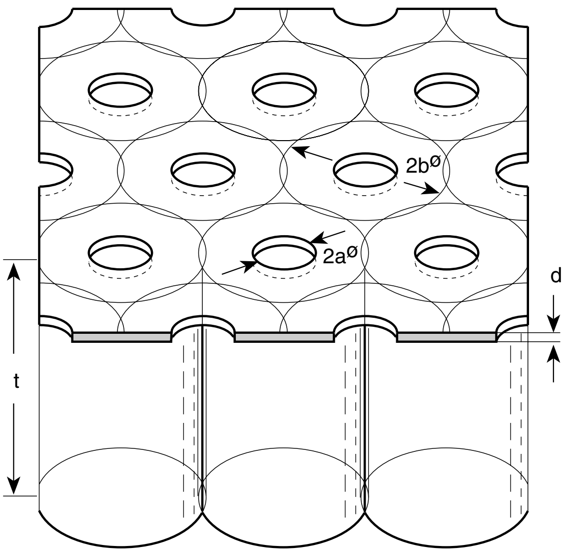

Zones I and III are supposed to be dissipationless; the necks (zone II) have viscous and thermal losses, or the neck walls may be absorbent.

The sketch (with a resonator volume for the next section) shows field quantities which have to satisfy boundary conditions at the indicated surfaces, mode amplitudes in the zones, and wave numbers.

The fundamentals of this section correspond widely to those of Sect. H.7 for slit arrays with losses, except the losses in zones I and III are neglected here (their effect is unimportant).

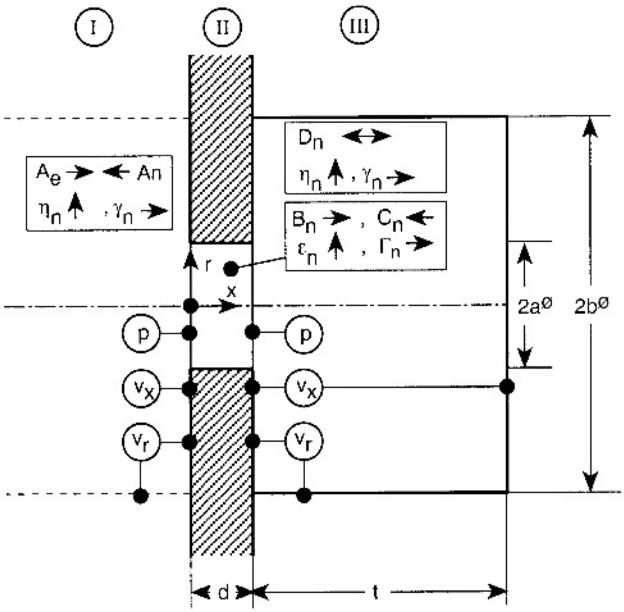

Sound field formulations:

in *Zone I*:

$$p_I(x, r) = A_e e^{-jk_0x} + \sum_{n\geq 0} A_n\, e^{\gamma_n x} J_0(\eta_n r)$$
$$Z_0 v_{Ix}(x, r) = A_e e^{-jk_0x} + j \sum_{n\geq 0} A_n\, \frac{\gamma_n}{k_0}\, e^{\gamma_n x} J_0(\eta_n r) \tag{1}$$

in *Zone II*:

$$p_{II}(x, r) = \sum_{n\geq 0} [B_n e^{-\Gamma_n x} + C_n e^{\Gamma_n x}]\, J_0(\varepsilon_n r)$$
$$Z_0 v_{IIx}(x, r) = -j \sum_{n\geq 0} \frac{\Gamma_n}{k_0}\, [B_n e^{-\Gamma_n x} - C_n e^{\Gamma_n x}]\, J_0(\varepsilon_n r) \tag{2}$$

in *Zone III*:

$$p_{III}(x, r) = \sum_{n\geq 0} D_n\, e^{-\gamma_n x} J_0(\eta_n r)$$
$$Z_0 v_{IIIx}(x, r) = -j \sum_{n\geq 0} D_n\, \frac{\gamma_n}{k_0}\, e^{-\gamma_n x} J_0(\eta_n y) \tag{3}$$

The sound field in the neck (zone II) is formulated as a mode sum. Some cases can be treated as follows:

(1) Use the formulation as it is if the neck walls are absorbent with an admittance G and higher neck modes shall be considered. Solve the characteristic equation

$$\varepsilon_n a \, \frac{J_1(\varepsilon_n a)}{J_0(\varepsilon_n a)} = j\, k_0 a\; Z_0 G \tag{4}$$

for a sufficiently large set of wave numbers ε_n and determine the axial propagation constants Γ_n from $\Gamma_n^2 = \varepsilon_n^2 - k_0^2$.

(2) The neck wall is absorbent, but the neck is narrow, so that only the fundamental neck mode must be retained: determine ε_0, Γ_0 as above and set $B_{n>0} = 0$ and $C_{n>0} = 0$.

(3) The neck wall is hard, and higher neck modes shall be considered: proceed as in (1), but with the characteristic equation for $G = 0$.

(4) The neck wall is hard, and only a plane wave is assumed in the neck: proceed as in (2), but with ε_0, Γ_0 for $G = 0$.

(5) The neck wall is hard, and only the fundamental capillary mode shall be considered (the neck is very narrow; viscous and thermal losses in it shall be considered): take for Γ_0 the propagation constant in circular capillaries (see sections about capillaries in *Ch. J*, "Duct Acoustics") and evaluate ε_0 from $\varepsilon_0^2 = \Gamma_0^2 + k_0^2$. (5)

(6) A somewhat exotic model assumes a very narrow neck, but with higher capillary modes. Either solve the characteristic equation of circular capillaries for a set of higher-mode propagation constants (which is not easy) or solve

$$\varepsilon_n a \, \frac{J_1(\varepsilon_n a)}{J_0(\varepsilon_n a)} = j\, k_0 a\; Z_0 G \tag{6}$$

with an equivalent $Z_0 G$:

$$Z_0 G = \frac{j}{k_0 a} \, \frac{(k_\rho a)^2 \left(1 - \dfrac{\Theta_\rho}{\Theta_\alpha}\right) \dfrac{J_1(k_\nu a)}{k_\nu a\, J_0(k_\nu a)} - \dfrac{\Theta_\rho}{\Theta_\alpha} k_\alpha a \, \dfrac{J_1(k_\alpha a)}{J_0(k_\alpha a)}}{1 - 2\left(1 - \dfrac{\Theta_\rho}{\Theta_\alpha}\right) \dfrac{J_1(k_\nu a)}{k_\nu a\, J_0(k_\nu a)}} \tag{7}$$

for a set of ε_n and then Γ_n from $\Gamma_n^2 = \varepsilon_n^2 - k_0^2$. (8)

Relations between wave numbers and propagation constants are:

$$\gamma_n^2 = \eta_n^2 - k_0^2 \quad ; \quad \Gamma_n^2 = \varepsilon_n^2 - k_0^2. \tag{9}$$

$z_n = \eta_n b$ are solutions ($n = 0, 1, 2, \ldots$) of $J_1(z) = 0$ with $z_0 = 0$.

Mode-coupling coefficients:

$$
\begin{aligned}
T_{n,m} &= \frac{1}{a^2}\int_0^a J_0(\varepsilon_n r)\, J_0(\eta_m r)\cdot r\,dr \\
&= \frac{\varepsilon_n a\ J_1(\varepsilon_n a)\ J_0\left(z_m \frac{a}{b}\right) - z_m \frac{a}{b}\ J_0(\varepsilon_n a)\ J_1\left(z_m \frac{a}{b}\right)}{(\varepsilon_n a)^2 - z_m^2\left(\frac{a}{b}\right)^2} \\
&= \frac{J_0(\varepsilon_n a)\ J_0(\eta_m a)}{(\varepsilon_n a)^2 - (\eta_m)^2}\left[j\,k_0 a\,Z_0 G - \eta_m a\,\frac{J_1(\eta_m a)}{J_0(\eta_m a)}\right]
\end{aligned} \tag{10}
$$

$$
T_{m,0} = \frac{1}{a^2}\int_0^a J_0(\varepsilon_m r)\cdot r\,dr = \frac{J_1(\varepsilon_m a)}{\varepsilon_m a} = \frac{J_0(\varepsilon_m a)}{(\varepsilon_m a)^2}\cdot j\,k_0 a\,Z_0 G
$$

$$
T_{m,i}T_{n,i} = J_0^2(\eta_i a)\ \frac{J_0(\varepsilon_m a)}{(\varepsilon_m a)^2-(\eta_i a)^2}\ \frac{J_0(\varepsilon_n a)}{(\varepsilon_n a)^2-(\eta_i a)^2}\ \left(j\,k_0 a\,Z_0 G-\eta_i a\,\frac{J_1(\eta_i a)}{J_0(\eta_i a)}\right)^2
$$

and

$$
R_m = \frac{1}{a^2}\int_0^a J_0(\varepsilon_n r)\ J_0(\varepsilon_m r)\cdot r\,dr = \frac{1}{2}J_0^2(\varepsilon_m a)\left[1 - \frac{(k_0 a)^2}{(\varepsilon_m a)^2}(Z_0 G)^2\right]. \tag{11}
$$

The boundary conditions lead to a coupled system of equations for the auxiliary quantities;

$$
X_{n\pm} := B_n \pm C_n \quad ; \quad Y_{n\pm} := B_n e^{-\Gamma_n d} \pm C_n e^{\Gamma_n d} \tag{12}
$$

with intrinsic relations

$$
\begin{aligned}
X_{n+} &= X_{n-}\cdot\frac{1+e^{-2\Gamma_n d}}{1-e^{-2\Gamma_n d}} - 2Y_{n-}\cdot\frac{e^{-\Gamma_n d}}{1-e^{-2\Gamma_n d}}\,, \\
Y_{n+} &= 2X_{n-}\cdot\frac{e^{-\Gamma_n d}}{1-e^{-2\Gamma_n d}} - Y_{n-}\cdot\frac{1+e^{-2\Gamma_n d}}{1-e^{-2\Gamma_n d}}.
\end{aligned} \tag{13}
$$

The system of equations has the form ($m = 0, 1, \ldots$):

$$
\begin{aligned}
&\sum_{n\geq 0} a_{mn}\cdot X_{n-} + c_m\cdot Y_{m-} = b_m\cdot A_e \\
&c_m\cdot X_{m-} + \sum_{n\geq 0} a_{mn}\cdot Y_{n-} = 0
\end{aligned} \tag{14}
$$

with coefficients:

$$
\begin{aligned}
a_{m,n} &= 2\left(\frac{a}{b}\right)^2\ \frac{\Gamma_n}{k_0}\ \sum_{i\geq 0}\frac{k_0}{\gamma_i J_0^2(z_i)}\ T_{m,i}T_{n,i} + \delta_{m,n}\ \frac{1+e^{-2\Gamma_m d}}{1-e^{-2\Gamma_m d}} \\
c_m &= -2\,R_m\,\frac{e^{-\Gamma_m d}}{1-e^{-2\Gamma_m d}} \quad ; \quad b_m = T_{m,0}\left(1 + j\,\frac{k_0}{\gamma_0}\right).
\end{aligned} \tag{15}
$$

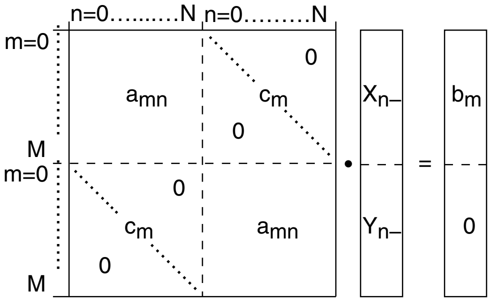

The mode amplitudes follow from solutions with:

$$
\begin{aligned}
A_n &= \frac{k_0}{\gamma_n J_0^2(z_n)} \left[\delta_{0,n} \cdot jA_e - 2\left(\frac{a}{b}\right)^2 \sum_{i\geq 0} \frac{\Gamma_i}{k_0}\, T_{i,n} \cdot X_{i-} \right] , \\
B_n &= \frac{1}{2}(X_{n+} + X_{n-}) = \frac{1}{2}(Y_{n+} + Y_{n-}) e^{+\Gamma_n d} , \\
C_n &= \frac{1}{2}(X_{n+} - X_{n-}) = \frac{1}{2}(Y_{n+} - Y_{n-}) e^{-\Gamma_n d} , \\
D_n &= 2\left(\frac{a}{b}\right)^2 \frac{k_0\, e^{\gamma_n d}}{\gamma_n J_0^2(z_n)} \sum_{i\geq 0} \frac{\Gamma_i}{k_0}\, T_{i,n} \cdot Y_{i-} .
\end{aligned}
\tag{16}
$$

The front side and back side orifice impedances Z_{sf}, Z_{sb} are obtained from:

$$
\begin{aligned}
\frac{Z_{sf}}{Z_0} &= \frac{< p_{II}(0,r) >_a}{Z_0 < v_{IIx}(0,r) >_a} = j\, \frac{\sum\limits_{n\geq 0} T_{n,0} \cdot X_{n+}}{\sum\limits_{n\geq 0} \frac{\Gamma_n}{k_0}\, T_{n,0} \cdot X_{n-}} , \\
\frac{Z_{sb}}{Z_0} &= \frac{< p_{II}(d,r) >_a}{Z_0 < v_{IIx}(d,r) >_a} = j\, \frac{\sum\limits_{n\geq 0} T_{n,0} \cdot Y_{n+}}{\sum\limits_{n\geq 0} \frac{\Gamma_n}{k_0}\, T_{n,0} \cdot Y_{n-}} .
\end{aligned}
\tag{17}
$$

If only the fundamental mode $n = 0$ is retained in the neck, the system of equations becomes:

$$
a_{0,0} \cdot X_{0-} + c_0 \cdot Y_{0-} = b_0 \cdot A_e \quad ; \quad c_0 \cdot X_{0-} + a_{0,0} \cdot Y_{0-} = 0 \tag{18}
$$

or $$X_{0-} = \frac{b_0\, a_{0,0}}{a_{0,0}^2 - c_0^2} \quad ; \quad Y_{0-} = \frac{-b_0\, c_0}{a_{0,0}^2 - c_0^2} \tag{19}$$

with

$$
\begin{aligned}
a_{0,0} &= 2\left(\frac{a}{b}\right)^2 \frac{\Gamma_0}{k_0} \sum_{i\geq 0} \frac{k_0}{\gamma_i J_0^2(z_i)}\, T_{0,i} T_{0,i} + \frac{1 + e^{-2\Gamma_0 d}}{1 - e^{-2\Gamma_0 d}} , \\
b_0 &= T_{0,0}\left(1 + j\frac{k_0}{\gamma_0}\right) \quad ; \quad c_0 = -2\, R_0\, \frac{e^{-\Gamma_0 d}}{1 - e^{-2\Gamma_0 d}} .
\end{aligned}
\tag{20}
$$

The end correction $\Delta\ell/a$ of an orifice follows from: $$\frac{\Delta\ell}{a} = \frac{\mathrm{Im}\{Z_{sb}/Z_0\}}{k_0 a}. \tag{21}$$

Analytical results for necks with viscous and thermal losses in a free plate can be represented by the regression:

$$\begin{aligned}\frac{\Delta\ell}{a} = &-0.0454\,728 - 0.728\,326\,x - 0.177\,078\,x^2 + 0.0339\,531\,y \\ &+ 0.00810\,471\,y^2 - 0.00100\,762\,xy,\end{aligned} \tag{22}$$

$$x = \lg(\sigma) = \lg(a^2/b^2) \quad ; \quad y = \lg(b/\lambda_0).$$

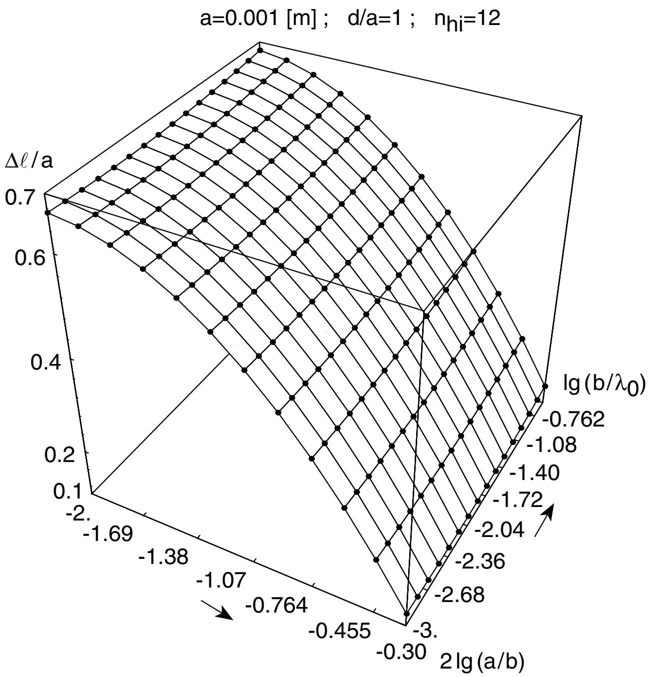

End correction $\Delta\ell/a$ of an orifice of an array of circular necks in a free plate, with losses in the neck; points: analytical solution; curves: regression

H.9 Array of Helmholtz Resonators with Circular Necks

▸ *See also:* Mechel, Vol. II, Ch. 21 (1995)

The arrangement is as shown in *Sect. H.8*, but now with a finite length t of the cells behind the necks. The fields in zones I and III are formulated as in *Sect. H.8*. The field formulation in zone III now is:

$$\begin{aligned} p_{III}(x,r) &= \sum_{n\geq 0} D_n \cosh(\gamma_n(x-d-t))\, J_0(\eta_n r)\,, \\ Z_0 v_{IIIx}(x,r) &= j\sum_{n\geq 0} D_n \frac{\gamma_n}{k_0} \sinh(\gamma_n(x-d-t))\, J_0(\eta_n y) \end{aligned} \tag{1}$$

with wave numbers as in *Sect. H.8*. The auxiliary quantities X_{n-}, Y_{n-} of that section are now solutions of the following coupled system of equations ($m = 0, 1, 2, \ldots$):

$$\begin{aligned} &\sum_{n\geq 0} a_{mn}\cdot X_{n-} + c_m\cdot Y_{m-} = b_m\cdot A_e\,, \\ &c_m\cdot X_{m-} + \sum_{n\geq 0} d_{mn}\cdot Y_{n-} = 0 \end{aligned} \tag{2}$$

with the coefficients $a_{m,n}, b_m, c_m$ from *Sect. H.8*, and

$$d_{m,n} = 2\left(\frac{a}{b}\right)^2 \frac{\Gamma_n}{k_0} \sum_{i\geq 0} \frac{k_0 \coth(\gamma_i t)}{\gamma_i J_0^2(z_i)} T_{m,i}T_{n,i} + \delta_{m,n} \frac{1+e^{-2\Gamma_m d}}{1-e^{-2\Gamma_m d}}. \tag{3}$$

The new mode amplitudes D_n are evaluated with solutions by:

$$D_n = 2\left(\frac{a}{b}\right)^2 \frac{k_0}{\gamma_n \sinh(\gamma_n d)\cdot J_0^2(z_n)} \sum_{i=0} \frac{\Gamma_i}{k_0} T_{i,n}\cdot Y_{i-}. \tag{4}$$

The front side and backside orifice impedances Z_{sf}, Z_{sb} are:

$$\begin{aligned} \frac{Z_{sf}}{Z_0} &= \frac{\langle p_{II}(0,r)\rangle_a}{Z_0 \langle v_{IIx}(0,r)\rangle_a} = j\,\frac{\sum\limits_{n\geq 0} T_{n,0}\cdot X_{n+}}{\sum\limits_{n\geq 0} \frac{\Gamma_n}{k_0} T_{n,0}\cdot X_{n-}}\,, \\ \frac{Z_{sb}}{Z_0} &= \frac{\langle p_{II}(d,r)\rangle_a}{Z_0 \langle v_{IIx}(d,r)\rangle_a} = j\,\frac{\sum\limits_{n\geq 0} T_{n,0}\cdot Y_{n+}}{\sum\limits_{n\geq 0} \frac{\Gamma_n}{k_0} T_{n,0}\cdot Y_{n-}}. \end{aligned} \tag{5}$$

If losses can be neglected in the neck, i.e. $\varepsilon_n a = z_n$ with z_n the solutions of $J_1(z_n) = 0$; $n = 0, 1, 2, \ldots; z_0 = 0$, then:

$$\begin{aligned} &\eta_n b = z_n \quad;\quad \eta_0 = 0 \quad;\quad \gamma_n^2 = \eta_n^2 - k_0^2 \quad;\quad \gamma_0 = jk_0\,, \\ &\varepsilon_n a = z_n \quad;\quad \varepsilon_0 = 0 \quad;\quad \Gamma_n^2 = \varepsilon_n^2 - k_0^2 \quad;\quad \Gamma_0 = jk_0 \end{aligned} \tag{6}$$

and

$$R_m = \frac{1}{a^2}\int_0^a J_0^2(\varepsilon_m r)\cdot r\,dr = \frac{1}{2}J_0^2(\varepsilon_m a)\,,$$

$$\begin{aligned}T_{n,m} &= \frac{1}{a^2}\int_0^a J_0(\varepsilon_n r)\,J_0(\eta_m r)\cdot r\,dr \\ &= \frac{\varepsilon_n a\,J_1(\varepsilon_n a)\,J_0\left(z_m\frac{a}{b}\right) - z_m\frac{a}{b}\,J_0(\varepsilon_n a)\,J_1\left(z_m\frac{a}{b}\right)}{(\varepsilon_n a)^2 - z_m^2\left(\frac{a}{b}\right)^2} \\ &= -\frac{\eta_m a\,J_0(\varepsilon_n a)\,J_1(\eta_m a)}{(\varepsilon_n a)^2-(\eta_m)^2}\,,\end{aligned} \tag{7}$$

$$T_{n,0} = \frac{1}{a^2}\int_0^a J_0(\varepsilon_n r)\cdot r\,dr = \frac{J_1(\varepsilon_n a)}{\varepsilon_n a} = 0 \quad ; \quad n > 0\,,$$

$$T_{0,m} = \frac{1}{a^2}\int_0^a J_0(\eta_m r)\cdot r\,dr = \frac{J_1(\eta_m a)}{\eta_m a} \quad ; \quad m > 0\,,$$

$$T_{0,0} = \frac{1}{2}$$

further: $b_m = \delta_{0,m}$. The orifice impedances then become:

$$\frac{Z_{sb}}{Z_0} = \frac{< p_{II}(d,r) >_a}{Z_0 < v_{IIx}(d,r) >_a} = \frac{Y_{0+}}{Y_{0-}} \quad ; \quad \frac{Z_{sf}}{Z_0} = \frac{< p_{II}(0,r) >_a}{Z_0 < v_{IIx}(0,r) >_a} = \frac{X_{0+}}{X_{0-}}. \tag{8}$$

The equivalent network of a Helmholtz resonator can be conceived as in the diagram.

Z_R is the radiation resistance of the front orifice;

Z_1, Z_2 represent the neck;

Z_F is the spring reactance of the resonator volume.

Then M_f, M_b represent the oscillating masses of the front and back orifices.

$$Z_1 = j\,Z_0\,\sin(k_0 d) \quad ; \quad Z_2 = -j\,Z_0\,\frac{\sin(k_0 d)}{1-\cos(k_0 d)} \quad ; \quad Z_F = -j\,\sigma\,\cot(k_0 t) \tag{9}$$

with $\sigma = (a/b)^2$ the surface porosity of the neck plate.

The end corrections are given by: $$\frac{\Delta\ell}{a} = \frac{\mathrm{Im}\{Z_M/Z_0\}}{k_0 a} = \frac{\omega M/Z_0}{k_0 a}. \tag{10}$$

The front side end correction $\Delta\ell_f/a$ is that of the front side orifice of a free plate (Sect. H.8).

With the back side orifice impedance Z_{sb} written as:

$$\frac{Z_{sb}}{Z_0} = \frac{Z_{Mb}}{Z_0} - j\,\sigma\,\cot(k_0 t). \tag{11}$$

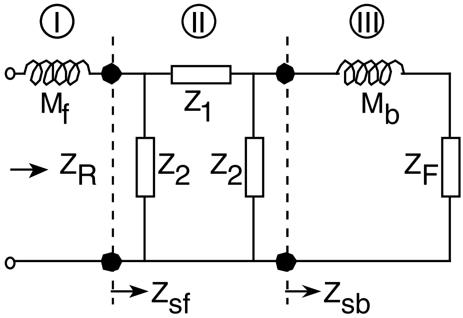

the interior end correction can be represented for $t/b \geq 0.5$ by:

$$x = \lg\sigma = 2\lg(a/b) \quad ; \quad y = \lg(b/\lambda_0)$$

$$\begin{aligned}\frac{\Delta\ell_b}{a} &= -0.0481\,939 - 0.731\,823\,x - 0.179\,629\,x^2 + 0.0342\,687\,y \\ &\quad + 0.00818\,059\,y^2 - 0.00101\,281\,xy.\end{aligned} \tag{12}$$

The resonance (angular) frequency ω_0 follows from the resonance condition:

$$\begin{aligned}k_0a\left(\frac{\Delta\ell_f}{a}+\frac{\Delta\ell_b}{a}\right) - \sigma\cot(k_0t) + \Bigg[1-(k_0a)^2\frac{\Delta\ell_f}{a}\frac{\Delta\ell_b}{a} \\ +\sigma k_0a\frac{\Delta\ell_f}{a}\cot(k_0t)\Bigg]\cdot\tan(k_0d) = 0\end{aligned} \tag{13}$$

with an approximation for $k_0d \ll 1$ and $k_0t \ll 1$ (with S_a the neck cross-section area and V the resonator volume):

$$\begin{aligned}(k_0a)^2 &\approx \frac{\sigma\,\dfrac{d}{t}}{\dfrac{d}{a}\left[\dfrac{d}{a}+\sigma\,\dfrac{d}{t}\,\dfrac{\Delta\ell_f}{a}+\dfrac{\Delta\ell_f}{a}+\dfrac{\Delta\ell_b}{a}\right]} \\ \omega_0 &\approx c_0\sqrt{\frac{S_a}{V\,(d+\Delta\ell_f+\Delta\ell_b)+S_a d\,\Delta\ell_f}}.\end{aligned} \tag{14}$$

H.10 Slit Resonator Array with Porous Layer in the Volume, Fields

▸ *See also:* Mechel, Vol. II, Ch. 23 (1995)

The arrangement consists of a stiff plate at a distance t + s of a hard wall, which contains an array of parallel slits with width a and a mutual distance L. Behind the plate is a porous layer with thickness s (backed by the wall) and a distance t to the plate.

A plane wave with amplitude A_e is obliquely incident under a polar angle Θ.

Special cases, such as $\Theta = 0$; $t = 0$; $s = \infty$, will be considered. A great interest lies in the influence of the porous layer on the back side end correction.

The arrangement is treated as a periodic structure with period length L. The field in the necks is composed of mode sums in a hard duct (viscous and thermal losses generally can be neglected compared with the losses introduced by the porous layer). As a special case, only plane waves in the necks will be assumed also.

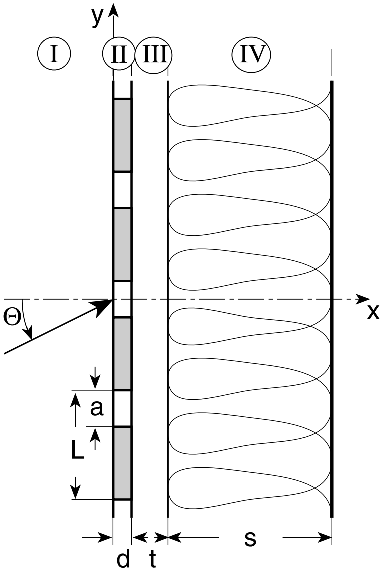

Below is $$\delta_m = \begin{cases} 1\,;\ m=0 \\ 2\,;\ m>0 \end{cases}. \tag{1}$$

Oblique incidence; t > 0; *higher neck modes*

Field formulation in zone I:

$$\begin{aligned} p_I(x,y) &= A_e\, e^{-j(k_x x + k_y y)} + \sum_{n=-\infty}^{+\infty} A_n \cdot e^{\gamma_n x} \cdot e^{-j\beta_n y} \\ Z_0\, v_{Ix}(x,y) &= A_e \frac{k_x}{k_0} e^{-j(k_x x + k_y y)} + j \sum_{n=-\infty}^{+\infty} A_n \frac{\gamma_n}{k_0} \cdot e^{\gamma_n x} \cdot e^{-j\beta_n y} \end{aligned} \tag{2}$$

with $k_x = k_0 \cos\Theta \quad ; \quad k_y = k_0 \sin\Theta$

and
$$\begin{aligned} &\beta_0 = k_y = k_0 \sin\Theta; \quad \beta_n = \beta_0 + n\frac{2\pi}{L} = k_0\left(\sin\Theta + n\frac{\lambda_0}{L}\right); \\ &\gamma_n^2 = \beta_n^2 - k_0^2; \ \gamma_0 = j\,k_x = j\,k_0 \cos\Theta; \ \gamma_n = k_0\sqrt{(\sin\theta + n\,\lambda_0/L)^2 - 1}. \end{aligned} \tag{3}$$

The necks in zone II are numbered with $\nu = 0, \pm1, \pm2, \ldots$, beginning with the neck which contains the x axis. The local co-ordinate in the ν-th neck is $y_\nu = y - \nu \cdot L$ with $|y_\nu| \le a/2$:

$$\begin{aligned} p_{II}(x,y_\nu) &= e^{-j\beta_0 \nu L} \sum_{m=0}^{\infty} \left(B_m\, e^{-j\kappa_m x} + C_m\, e^{+j\kappa_m x}\right) \cos\left(m\pi\left(\frac{y_\nu}{a} - \frac{1}{2}\right)\right) \\ Z_0\, v_{IIx}(x,y_\nu) &= e^{-j\beta_0 \nu L} \sum_{m=0}^{\infty} \frac{\kappa_m}{k_0}\left(B_m\, e^{-j\kappa_m x} - C_m\, e^{+j\kappa_m x}\right) \cos\left(m\pi\left(\frac{y_\nu}{a} - \frac{1}{2}\right)\right) \end{aligned} \tag{4}$$

$$\text{with} \quad \kappa_m = \begin{cases} \sqrt{k_0^2 - (m\pi/a)^2}\,; & m \le m_g \\ -j\sqrt{(m\pi/a)^2 - k_0^2}; & m > m_g \end{cases} \; ; \; m_g = \mathrm{INT}(k_0 a/\pi) = \mathrm{INT}(2a/\lambda_0). \quad (5)$$

The index limit m_g defines the transition from propagating modes to cut-off modes.

In the air gap of zone III (with wave numbers as in zone I):

$$\begin{aligned} p_{III}(x,y) &= \sum_{n\ge 0} (D_n\, e^{-\gamma_n y} + E_n\, e^{+\gamma_n x}) \cdot e^{-j\beta_n y}\,, \\ Z_0\, v_{IIIx}(x,y) &= -j \sum_{n\ge 0} \frac{\gamma_n}{k_0} (D_n\, e^{-\gamma_n y} - E_n\, e^{+\gamma_n x}) \cdot e^{-j\beta_n y}. \end{aligned} \quad (6)$$

In the absorber layer, zone IV:

$$\begin{aligned} p_{IV}(x,y) &= \sum_{n\ge 0} F_n\, \cosh(\varepsilon_n\,(x-d-t-s)) \cdot e^{-j\beta_n y}\,, \\ Z_0\, v_{IVx}(x,y) &= -\frac{k_0 Z_0}{\Gamma_a Z_a} \sum_{n\ge 0} \frac{\varepsilon_n}{k_0} F_n\, \sinh(\varepsilon_n\,(x-d-t-s)) \cdot e^{-j\beta_n y} \end{aligned} \quad (7)$$

with the characteristic propagation constant Γ_a and wave impedance Z_a of the porous material

$$\text{and} \quad \varepsilon_n = \sqrt{\beta_n^2 + \Gamma_a^2} = k_0\sqrt{(\sin\Theta + n\,\lambda_0/L)^2 + (\Gamma_a/k_0)^2}. \quad (8)$$

Auxiliary amplitudes are introduced:

$$X_{m\pm} =: B_m \pm C_m \quad ; \quad Y_{m\pm} =: B_m\, e^{-j\kappa_m d} \pm C_m\, e^{+j\kappa_m d} \quad (9)$$

with intrinsic relations

$$\begin{aligned} X_{m+} &= X_{m-} \frac{1+e^{-2j\kappa_m d}}{1-e^{-2j\kappa_m d}} - 2Y_{m-} \frac{e^{-j\kappa_m d}}{1-e^{-2j\kappa_m d}}\,, \\ Y_{m+} &= 2\,X_{m-} \frac{e^{-j\kappa_m d}}{1-e^{-2j\kappa_m d}} - Y_{m-} \frac{1+e^{-2j\kappa_m d}}{1-e^{-2j\kappa_m d}} \end{aligned} \quad (10)$$

and giving the other amplitudes by:

$$B_m = \frac{1}{2}(X_{m+} + X_{m-}) = \frac{1}{2}(Y_{m+} + Y_{m-})\, e^{+j\kappa_m d}\,,$$

$$C_m = \frac{1}{2}(X_{m+} - X_{m-}) = \frac{1}{2}(Y_{m+} - Y_{m-})\, e^{-j\kappa_m d}\,,$$

$$\begin{aligned} A_n &= j\frac{k_0}{\gamma_n}\left[\delta_{0,n}\cos\Theta - \frac{a}{2L}\sum_{m=0}^{\infty} X_{m-} \frac{\kappa_m}{k_0} s_{m,n}\right], \\ D_n &= j\frac{a}{2L}\frac{k_0}{\gamma_n}\frac{e^{+\gamma_n d}}{1 - r_n\, e^{-2\gamma_n t}} \sum_{m=0}^{\infty} Y_{m-}\frac{\kappa_m}{k_0} s_{m,n}\,, \\ E_n &= D_n \cdot r_n\, e^{-2\gamma_n (d+t)}\,, \\ F_n &= \frac{1}{\cosh(\varepsilon_n s)} (D_n\, e^{-\gamma_n (d+t)} + E_n\, e^{+\gamma_n (d+t)}). \end{aligned} \quad (11)$$

Here the modal reflection factors at the zone boundary III–IV are:

$$r_n = \frac{1 - j\,\dfrac{k_0 Z_0}{\Gamma_a Z_a}\,\dfrac{\varepsilon_n}{\gamma_n}\,\tanh(\varepsilon_n s)}{1 + j\,\dfrac{k_0 Z_0}{\Gamma_a Z_a}\,\dfrac{\varepsilon_n}{\gamma_n}\,\tanh(\varepsilon_n s)}. \tag{12}$$

The X_{n-}, Y_{n-} are solutions of the coupled system of linear equations

$$\sum_{n=0}^{\infty} a_{m,n}\, X_{n-} + c_m\, Y_{m-} = b_m \quad ; \quad \sum_{n=0}^{\infty} d_{m,n}\, Y_{n-} + c_m\, X_{m-} = 0 \tag{13}$$

with the coefficients:

$$a_{m,n} = j\,\frac{a}{2L}\,\frac{\kappa_n}{k_0}\sum_{i=-\infty}^{\infty}\frac{k_0}{\gamma_i}\, s_{m,i}\, s_{n,i} \;+\; 2\,(-1)^m\frac{\delta_{m,n}}{\delta_m}\,\frac{1+e^{-2j\,\kappa_m d}}{1-e^{-2j\,\kappa_m d}}\,,$$

$$d_{m,n} = j\,\frac{a}{2L}\,\frac{\kappa_n}{k_0}\sum_{i=-\infty}^{\infty}\frac{k_0}{\gamma_i}\,\frac{1+r_i\, e^{-2\gamma_i t}}{1-r_i\, e^{-2\gamma_i t}}\, s_{m,i}\, s_{n,i} \;+\; 2\,(-1)^m\frac{\delta_{m,n}}{\delta_m}\,\frac{1+e^{-2j\,\kappa_m d}}{1-e^{-2j\,\kappa_m d}}\,, \tag{14}$$

$$c_m = -\frac{4\,(-1)^m}{\delta_m}\,\frac{e^{-j\,\kappa_m d}}{1-e^{-2j\,\kappa_m d}} \quad ; \quad b_m = 2\; s_{m,0}\,,$$

$$s_{m,n} = e^{j\,m\pi/2}\left[\frac{\sin((m\pi-\beta_n a)/2)}{(m\pi-\beta_n a)/2} + (-1)^m\frac{\sin((m\pi+\beta_n a)/2)}{(m\pi+\beta_n a)/2}\right]$$

$$= 2\,\frac{\beta_n a/2}{(\beta_n a/2)^2-(m\pi/2)^2}\cdot\begin{cases}\sin(\beta_n a/2)\,; & m = \text{even}\\ -j\,\cos(\beta_n a/2); & m = \text{odd}\end{cases}$$

$$= \begin{cases} 2 & ;\quad \beta_n a = m\pi\,, \quad m = 0\\ e^{jm\pi/2} & ;\quad \beta_n a = m\pi\,, \quad m \neq 0\end{cases}$$

$$= \begin{cases} 2 & ;-\beta_n a = m\pi\,, \quad m = 0\\ (-1)^m\, e^{jm\pi/2} & ;-\beta_n a = m\pi\,, \quad m \neq 0\end{cases}$$

and $\quad s_{-m,n} = s_{m,n}.$ (15)

Oblique incidence; $t > 0$; *higher neck modes; infinite layer thickness* $t \to \infty$

Change the field formulation in zone IV to:

$$p_{IV}(x,y) = \sum_{n\geq 0} F_n\, e^{-\varepsilon_n x}\; e^{-j\,\beta_n y}\,,$$

$$Z_0\, v_{IVx}(x,y) = \frac{k_0 Z_0}{\Gamma_a Z_a}\sum_{n\geq 0}\frac{\varepsilon_n}{k_0}\, F_n\, e^{-\varepsilon_n x}\; e^{-j\,\beta_n y}, \tag{16}$$

substitute in r_n: $\qquad \tanh(\varepsilon_n s) \to 1,$

and evaluate the amplitudes from: $F_n = e^{\varepsilon_n(d+t)}\,(D_n\,e^{-\gamma_n(d+t)} + E_n\,e^{+\gamma_n(d+t)})$. (17)
The other expressions remain.

Normal incidence; $t > 0$; *higher neck modes*

It is not advisable to treat this case as a special case $\Theta = 0$ of the above results because the anti-symmetrical modes for oblique incidence (odd m) will vanish and the matrix will get a banded structure.

Field in zone I:

$$\begin{aligned} p_I(x,y) &= A_e\,e^{-j\,k_0 x} + \sum_{n\geq 0} \delta_n\,A_n\,e^{\gamma_n x}\,\cos(\eta_n y)\,, \\ Z_0\,v_{Ix}(x,y) &= A_e\,e^{-j\,k_0 x} + j\sum_{n\geq 0} \delta_n\,\frac{\gamma_n}{k_0}\,A_n\,e^{\gamma_n x}\,\cos(\eta_n y) \end{aligned} \tag{18}$$

$$\text{with}\quad \delta_n = \begin{cases} 1 & ;\ n=0 \\ 2 & ;\ n>0 \end{cases}\;;\quad \eta_n = n\,\frac{2\pi}{L};\quad \gamma_n = \sqrt{\eta_n^2 - k_0^2};\quad \gamma_0 = j\,k_0. \tag{19}$$

Field in zone II:

$$\begin{aligned} p_{II}(x,y) &= \sum_{m\geq 0} (B_m\,e^{-j\kappa_m x} + C_m\,e^{+j\kappa_m x})\,\cos(2m\pi\,y/a)\,, \\ Z_0\,v_{IIx}(x,y) &= \sum_{m\geq 0} \frac{\kappa_m}{k_0}\,(B_m\,e^{-j\kappa_m x} - C_m\,e^{+j\kappa_m x})\,\cos(2m\pi\,y/a) \end{aligned} \tag{20}$$

$$\text{with}\quad \kappa_m = \begin{cases} \sqrt{k_0^2 - (2m\pi/a)^2}; & m \leq m_g \\ -j\sqrt{(2m\pi/a)^2 - k_0^2}; & m > m_g \end{cases}\;;\quad \kappa_0 = k_0, \tag{21}$$

and the limit index for cut-off: $m_g = \mathrm{INT}(a/\lambda_0)$.

Field in zone III:

$$\begin{aligned} p_{III}(x,y) &= \sum_{n\geq 0} \delta_n\,(D_n\,e^{-\gamma_n x} + E_n\,e^{+\gamma_n x})\,\cos(\eta_n y)\,, \\ Z_0\,v_{IIIx}(x,y) &= -j\sum_{n\geq 0} \delta_n\,\frac{\gamma_n}{k_0}\,(D_n\,e^{-\gamma_n x} - E_n\,e^{+\gamma_n x})\,\cos(\eta_n y). \end{aligned} \tag{22}$$

Field in zone IV:

$$\begin{aligned} p_{IV}(x,y) &= \sum_{n\geq 0} \delta_n\,F_n\,\cosh(\varepsilon_n(x-d-t-s))\,\cos(\eta_n y)\,, \\ Z_0\,v_{IVx}(x,y) &= -\frac{k_0 Z_0}{\Gamma_a Z_a}\sum_{n\geq 0} \delta_n\,\frac{\varepsilon_n}{k_0}\,F_n\,\sinh(\varepsilon_n(x-d-t-s))\,\cos(\eta_n y) \end{aligned} \tag{23}$$

$$\text{with}\quad \varepsilon_n = \sqrt{\eta_n^2 + \Gamma_a^2};\quad \varepsilon_0 = \Gamma_a. \tag{24}$$

Mode-coupling coefficients:

$$
\begin{aligned}
S_{m,n} := &\frac{1}{a}\int_{-a/2}^{+a/2} \cos(2m\pi\, y/a)\ \cos(\eta_n y)\ dy \\
= &\frac{1}{2}\left[\frac{\sin(m\pi - n\pi\, a/L)}{m\pi - n\pi\, a/L} + \frac{\sin(m\pi + n\pi\, a/L)}{m\pi + n\pi\, a/L}\right]; \quad m, n > 0 \\
= &\frac{-(-1)^m}{\pi}\,\frac{n\, a/L}{m^2 - (n\, a/L)^2}\ \sin(n\pi\, a/L); \quad m, n > 0; \quad m \neq n\, a/L \\
= &\frac{\sin(n\pi\, a/L)}{n\pi\, a/L}; \quad m = 0; \quad n \geq 0 \\
= &\ 0; \quad m > 0; \quad n = 0 \\
= &\ 1; \quad m = n = 0 \\
= &\frac{1}{2}; \quad m = n\, a/L \neq 0.
\end{aligned}
\tag{25}
$$

The auxiliary amplitudes X_{n-}, Y_{n-} from above again are solutions of two coupled systems of equations as above, but with the following coefficients:

$$
\begin{aligned}
a_{m,n} &= j\,\frac{a}{L}\,\frac{\kappa_n}{k_0}\sum_{i\geq 0}\delta_i\,\frac{k_0}{\gamma_i}\,S_{m,i}\,S_{n,i} + \frac{\delta_{m,n}}{\delta_m}\,\frac{1 + e^{-2j\kappa_m d}}{1 - e^{-2j\kappa_m d}}, \\
d_{m,n} &= j\,\frac{a}{L}\,\frac{\kappa_n}{k_0}\sum_{i\geq 0}\delta_i\,\frac{k_0}{\gamma_i}\,S_{m,i}\,S_{n,i}\,\frac{1 + r_i\, e^{-2\gamma_i t}}{1 - r_i\, e^{-2\gamma_i t}} + \frac{\delta_{m,n}}{\delta_m}\,\frac{1 + e^{-2j\kappa_m d}}{1 - e^{-2j\kappa_m d}}, \\
c_m &= -\frac{2}{\delta_m}\,\frac{e^{-j\kappa_m d}}{1 - e^{-2j\kappa_m d}}; \quad b_m = 2\,\delta_{0,m}.
\end{aligned}
\tag{26}
$$

The mode amplitudes follow from solutions of this system as

$$
\begin{aligned}
A_m &= j\,\frac{k_0}{\gamma_m}\left[\delta_{0,m} - \frac{a}{L}\sum_{n\geq 0}\frac{\kappa_n}{k_0}\,S_{n,m}\ X_{n-}\right], \\
B_m &= \frac{1}{2}\,(X_{m+} + X_{m-}) = \frac{1}{2}\,(Y_{m+} + Y_{m-})\, e^{+j\kappa_m d}, \\
C_m &= \frac{1}{2}\,(X_{m+} - X_{m-}) = \frac{1}{2}\,(Y_{m+} - Y_{m-})\, e^{-j\kappa_m d}, \\
D_m &= j\,\frac{a}{L}\,\frac{e^{+\gamma_m d}}{1 - r_m\, e^{-2\gamma_m t}}\,\frac{k_0}{\gamma_m}\sum_{n\geq 0}\frac{\kappa_n}{k_0}\,S_{n,m}\ Y_{n-}, \\
E_m &= r_m\, e^{-2\gamma_m (d+t)}\ D_m, \\
F_m &= \frac{1}{\cosh(\varepsilon_m s)}\,\left(D_m\, e^{-\gamma_m (d+t)} + E_m\, e^{+\gamma_m (d+t)}\right).
\end{aligned}
\tag{27}
$$

Normal incidence; $t>0$; *only plane waves in the neck*

The system of equations to be solved simplifies to:

$$a_{0,0}\cdot X_{0-}+c_0\cdot Y_{0-}=b_0 \quad ; \quad c_0\cdot X_{0-}+d_{0,0}\cdot Y_{0-}=0 \tag{28}$$

or

$$X_{0-}=\frac{b_0 d_{0,0}}{a_{0,0}d_{0,0}-c_0^2} \quad ; \quad Y_{0-}=\frac{-b_0 c_0}{a_{0,0}d_{0,0}-c_0^2} \quad ; \quad \frac{X_{0-}}{Y_{0-}}=-\frac{d_{0,0}}{c_0} \tag{29}$$

with coefficients

$$\begin{aligned}
a_{0,0}&=j\frac{a}{L}\sum_{i\geq 0}\delta_i\frac{k_0}{\gamma_i}\left(\frac{\sin(i\pi\, a/L)}{i\pi\, a/L}\right)^2-j\cot(k_0 d)\,,\\
d_{0,0}&=j\frac{a}{L}\sum_{i\geq 0}\delta_i\frac{k_0}{\gamma_i}\left(\frac{\sin(i\pi\, a/L)}{i\pi\, a/L}\right)^2\frac{1+r_i\,e^{-2\gamma_i t}}{1-r_i\,e^{-2\gamma_i t}}-j\cot(k_0 d)\,,\\
c_0&=\frac{j}{\sin(k_0 d)} \quad ; \quad b_0=2.
\end{aligned} \tag{30}$$

The modal reflection factors are:

$$r_n=\frac{1-j\,\dfrac{k_0 Z_0}{\Gamma_a Z_a}\,\dfrac{\varepsilon_n}{\gamma_n}\,\tanh(\varepsilon_n s)}{1+j\,\dfrac{k_0 Z_0}{\Gamma_a Z_a}\,\dfrac{\varepsilon_n}{\gamma_n}\,\tanh(\varepsilon_n s)} \tag{31}$$

and the mode amplitudes

$$\begin{aligned}
B_0&=\frac{1}{2}\,(X_{0+}+X_{0-})=\frac{1}{2}\,(Y_{0+}+Y_{0-})\,e^{+j\,k_0 d}\,,\\
C_0&=\frac{1}{2}\,(X_{0+}-X_{0-})=\frac{1}{2}\,(Y_{0+}-Y_{0-})\,e^{-j\,k_0 d}\,,\\
A_n&=j\,\frac{k_0}{\gamma_n}\left[\delta_{0,n}-\frac{a}{L}\,\frac{\sin(n\pi\, a/L)}{n\pi\, a/L}\,X_{0-}\right],
\end{aligned} \tag{32a}$$

$$\begin{aligned}
D_n&=j\,\frac{a}{L}\,\frac{e^{+\gamma_n d}}{1-r_n\,e^{-2\gamma_n t}}\,\frac{k_0}{\gamma_n}\,\frac{\sin(n\pi\, a/L)}{n\pi\, a/L}\,Y_{0-}\,,\\
E_n&=r_n\,e^{-2\gamma_n(d+t)}\,D_n\,,\\
F_n&=\frac{1}{\cosh(\varepsilon_n s)}\,(D_n\,e^{-\gamma_n(d+t)}+E_n\,e^{+\gamma_n(d+t)}).
\end{aligned} \tag{32b}$$

Normal incidence; $t = 0$; *higher neck modes*

If the neck plate is in contact with the porous layer, zone III is obsolete; the amplitudes D_n, E_n are not needed. The axial function in zone IV changes to $\cosh(\varepsilon_n(x-d-s))$; $\sinh(\varepsilon_n(x-d-s))$. The system of equations for X_{n-}, Y_{n-} has the following coefficients:

$$
\begin{aligned}
a_{m,n} &= j\,\frac{a}{L}\,\frac{\kappa_n}{k_0}\sum_{i\ge 0}\delta_i\,\frac{k_0}{\gamma_i}\,S_{m,i}\,S_{n,i} + \frac{\delta_{m,n}}{\delta_m}\,\frac{1+e^{-2j\kappa_m d}}{1-e^{-2j\kappa_m d}}\,,\\
d_{m,n} &= j\,\frac{a}{L}\,\frac{\kappa_n}{k_0}\,\frac{\Gamma_a Z_a}{k_0 Z_0}\sum_{i\ge 0}\delta_i\,\frac{k_0}{\varepsilon_i}\,S_{m,i}\,S_{n,i}\,\coth(\varepsilon_i s) + \frac{\delta_{m,n}}{\delta_m}\,\frac{1+e^{-2j\kappa_m d}}{1-e^{-2j\kappa_m d}}\,,\\
c_m &= -\frac{2}{\delta_m}\,\frac{e^{-j\kappa_m d}}{1-e^{-2j\kappa_m d}}\quad;\quad b_m = 2\,\delta_{0,m}.
\end{aligned} \tag{33}
$$

The amplitudes F_m follow from:

$$
F_n = \frac{a}{L}\,\frac{\Gamma_a Z_a}{k_0 Z_0}\,\frac{k_0}{\varepsilon_n\cdot\sinh(\varepsilon_n s)}\sum_{m\ge 0}\frac{\kappa_m}{k_0}\,S_{m,n}\cdot Y_{m-}\,, \tag{34}
$$

the other amplitudes as above.

Normal incidence; $t = 0$; *only plane waves in the neck*

The coefficients of the two equations for X_{0-}, Y_{0-} become:

$$
\begin{aligned}
a_{0,0} &= j\,\frac{a}{L}\sum_{i\ge 0}\delta_i\,\frac{k_0}{\gamma_i}\left(\frac{\sin(i\pi a/L)}{i\pi a/L}\right)^2 + \frac{1+e^{-2j\,k_0 d}}{1-e^{-2j\,k_0 d}};\ b_0 = 2;\quad c_0 = -2\,\frac{e^{-j\,k_0 d}}{1-e^{-2j\,k_0 d}}\,,\\
d_{0,0} &= \frac{a}{L}\,\frac{\Gamma_a Z_a}{k_0 Z_0}\sum_{i\ge 0}\delta_i\,\frac{k_0}{\varepsilon_i}\left(\frac{\sin(i\pi a/L)}{i\pi a/L}\right)^2\coth(\varepsilon_i s) + \frac{1+e^{-2j\,k_0 d}}{1-e^{-2j\,k_0 d}}.
\end{aligned} \tag{35}
$$

H.11 Slit Resonator Array with Porous Layer in the Volume, Impedances

▸ *See also:* Mechel, Vol. II, Ch. 23 (1995)

The object here is the same as in › *Sect. H.10*.

The intention in this section is to evaluate the average impedance Z (without radiation resistance Z_R) of an array of slit Helmholtz resonators with a porous absorber layer in the resonator volume by a chain of equations, which represent a simple equivalent network. Some elements of the network are described with the help of the field evaluations in the previous › *Sect. H.10*.

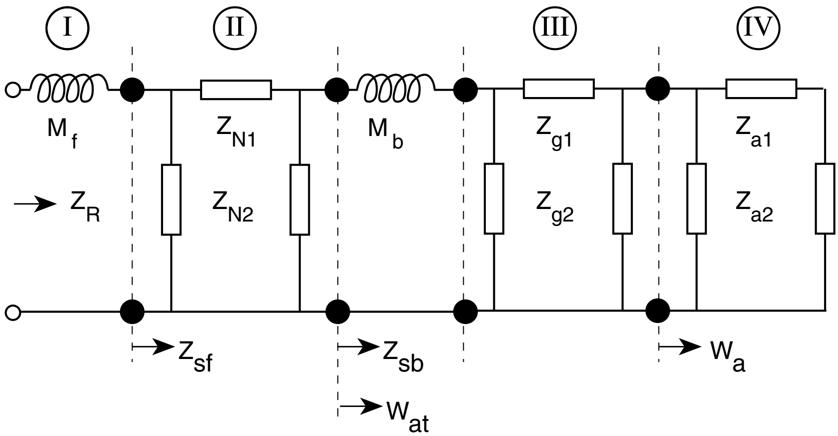

The symmetrical Π-fourpoles with $Z_{N1}, Z_{N2}; Z_{g1}, Z_{g2}; Z_{a1}, Z_{a2}$ represent, respectively, the neck, the air gap between the neck plate and the absorber layer, and the absorber layer. W_a is the input impedance of the absorber layer; W_{at} is that impedance transformed to the back side surface of the neck plate; Z_{sf}, Z_{sb} are the orifice impedances of the front side orifice and back side orifice. M_f, M_b are the oscillating masses of the two orifices.

The equations are as follows:

$$\begin{aligned}
\frac{Z}{Z_0} &= \frac{L}{a}\left[j\,k_0 a\,\frac{\Delta\ell}{a} + \frac{Z_{sf}}{Z_0}\right], \\
\frac{Z_{sf}}{Z_0} &= \frac{j\ \tan(k_0 d) + Z_{sb}/Z_0}{1 + j\ Z_{sb}/Z_0 \cdot \tan(k_0 d)}, \\
\frac{Z_{sb}}{Z_0} &= \frac{Z_{Msb}}{Z_0} + \frac{a}{L}\,\frac{W_{at}}{Z_0}; \qquad \frac{Z_{Msb}}{Z_0} = j\,k_0 a\,\frac{\Delta\ell_b}{a}, \\
\frac{W_{at}}{Z_0} &= \frac{j\ \tan(k_0 t) + W_a/Z_0}{1 + j\ W_a/Z_0 \cdot \tan(k_0 t)}; \qquad \frac{W_a}{Z_0} = \frac{Z_a/Z_0}{\tanh(\Gamma_a s)}
\end{aligned} \tag{1}$$

where $\Delta\ell/a$ is the front side end correction; the third line is a defining equation for the back side end correction $\Delta\ell_b/a$ using the back side orifice impedance Z_{sb} evaluated from the sound field as given in *Sect. H.10* for different conditions. Some of these conditions will be considered below. There $\Gamma_{an} = \Gamma_a/k_0$; $Z_{an} = Z_a/Z_0$ are the normalised characteristic values of the porous material.

Normal sound incidence, absorber layer in contact with neck plate, t = 0, *plane wave in the neck*

The back side orifice impedance Z_{sb} is (with quantities from *Sect. H.10*):

$$\begin{aligned}\frac{Z_{sb}}{Z_0} &= \frac{\langle p_{II}(d,y)\rangle_a}{Z_0\,\langle v_{IIx}(d,y)\rangle_a} = \frac{Y_{0+}}{Y_{0-}}\\ &= -2\,\frac{e^{-jk_0d}}{1-e^{-2jk_0d}}\,\frac{d_{0,0}}{c_0} - \frac{1+e^{-2jk_0d}}{1-e^{-2jk_0d}} = d_{0,0} - \frac{1+e^{-2jk_0d}}{1-e^{-2jk_0d}}\\ &= \frac{a}{L}\,\frac{\Gamma_a Z_a}{k_0 Z_0}\sum_{n\geq 0}\delta_n\frac{k_0}{\varepsilon_n}\left(\frac{\sin(n\pi\,a/L)}{n\pi\,a/L}\right)^2\coth(\varepsilon_n s)\\ &= \frac{a}{L}\left[\frac{Z_a/Z_0}{\tanh(\Gamma_a s)} + 2\frac{\Gamma_a Z_a}{k_0 Z_0}\sum_{n>0}\frac{k_0}{\varepsilon_n}\left(\frac{\sin(n\pi\,a/L)}{n\pi\,a/L}\right)^2\coth(\varepsilon_n s)\right].\end{aligned} \tag{2}$$

For the absorber layer in contact with the neck plate, as assumed here, $W_a = W_{at}$; therefore, evidently:

$$\frac{Z_{Mb}}{Z_0} = 2\frac{a}{L}\,\frac{\Gamma_a Z_a}{k_0 Z_0}\sum_{n>0}\frac{k_0}{\varepsilon_n}\left(\frac{\sin(n\pi\,a/L)}{n\pi\,a/L}\right)^2\coth(\varepsilon_n s) \tag{3}$$

and

$$\begin{aligned}\frac{\Delta\ell_b}{a} &= \frac{-j}{k_0 a}\,\frac{Z_{Mb}}{Z_0} = -2j\,\frac{s}{L}\,\frac{\Gamma_a Z_a}{k_0 Z_0}\sum_{n>0}\left(\frac{\sin(n\pi\,a/L)}{n\pi\,a/L}\right)^2\frac{\coth(\varepsilon_n s)}{\varepsilon_n s}\\ &= 2\frac{\sigma}{\sigma_a}\,\frac{\rho_{eff}}{\rho_0}\,\frac{s}{a}\sum_{n>0}\left(\frac{\sin(n\pi\,a/L)}{n\pi\,a/L}\right)^2\frac{\coth(\varepsilon_n s)}{\varepsilon_n s}\end{aligned}$$

$$\text{with}\quad \frac{\Gamma_a Z_a}{k_0 Z_0} = \frac{j}{\sigma_a}\,\frac{\rho_{eff}}{\rho_0}, \tag{4}$$

where σ_a is the porosity of the porous material and ρ_{eff} its (acoustical) effective density.

A set of variables for $\Delta\ell_b/a$ is:

$$F = \frac{L}{\lambda_0}\quad;\quad R = \frac{\Xi\, s}{Z_0}\quad;\quad E = \frac{\rho_0 f}{\Xi} = \frac{s}{L}\,\frac{F}{R}\,;\quad \frac{a}{L}\,;\quad \frac{d}{a}\,;\quad \frac{t}{L}\,;\quad \frac{s}{L}. \tag{5}$$

A regression through analytically evaluated end correction values for the absorber layer in contact with the neck plate is:

$$\begin{aligned}\frac{\Delta\ell_b}{a} = j\frac{\Gamma_a Z_a}{k_0 Z_0}\cdot(&0.0389998 + 0.454066\cdot x - 0.345328\cdot x^2 - 0.125386\cdot x^3\\ &- 0.0143782\cdot y + 0.00418541\cdot y^2 + 0.0170766\cdot y^3\\ &- 0.0142094\cdot z - 0.0715597\cdot z^2 + 0.0915584\cdot z^3\\ &- 0.0115326\cdot x\cdot y - 0.0195509\cdot x\cdot z - 0.0595634\cdot y\cdot z)\end{aligned} \tag{6}$$

$$x = \lg(a/L)\quad;\quad y = \lg(R) = \lg(\Xi\, s/Z_0)\quad;\quad z = \lg(s/L).$$

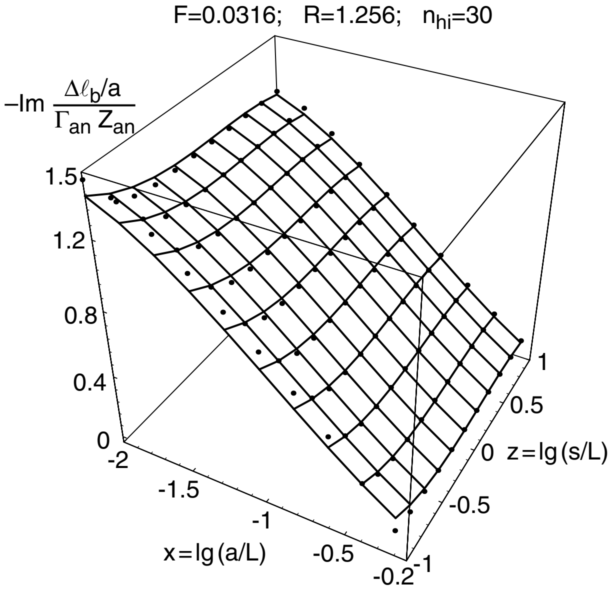

Back side orifice end correction $\Delta\ell_b/a$ if the absorber layer is in contact with the neck plate; points: analytic evaluation; curves: regression

Normal sound incidence, $t > 0$, *plane wave in the neck*

The back side orifice impedance Z_{sb} is (with quantities from *Sect. H.10*):

$$
\begin{aligned}
\frac{Z_{sb}}{Z_0} &= \frac{\langle p_{II}(d,y)\rangle_a}{Z_0\,\langle v_{IIx}(d,y)\rangle_a} = \frac{Y_{0+}}{Y_{0-}} \\
&= -2\,\frac{e^{-jk_0 d}}{1-e^{-2jk_0 d}}\,\frac{d_{0,0}}{c_0} - \frac{1+e^{-2jk_0 d}}{1-e^{-2jk_0 d}} = d_{0,0} - \frac{1+e^{-2jk_0 d}}{1-e^{-2jk_0 d}} \\
&= j\,\frac{a}{L}\sum_{n\ge 0}\delta_n\frac{k_0}{\gamma_n}\left(\frac{\sin(n\pi\,a/L)}{n\pi\,a/L}\right)^2\frac{1+r_n\,e^{-2\gamma_n t}}{1-r_n\,e^{-2\gamma_n t}} \\
&= \frac{a}{L}\left[\frac{1+r_0\,e^{-2jk_0 t}}{1-r_0\,e^{-2jk_0 t}} + 2j\sum_{n>0}\frac{k_0}{\gamma_n}\left(\frac{\sin(n\pi\,a/L)}{n\pi\,a/L}\right)^2\frac{1+r_n\,e^{-2\gamma_n t}}{1-r_n\,e^{-2\gamma_n t}}\right]
\end{aligned}
\tag{7}
$$

and

$$
\frac{Z_{Mb}}{Z_0} = 2j\,\frac{a}{L}\sum_{n>0}\frac{k_0}{\gamma_n}\left(\frac{\sin(n\pi\,a/L)}{n\pi\,a/L}\right)^2\frac{1+r_n\,e^{-2\gamma_n t}}{1-r_n\,e^{-2\gamma_n t}}. \tag{8}
$$

The variation of Z_{Mb} in the parameter space makes it unsuited for the definition of an end correction with a representation by regression in this case.

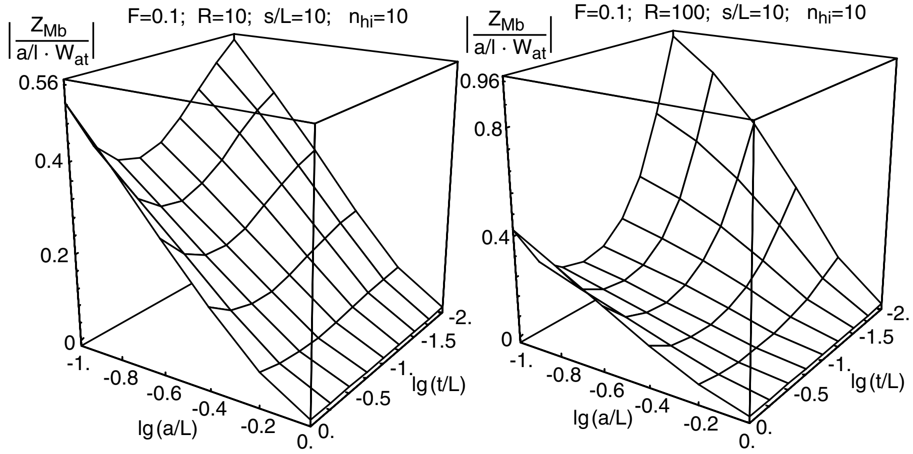

Normal sound incidence, infinite absorber layer in contact with neck plate, $t = 0$; $s = \infty$, *plane wave in the neck*

The impedance Z_{Mb} of the back orifice oscillating mass is (with quantities from *Sect. H.10*):

$$\frac{Z_{Mb}}{Z_0} = 2\,\frac{a}{L}\,\Gamma_{an} Z_{an} \sum_{n>0} \left(\frac{\sin(n\pi\, a/L)}{n\pi\, a/L}\right)^2 \frac{1}{\sqrt{(n\,\lambda_0/L)^2 + \Gamma_{an}^2}} \tag{9}$$

From the comparison with the corresponding impedance Z_{Mb0} of a free neck plate, and assuming $n \cdot \lambda_0/L \gg |\Gamma_{an}|^2$; $n \cdot \lambda_0/L \gg 1$ for all $n \geq 1$, one gets:

$$\frac{Z_{Mb}}{Z_0} \approx -j\,\Gamma_{an} Z_{an}\,\frac{Z_{Mb0}}{Z_0} = k_0 a\,\Gamma_{an} Z_{an}\,\frac{\Delta\ell}{a}. \tag{10}$$

With a higher order approximation for $\lambda_0/L \gg 1$:

$$\begin{aligned} \frac{Z_{Mb}}{Z_0} &\approx -j\,\Gamma_{an} Z_{an}\,\frac{Z_{Mb0}}{Z_0} + 2\,\frac{a}{L}\left(\frac{\sin(\pi\, a/L)}{\pi a/L}\right)^2 \Gamma_{an} Z_{an} \\ &\quad\times\left(\frac{1}{\sqrt{(\lambda_0/L)^2 + \Gamma_{an}^2}} - \frac{1}{\sqrt{(\lambda_0/L)^2 - 1}}\right) \\ &\approx k_0 a\,\Gamma_{an} Z_{an}\left[\frac{\Delta\ell}{a} + \frac{1}{\pi}\left(\frac{\sin(\pi\, a/L)}{\pi a/L}\right)^2\left(\frac{1}{\sqrt{1-(L/\lambda_0\cdot\Gamma_{an})^2}} - 1\right)\right], \end{aligned} \tag{11}$$

where $\Delta\ell/a$ is the front side orifice end correction.

Normal sound incidence, infinite absorber layer, $s = \infty$, *air gap between neck plate and porous layer*, $t > 0$ *plane wave in the neck*

The back orifice oscillating mass impedance is:

$$\frac{Z_{Mb}}{Z_0} = 2j\,\frac{a}{L}\sum_{n>0}\frac{k_0}{\gamma_n}\left(\frac{\sin(n\pi\, a/L)}{n\pi\, a/L}\right)^2 \frac{1 + r_n\, e^{-2\gamma_n t}}{1 - r_n\, e^{-2\gamma_n t}}, \tag{12}$$

and the modal reflection factors in this case are:

$$r_n = \left(1 - \frac{j}{\Gamma_{an} Z_{an}} \frac{\varepsilon_n}{\gamma_n}\right) \Big/ \left(1 + \frac{j}{\Gamma_{an} Z_{an}} \frac{\varepsilon_n}{\gamma_n}\right) \tag{13}$$

with the wave number ratio

$$\frac{\varepsilon_n}{\gamma_n} = \sqrt{\frac{(n\,\lambda_0/L)^2 + \Gamma_{an}^2}{(n\,\lambda_0/L)^2 - 1}}, \tag{14}$$

consequently:

$$\frac{1 + r_n\, e^{-2\gamma_n t}}{1 - r_n\, e^{-2\gamma_n t}} = \frac{1 + \dfrac{j}{\Gamma_{an} Z_{an}} \dfrac{\varepsilon_n}{\gamma_n} \tanh(\gamma_n t)}{\tanh(\gamma_n t) + \dfrac{j}{\Gamma_{an} Z_{an}} \dfrac{\varepsilon_n}{\gamma_n}}. \tag{15}$$

Under the condition and ensuing approximations

$$(n\,\lambda_0/L)^2 \gg \begin{cases} 1 \\ |\Gamma_{an}|^2 \end{cases} ; \frac{\varepsilon_n}{\gamma_n} \approx 1 \quad ; \quad \gamma_n t \approx k_0 t \cdot n\,\lambda_0/L = 2\pi n\ t/L, \tag{16}$$

one gets

$$\frac{1 + r_n\, e^{-2\gamma_n t}}{1 - r_n\, e^{-2\gamma_n t}} \approx \frac{1 + \dfrac{j}{\Gamma_{an} Z_{an}} \tanh(2\pi n\, t/L)}{\tanh(2\pi n\, t/L) + \dfrac{j}{\Gamma_{an} Z_{an}}} \xrightarrow[\pi t/L > 1]{} \frac{1 + \dfrac{j}{\Gamma_{an} Z_{an}}}{1 + \dfrac{j}{\Gamma_{an} Z_{an}}} = 1. \tag{17}$$

Thus for $t/L > 1/\pi$: $\dfrac{Z_{Mb}}{Z_0} \approx \dfrac{Z_{Mb0}}{Z_0}$.

An approximation of higher order is:

$$\frac{Z_{msh}}{Z_0} \xrightarrow[\substack{s \to \infty \\ \lambda_0/L \gg 1}]{} j\,k_0 a \left[\frac{\Delta\ell}{a} + \frac{1}{\pi} \left(\frac{\sin(\pi\, a/L)}{\pi\, a/L}\right)^2 \frac{\left(1 - \dfrac{j}{\Gamma_{an} Z_{an}} \sqrt{\dfrac{(\lambda_0/L)^2 + \Gamma_{an}^2}{(\lambda_0/L)^2 - 1}}\right) (1 - \tanh(2\pi\, t/L))}{\tanh(2\pi\, t/L) + \dfrac{j}{\Gamma_{an} Z_{an}} \sqrt{\dfrac{(\lambda_0/L)^2 + \Gamma_{an}^2}{(\lambda_0/L)^2 - 1}}} \right] \tag{18}$$

$$\approx j\,k_0 a \left[\frac{\Delta\ell}{a} + \frac{1}{\pi} \left(\frac{\sin(\pi\, a/L)}{\pi\, a/L}\right)^2 \frac{\left(1 - \dfrac{j}{\Gamma_{an} Z_{an}} \sqrt{1 + (\Gamma_{an}\, L/\lambda_0)^2}\right) (1 - \tanh(2\pi\, t/L))}{\tanh(2\pi\, t/L) + \dfrac{j}{\Gamma_{an} Z_{an}} \sqrt{1 + (\Gamma_{an}\, L/\lambda_0)^2}} \right].$$

H.12 Slit Resonator Array with Porous Layer on Back Orifice

► *See also:* Mechel, Vol. II, Ch. 24 (1995)

The object here is similar to that in *Sects. H.10 and H.11*, but a (possibly thin) absorber layer covers the back side orifices and allows an air space deeper in the resonator volume. This is a common method for introducing an additional loss to Helmholtz resonators.

A (stiff) plate of thickness d contains an array of parallel slits, width a, mutual distance L, each of which is backed with a resonator volume V of depth t. A porous material layer of thickness $s < t$ is in contact with the back side of the plate. The characteristic values of the layer material are Γ_a, Z_a, and in normalised form $\Gamma_{an} = \Gamma_a/k_0$; $Z_{an} = Z_a/Z_0$. If the layer becomes a cloth, wire mesh, felt, etc., the limit transition $s \to 0$ is made with its flow resistance $R = \Xi s/Z_0$ kept constant.

A normally incident plane wave with amplitude A_e is assumed.

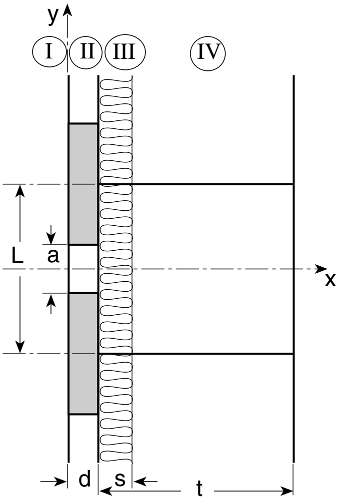

The field formulations in zones I and II are taken from *Sect. H.10*.

Field formulation in zone III:

$$
\begin{aligned}
p_{III}(x, y) &= \sum_{n\geq 0} \delta_n \left(D_n\, e^{-\varepsilon_n x} + E_n\, e^{+\varepsilon_n x}\right) \cos(\eta_n y)\,, \\
Z_0\, v_{IIIx}(x, y) &= \frac{k_0 Z_0}{\Gamma_a Z_a} \sum_{n\geq 0} \delta_n \frac{\varepsilon_n}{k_0} \left(D_n\, e^{-\varepsilon_n x} - E_n\, e^{+\varepsilon_n x}\right) \cos(\eta_n y)
\end{aligned}
\tag{1}
$$

Field formulation in zone IV:

$$
\begin{aligned}
p_{IV}(x, y) &= \sum_{n\geq 0} \delta_n F_n \cosh(\gamma_n(x-d-t)) \cdot \cos(\eta_n y)\,, \\
Z_0 v_{IVx}(x, y) &= j \sum_{n\geq 0} \delta_n \frac{\gamma_n}{k_0} F_n \sinh(\gamma_n(x-d-t)) \cdot \cos(\eta_n y)
\end{aligned}
\tag{2}
$$

with wave numbers and propagation constants

$$
\eta_n = 2n\pi/L \quad ; \quad \gamma_n = \sqrt{\eta_n^2 - k_0^2} \quad ; \quad \gamma_0 = j\,k_0\,,
$$

$$
\kappa_m = \begin{cases} \sqrt{k_0^2 - (2m\pi\, a/L)^2}\,; & m \leq m_g \\ -j\sqrt{(2m\pi\, a/L)^2 - k_0^2}\,; & m > m_g \end{cases} \quad ; \quad m_g = \mathrm{INT}(a/\lambda_0)\,; \quad \kappa_0 = k_0\,,
\tag{3}
$$

$$
\varepsilon_n = \sqrt{\eta_n^2 + \Gamma_a^2}; \quad \varepsilon_0 = \Gamma_a\,.
$$

The limit order m_g separates cut-on and cut-off (i.e. radiating and non-radiating) spatial harmonics.

Modal reflection factors at the back surface of the porous layer are:

$$r_n = \frac{\dfrac{j}{\Gamma_{an} Z_{an}} \dfrac{\varepsilon_n}{\gamma_n} \coth(\gamma_n(t-s)) - 1}{\dfrac{j}{\Gamma_{an} Z_{an}} \dfrac{\varepsilon_n}{\gamma_n} \coth(\gamma_n(t-s)) + 1}. \tag{4}$$

The auxiliary amplitudes $X_{n\pm}, Y_{n\pm}$ are defined as in Sect. H.10. X_{n-} and Y_{n-} are solutions of the coupled system of equations:

$$\sum_{n=0}^{\infty} a_{m,n} X_{n-} + c_m Y_{m-} = b_m \quad ; \quad \sum_{n=0}^{\infty} d_{m,n} Y_{n-} + c_m X_{m-} = 0 \tag{5}$$

with the coefficients

$$\begin{aligned} a_{m,n} &= j \frac{a}{L} \frac{\kappa_n}{k_0} \sum_{i \ge 0} \delta_i \frac{k_0}{\gamma_i} S_{m,i} S_{n,i} + \frac{\delta_{m,n}}{\delta_m} \frac{1+e^{-2j\kappa_m d}}{1-e^{-2j\kappa_m d}} \\ d_{m,n} &= \frac{a}{L} \frac{\Gamma_a Z_a}{k_0 Z_0} \frac{\kappa_n}{k_0} \sum_{i \ge 0} \delta_i \frac{k_0}{\varepsilon_i} S_{m,i} S_{n,i} \frac{1+r_i e^{-2\varepsilon_i s}}{1-r_i e^{-2\varepsilon_i s}} + \frac{\delta_{m,n}}{\delta_m} \frac{1+e^{-2j\kappa_m d}}{1-e^{-2j\kappa_m d}} \\ c_m &= \frac{-2}{\delta_m} \frac{e^{-j\kappa_m d}}{1-e^{-2j\kappa_m d}} \quad ; \quad b_m = 2\,\delta_{0,m} \end{aligned} \tag{6}$$

$$\text{where} \quad \delta_m = \begin{cases} 1\,; & m=0 \\ 2\,; & m>0 \end{cases} \quad ; \quad \delta_{m,n} = \begin{cases} 1\,; & m=n \\ 0\,; & m \ne n \end{cases} \tag{7}$$

and $S_{m,n}$ is found in Sect. H.10.

The field term amplitudes follow from the solutions X_{n-}, Y_{n-} as:

$$A_n = -j \frac{k_0}{\gamma_n} \left[\frac{a}{L} \sum_{m \ge 0} \frac{\kappa_m}{k_0} S_{m,n} \cdot X_{m-} - \delta_{0,n} A_e \right], \tag{8}$$

$$\begin{aligned} B_m &= \frac{1}{2}(X_{m+} + X_{m-}) = \frac{1}{2}(Y_{m+} + Y_{m-})\, e^{+j\kappa_m d}, \\ C_m &= \frac{1}{2}(X_{m+} - X_{m-}) = \frac{1}{2}(Y_{m+} - Y_{m-})\, e^{-j\kappa_m d}, \end{aligned} \tag{9}$$

$$\begin{aligned} D_n &= \frac{a}{L} \frac{\Gamma_a Z_a}{k_0 Z_0} \frac{k_0}{\varepsilon_n} \frac{e^{\varepsilon_n d}}{1 - e^{-\varepsilon_n s}\,[1 + r_n e^{-2\varepsilon_n s} - e^{-\varepsilon_n s}]} \sum_{m \ge 0} \frac{\kappa_m}{k_0} S_{m,n} \cdot Y_{m-}, \\ E_n &= D_n e^{-2\varepsilon_n (d+s)}\, [1 - e^{\varepsilon_n s} + r_n e^{-\varepsilon_n s}], \\ F_n &= \frac{1}{\cosh(\gamma_n (t-s))} [D_n e^{-\varepsilon_n (d+s)} + E_n e^{+\varepsilon_n (d+s)}]. \end{aligned} \tag{10}$$

The back orifice impedance Z_{sb} becomes:

$$\frac{Z_{sb}}{Z_0} = \frac{a}{L} Z_{an} \left[\frac{1 + r_0\, e^{-2\Gamma_a s}}{1 - r_0\, e^{-2\Gamma_a s}} + 2\Gamma_{an} \sum_{i>0} \left(\frac{\sin(i\pi\, a/L)}{i\pi\, a/L} \right)^2 \frac{k_0}{\varepsilon_i} \frac{1 + r_i\, e^{-2\varepsilon_i s}}{1 - r_i\, e^{-2\varepsilon_i s}} \right], \tag{11}$$

and the impedance Z_{Mb} of the oscillating mass at the back orifice becomes:

$$\frac{Z_{Mb}}{Z_0} = 2\frac{a}{L} \Gamma_{an} Z_{an} \sum_{i>0} \left(\frac{\sin(i\pi\, a/L)}{i\pi\, a/L} \right)^2 \frac{k_0}{\varepsilon_i} \frac{1 + r_i\, e^{-2\varepsilon_i s}}{1 - r_i\, e^{-2\varepsilon_i s}}. \tag{12}$$

In the limit $s \to 0$ for thin orifice covers:

$$\frac{Z_{sb}}{Z_0} = \frac{a}{L} \left[R - j\, \cot(k_0 t) + 2j \sum_{i>0} \left(\frac{\sin(i\pi\, a/L)}{i\pi\, a/L} \right)^2 \frac{k_0}{\gamma_i} \coth(\gamma_i t) \right]. \tag{13}$$

This is the value for an empty resonator volume except the term R for the flow resistance of the thin cover. If R has no reactive component, the tuning of the resonator is not changed either by the additional resistance or by the end correction of the interior orifice.

If the porous foil can freely oscillate, the substitution $R \to R_{eff}$ should be made, with

$$R_{eff} = \frac{1}{Z_0} \frac{j\omega m_f \cdot \Xi s}{j\omega m_f + \Xi s} = \frac{j\, k_0 s \cdot \rho_f/\rho_0 \cdot R}{j\, k_0 s \cdot \rho_f/\rho_0 + R}, \tag{14}$$

where m_f is the surface mass density of the foil, and ρ_f the density of the foil material.

H.13 Slit Resonator Array with Porous Layer on Front Orifice

► *See also:* Mechel, Vol. II, Ch. 24 (1995)

Sections H.10–H.12 deal with additional damping of Helmholtz resonators with porous layers. This section considers an arrangement of the porous layer which gives the possibility of combining the broad-band absorption of a porous layer with the peak absorption of a resonator.

In contrast to the previous sections, the porous layer now is placed on the front side of the resonator array.

A plane wave with amplitude A_e is normally incident.

The characteristic values of the layer material are Γ_a, Z_a, and in normalised form $\Gamma_{an} = \Gamma_a/k_0$; $Z_{an} = Z_a/Z_0$. If the layer is a cloth, wire mesh, felt, etc., the limit transition $s \to 0$ is made with its flow resistance $R = \Xi s/Z_0$ kept constant.

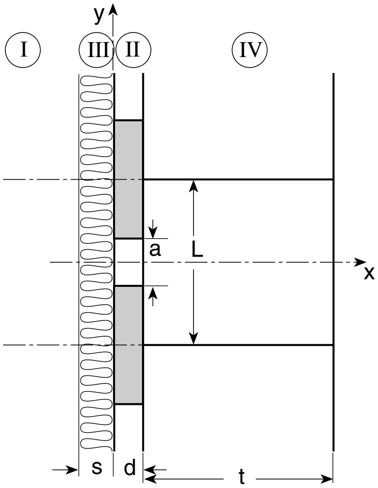

The field formulations in the zones are as follows:

Zone I:

$$\begin{aligned} p_I(x,y) &= A_e\, e^{-jk_0 x} + \sum_{n\geq 0} \delta_n A_n\, e^{\gamma_n x}\, \cos(\eta_n y)\ , \\ Z_0 v_{Ix}(x,y) &= A_e\, e^{-jk_0 x} + j \sum_{n\geq 0} \delta_n \frac{\gamma_n}{k_0} A_n\, e^{\gamma_n x}\, \cos(\eta_n y)\ . \end{aligned} \tag{1}$$

Zone III:

$$\begin{aligned} p_{III}(x,y) &= \sum_{n\geq 0} \delta_n (D_n\, e^{-\varepsilon_n x} + E_n\, e^{+\varepsilon_n x})\ \cos(\eta_n y)\ , \\ Z_0 v_{IIIx}(x,y) &= \frac{k_0 Z_0}{\Gamma_a Z_a} \sum_{n\geq 0} \delta_n \frac{\varepsilon_n}{k_0} (D_n\, e^{-\varepsilon_n x} - E_n\, e^{+\varepsilon_n x})\ \cos(\eta_n y)\ . \end{aligned} \tag{2}$$

Zone II:

$$\begin{aligned} p_{II}(x,y) &= \sum_{m\geq 0} (B_m\, e^{-j\kappa_m x} + C_m\, e^{+j\kappa_m x})\ \cos(2m\pi\, y/a)\ , \\ Z_0 v_{IIx}(x,y) &= \sum_{m\geq 0} \frac{\kappa_m}{k_0} (B_m\, e^{-j\kappa_m x} - C_m\, e^{+j\kappa_m x})\ \cos(2m\pi\, y/a)\ . \end{aligned} \tag{3}$$

Zone IV:

$$\begin{aligned} p_{IV}(x,y) &= \sum_{n\geq 0} \delta_n F_n\ \cosh(\gamma_n (x-d-t))\ \cos(\eta_n y)\ , \\ Z_0 v_{IVx}(x,y) &= j \sum_{n\geq 0} \delta_n \frac{\gamma_n}{k_0} F_n\ \sinh(\gamma_n (x-d-t))\ \cos(\eta_n y)\ . \end{aligned} \tag{4}$$

The wave numbers and propagation constants are:

$$\eta_n = 2n\pi/L; \quad \gamma_n = \sqrt{\eta_n^2 - k_0^2}; \quad \gamma_0 = j\,k_0\,,$$

$$\kappa_m = \begin{cases} \sqrt{k_0^2 - (2m\pi\,a/L)^2}\,; & m \le m_g \\ -j\sqrt{(2m\pi\,a/L)^2 - k_0^2}; & m > m_g \end{cases} \;;\quad m_g = \mathrm{INT}(a/\lambda_0); \quad \kappa_0 = k_0\,, \tag{5}$$

$$\varepsilon_n = \sqrt{\eta_n^2 + \Gamma_a^2}; \quad \varepsilon_0 = \Gamma_a\,.$$

The boundary conditions give the set of equations for the mode amplitudes:

$$\begin{aligned}
&\delta_{0,n}A_e\, e^{+jk_0 s} + j\,\frac{\gamma_n}{k_0}\,A_n\, e^{-\gamma_n s} = \frac{k_0 Z_0}{\Gamma_a Z_a}\,\frac{\varepsilon_n}{k_0}\,(D_n\, e^{+\varepsilon_n s} - E_n\, e^{-\varepsilon_n s})\,,\\
&\frac{k_0 Z_0}{\Gamma_a Z_a}\,\frac{\varepsilon_n}{k_0}\,(D_n - E_n) = \frac{a}{L}\sum_{m\ge 0}\frac{\kappa_m}{k_0}\,S_{m,n}\,(B_m - C_m)\,,\\
&\frac{\gamma_n}{k_0}\,F_n\,\sinh(\gamma_n t) = j\frac{a}{L}\sum_{m\ge 0}\frac{\kappa_m}{k_0}\,S_{m,n}\,(B_m\, e^{-j\kappa_m d} - C_m\, e^{+j\kappa_m d})\,,\\
&\delta_{0,n}A_e\, e^{+jk_0 s} + A_n\, e^{-\gamma_n s} = D_n\, e^{+\varepsilon_n s} + E_n\, e^{-\varepsilon_n s}\,,\\
&\frac{1}{\delta_m}\,(B_m + C_m) = \sum_{n\ge 0}\delta_n\, S_{m,n}\,(D_n + E_n)\,,\\
&\frac{1}{\delta_m}\,(B_m\, e^{-j\kappa_m d} + C_m\, e^{+j\kappa_m d}) = \sum_{n\ge 0}\delta_n\, S_{m,n}\, F_n\,\cosh(\gamma_n t)
\end{aligned} \tag{6}$$

with the mode coupling coefficients:

$$\begin{aligned}
S_{m,n} :&= \frac{1}{a}\int_{-a/2}^{+a/2}\cos(2m\pi\,y/a)\,\cos(\eta_n y)\,dy\\
&= \frac{1}{2}\left[\frac{\sin(m\pi - n\pi\,a/L)}{m\pi - n\pi\,a/L} + \frac{\sin(m\pi + n\pi\,a/L)}{m\pi + n\pi\,a/L}\right]; \quad m,n > 0\\
&= \frac{-(-1)^m}{\pi}\,\frac{n\,a/L}{m^2 - (n\,a/L)^2}\,\sin(n\pi\,a/L); \quad m,n > 0\,; \quad m \ne n\,a/L\\
&= \frac{\sin(n\pi\,a/L)}{n\pi\,a/L}; \quad m = 0\,; \quad n \ge 0\\
&= 0; \quad m > 0\,; \quad n = 0\\
&= 1; \quad m = n = 0\\
&= \frac{1}{2}; \quad m = n\,a/L \ne 0.
\end{aligned} \tag{7}$$

Henceforth *only plane waves* are supposed to exist in the necks, i.e. $B_{m>0} = C_{m>0} = 0$.

The equations of the boundary conditions simplify to:

$$\delta_{0,n}A_e\,e^{+jk_0 s}+j\,\frac{\gamma_n}{k_0}\,A_n\,e^{-\gamma_n s}=\frac{k_0Z_0}{\Gamma_aZ_a}\,\frac{\varepsilon_n}{k_0}\,\left(D_n\,e^{+\varepsilon_n s}-E_n\,e^{-\varepsilon_n s}\right)\;, \tag{8}$$

$$\frac{k_0Z_0}{\Gamma_aZ_a}\,\frac{\varepsilon_n}{k_0}\,(D_n-E_n)=\frac{a}{L}\,S_{0,n}\,(B_0-C_0)\;,$$

$$\frac{\gamma_n}{k_0}\,F_n\,\sinh(\gamma_n t)=j\frac{a}{L}\,S_{0,n}\,(B_0\,e^{-jk_0 d}-C_0\,e^{+jk_0 d})\;,$$

$$\delta_{0,n}A_e\,e^{+jk_0 s}+A_n\,e^{-\gamma_n s}=D_n\,e^{+\varepsilon_n s}+E_n\,e^{-\varepsilon_n s}\;, \tag{9}$$

$$B_0+C_0=\sum_{n>0}\delta_n\,S_{0,n}\,(D_n+E_n)\;,$$

$$B_0\,e^{-jk_0 d}+C_0\,e^{+jk_0 d}=\sum_{n\ge 0}\delta_n\,S_{0,n}\,F_n\,\cosh(\gamma_n t)$$

$$\text{with}\qquad S_{0,n}=\sin(n\pi a/L)/(n\pi a/L). \tag{10}$$

The auxiliary amplitudes $X_{0\pm}, Y_{0\pm}$ are introduced:

$$X_{0\pm}=:B_0\pm C_0;\qquad Y_{0\pm}=:B_0\,e^{-jk_0 d}\pm C_0\,e^{+jk_0 d} \tag{11}$$

with intrinsic relations

$$\begin{aligned}X_{0+}&=X_{0-}\,\frac{1+e^{-2jk_0 d}}{1-e^{-2jk_0 d}}-2Y_{0-}\,\frac{e^{-jk_0 d}}{1-e^{-2jk_0 d}}\;,\\ Y_{0+}&=2\,X_{0-}\,\frac{e^{-jk_0 d}}{1-e^{-2jk_0 d}}-Y_{0-}\,\frac{1+e^{-2jk_0 d}}{1-e^{-2jk_0 d}}\end{aligned} \tag{12}$$

and

$$\begin{aligned}B_0&=\frac{1}{2}\,(X_{0+}+X_{0-})=\frac{1}{2}\,(Y_{0+}+Y_{0-})\,e^{+jk_0 d}\;,\\ C_0&=\frac{1}{2}\,(X_{0+}-X_{0-})=\frac{1}{2}\,(Y_{0+}-Y_{0-})\,e^{-jk_0 d}.\end{aligned} \tag{13}$$

X_{0-} and Y_{0-} are solutions of the two equations:

$$Y_{0-}\left[-\cot(k_0 d)+\frac{a}{L}\sum_{n\ge 0}\frac{\delta_n\,S_{0,n}^2}{\gamma_n/k_0}\;\coth(\gamma_n t)\right]+\frac{1}{\sin(k_0 d)}\,X_{0-}=0 \tag{14}$$

and

$$\begin{aligned}&Y_{0-}\frac{j}{\sin(k_0 d)}+X_{0-}\left[-j\,\cot(k_0 d)+\frac{a}{L}\,\Gamma_{an}Z_{an}\sum_{n\ge 0}\frac{\delta_n\,S_{0,n}^2}{\varepsilon_n/k_0}\;\coth(\varepsilon_n s)\right.\\ &\left.+\frac{j\,\gamma_n/k_0}{\sinh^2(\varepsilon_n s)\left(\dfrac{1}{\Gamma_{an}Z_{an}}\,\dfrac{\varepsilon_n}{k_0}-j\,\dfrac{\gamma_n}{k_0}\,\coth(\varepsilon_n s)\right)}\right]=\frac{2\,Z_{an}\,e^{jk_0 s}}{\sinh(\Gamma_a s)+Z_{an}\,\cosh(\Gamma_a s)}.\end{aligned} \tag{15}$$

With the solutions, the amplitudes other than B_0 and C_0 may be evaluated from the boundary conditions. The average input impedance Z of the arrangement will be given by:

$$\begin{aligned}\frac{Z}{Z_0}=\frac{\langle p_{III}(-s,y)\rangle_L}{Z_0\,\langle v_{IIIx}(-s,y)\rangle_L}&=Z_{an}\,\frac{2\,e^{jk_0s}\,\cosh(\Gamma_a s)-a/L\cdot X_{0-}}{2\,e^{jk_0s}\,\sinh(\Gamma_a s)+a/L\,Z_{an}\cdot X_{0-}}\\&=Z_{an}\,\coth(\Gamma_a s)-\frac{a/L\,Z_{an}\,(1+Z_{an}\,\coth(\Gamma_a s))}{2\,e^{jk_0s}\,\sinh(\Gamma_a s)+a/L\,Z_{an}\cdot X_{0-}}\cdot X_{0-}.\end{aligned}\tag{16}$$

The first term in the last line is the input impedance (normalised) of the porous layer when it has a hard back; therefore the second term is a correction due to the backing by the resonator array.

H.14 Array of Slit Resonators with Subdivided Neck Plate

► *See also:* Mechel, Vol. II, Ch. 26 (1995)

The intention with arrangements as described in this (and the following) section may be twofold: first introduce new, differently tuned resonances, then introduce losses.

The object is an array of Helmholtz resonators with slit-shaped necks. The neck plate is subdivided, allowing a narrow gap between the parts. The graphs show two possibilities of realisation.

The plate parts are supposed to be stiff in this section.

The average surface impedance Z or the average surface admittance G = 1/Z of the arrangement shall be evaluated with the method of equivalent networks.

The equivalent network is shown in the third graph in a p/q-analogy (q = volume flow; the circuit elements are admittances).

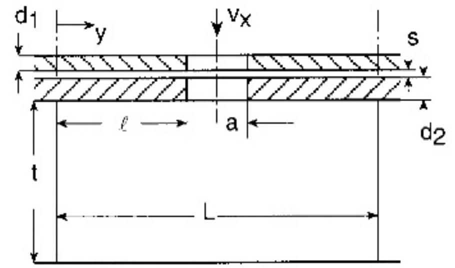

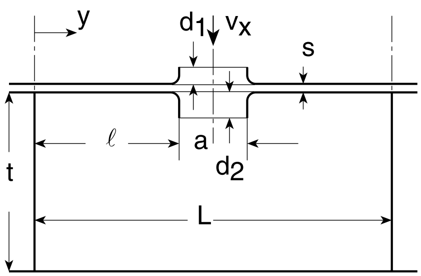

$\Delta\ell_f$	=	front side end correction;
$\Delta\ell_b$	=	end correction of neck orifice towards volume;
Z_1	=	entrance impedance of the first neck;
G_2	=	admittance of the second neck and air gap in parallel;
G_{f2}	=	entrance admittance of second neck;
Z_{sb}	=	output impedance of back orifice of second neck;
G_y	=	entrance admittance of air gap

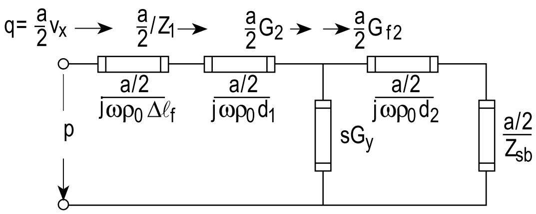

The chain of equations is (G is evaluated without radiation resistance):

$$\begin{aligned}
Z_0G &= \frac{a/L}{j\,k_0a\,\dfrac{\Delta\ell_f}{a}+\dfrac{Z_1}{Z_0}} \quad ; \quad \frac{Z_1}{Z_0}=\frac{1+j\,\tan(k_0d_1)\cdot Z_0G_2}{j\,\tan(k_0d_1)+Z_0G_2};\\
Z_0G_2 &= Z_0G_{f2}+2\,\frac{s}{a}\,Z_0G_y \quad ; \quad Z_0G_{f2}=\frac{1+j\,\tan(k_0d_2)\cdot Z_{sb}/Z_0}{j\,\tan(k_0d_2)+Z_{sb}/Z_0};\\
\frac{Z_{sb}}{Z_0} &= \frac{-j\,a/L}{\tan(k_0t)}+j\,k_0a\,\frac{\Delta\ell_b}{a}+R_{res} \quad ; \quad G_y=\frac{1}{Z_y}\,\tanh(\Gamma_y\ell).
\end{aligned} \tag{1}$$

Here $\Delta\ell_f$ and $\Delta\ell_b$ may be taken from a previous section on end corrections in a resonator array; R_{res} denotes a possibly added (normalised) resistance representing additional losses in the back side orifice and/or in the resonator volume. Γ_y, Z_y are the characteristic propagation constant and wave impedance, respectively, in a flat capillary of width s (see sections on capillaries in *Ch. J*, "Duct Acoustics").

If a poro-elastic foil (see later sections on foils) with effective surface mass density m_{eff} tightly covers the entrance orifice of the second neck, and if the air gap length ℓ is different on both sides of the neck, $\ell \to \ell_1, \ell_2$, then evaluate G_{f2} and G_2 from:

$$\begin{aligned}
\frac{1}{Z_0G_{f2}} &= j\,\frac{\omega\, m_{eff}}{Z_0}+\frac{j\,\tan(k_0d_2)+Z_{sb}/Z_0}{1+j\,\tan(k_0d_2)\cdot Z_{sb}/Z_0},\\
Z_0G_2 &= Z_0G_{f2}+\frac{s}{a}\,(Z_0G_{y1}+Z_0G_{y2}).
\end{aligned} \tag{2}$$

H.15 Array of Slit Resonators with Subdivided Neck Plate and Floating Foil in the Gap

► *See also:* Mechel, Vol. II, Ch. 26 (1995)

The object of this section is similar to that in the previous *Sect. H.14*, but the analysis is rather different. A freely floating poro-elastic foil (see later sections on foils) with effective surface mass density m_{eff} is placed in the air gap between the parts of the neck plate. From a technical point of view this is one way of protecting mechanical sensible foils; from an analytical point of view, sound transmission through the foil over all of its length must be considered. The analysis assumes (possibly different) air gap thicknesses s_1, s_2 in front of and behind the foil. The necks have the shown shapes only for analytical reasons: they indicate that no shift of the co-ordinates in front of and behind the neck plate is expressively considered.

Schematic arrangement:

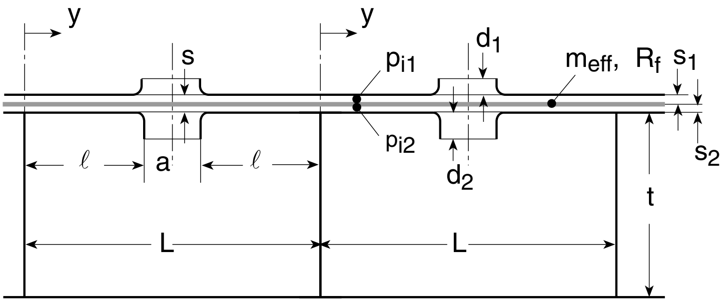

Schematic network:

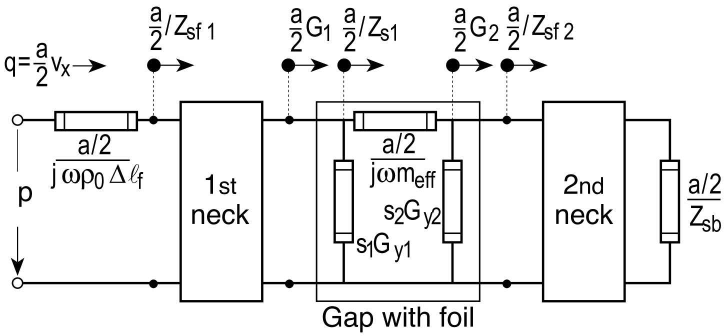

$\Delta\ell_f$	=	front orifice end correction;
$\Delta\ell_b$	=	end correction of orifice towards volume;
Z_{sf1}	=	entrance impedance of first neck;
Z_{sf2}	=	entrance impedance of second neck;
Z_{sb}	=	exit impedance of second neck;
G_1	=	admittance at exit of first neck;
G_2	=	load admittance of foil;
G_{y1}, G_{y2}	=	input admittances of air gaps

Detail in the air gaps:

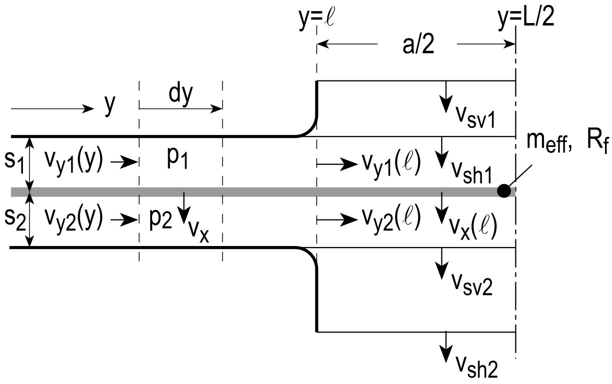

The chain of equations for the average surface admittance $G = 1/Z$ of the arrangement is, with the assumption that sound transmission through the foil in the gaps can be neglected, as follows:

$$\begin{aligned}
\frac{1}{Z_0 G} &= (jk_0 a \cdot \Delta\ell_f/a + Z_{sf1}/Z_0) \cdot L/a \;, \\
\frac{Z_{sf1}}{Z_0} &= \frac{1 + j\,\tan(k_0 d_1) \cdot Z_0 G_1}{j\,\tan(k_0 d_1) + Z_0 G_1} \;, \\
Z_0 G_1 &= \frac{Z_0}{Z_{s1}} + 2\,\frac{s_1}{a} \cdot Z_0 G_{y1} \;, \\
\frac{Z_{s1}}{Z_0} &= \frac{j\omega\, m_{eff}}{Z_0} + \frac{1}{Z_0 G_2} \;, \\
Z_0 G_2 &= \frac{Z_0}{Z_{sf2}} + 2\,\frac{s_2}{a} \cdot Z_0 G_{y2} \;, \\
\frac{Z_{sf2}}{Z_0} &= \frac{j\,\tan(k_0 d_2) + Z_{sh}/Z_0}{1 + j\,\tan(k_0 d_2) \cdot Z_{sh}/Z_0} \;, \\
\frac{Z_{sb}}{Z_0} &= \frac{-j\,a/L}{\tan(k_0 t)} + j\,k_0 a \cdot \Delta\ell_b/a + R_{res} \;,
\end{aligned} \tag{1}$$

$$G_{y1} = \frac{1}{Z_{y1}}\,\tanh(\Gamma_{y1}\ell) \quad ; \quad G_{y2} = \frac{1}{Z_{y2}}\,\tanh(\Gamma_{y2}\ell). \tag{2}$$

Γ_{y1}, Γ_{y2}	=	capillary propagation constants in the gaps;
Z_{y1}, Z_{y2}	=	capillary wave impedance in the gaps;
$\Delta\ell_f/a$	=	end correction of front side orifice;
$\Delta\ell_b/a$	=	end correction of orifice towards resonator;
m_{eff}	=	effective surface mass density of foil;
R_{res}	=	normalised resistance for possible additional loss in the volume

The two gaps on each side in fact are coupled wave guides; the differential equations for which are:

$$
\begin{aligned}
&p_1 - p_2 = j\omega m \cdot v_x \ , \\
&-\frac{\partial v_{y1}}{\partial y} - \frac{v_x}{s_1} = j\omega C_{eff,1} \cdot p_1 \quad ; \quad -\frac{\partial v_{y2}}{\partial y} + \frac{v_x}{s_2} = j\omega C_{eff,2} \cdot p_2 \ , \\
&-\frac{\partial p_1}{\partial y} = j\omega \rho_{eff} \cdot v_{y1} \quad ; \quad -\frac{\partial p_2}{\partial y} = j\omega \rho_{eff} \cdot v_{y2} ,
\end{aligned}
\tag{3}
$$

where the effective air densities $\rho_{eff,i}$ and air compressibilities $C_{eff,i}$ follow from the capillary propagation constants $\Gamma_{y,i}$ and wave impedances $Z_{y,i} (i = 1, 2)$ by:

$$
\frac{\Gamma_{y,i}}{k_0} = j\sqrt{\frac{\rho_{eff,i}}{\rho_0} \cdot \frac{C_{eff,i}}{C_0}} \quad ; \quad \frac{Z_{y,i}}{Z_0} = \sqrt{\frac{\rho_{eff,i}}{\rho_0} \bigg/ \frac{C_{eff,i}}{C_0}} . \tag{4}
$$

One gets two coupled, inhomogeneous wave equations for the fields in the air gaps:

$$
\begin{aligned}
&\frac{\partial^2 p_1}{\partial y^2} + \left[\omega^2 \rho_{eff,1} C_{eff,1} - \frac{\rho_{eff,1}}{m s_1}\right] \cdot p_1 = -\frac{\rho_{eff,1}}{m s_1} \cdot p_2 \ , \\
&\frac{\partial^2 p_2}{\partial y^2} + \left[\omega^2 \rho_{eff,2} C_{eff,2} - \frac{\rho_{eff,2}}{m s_2}\right] \cdot p_2 = -\frac{\rho_{eff,2}}{m s_2} \cdot p_1
\end{aligned}
\tag{5}
$$

with solutions satisfying the symmetry conditions

$$
p_i = A_i \cdot \cosh(\Gamma_a y) + B_i \cdot \cosh(\Gamma_b y) \quad ; \quad i = 1, 2 \ . \tag{6}
$$

The characteristic equation of the system has the solutions:

$$
\Gamma_a^2 = \Gamma_b^2 = \frac{\Gamma_{y1}^2 \dfrac{\rho_{eff,2}}{m\, s_2} - \Gamma_{y2}^2 \dfrac{\rho_{eff,1}}{m\, s_1}}{\dfrac{\rho_{eff,2}}{m\, s_2} - \dfrac{\rho_{eff,1}}{m\, s_1}} := \Gamma^2 . \tag{7}
$$

Therefore the gap fields are:

$$
p_i(y) = A_i \cdot \cosh(\Gamma y) \quad ; \quad v_{yi}(y) = -A_i \frac{\Gamma}{j\omega \rho_{eff,i}} \cdot \sinh(\Gamma y) \quad ; \quad i = 1,\ 2, \tag{8}
$$

and the gap input admittances are:

$$
G_{yi} = -\frac{v_{yi}(\ell)}{p_i(\ell)} = \frac{\Gamma}{j\omega \rho_{eff,i}} \tanh(\Gamma \ell). \tag{9}
$$

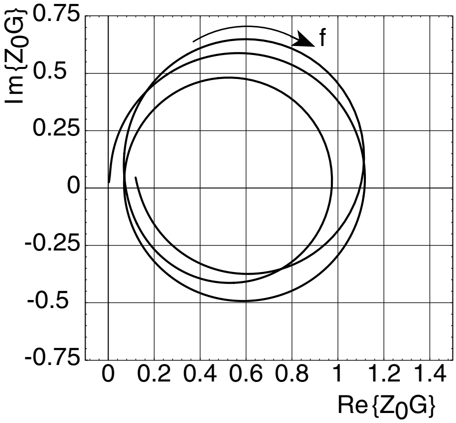

Normalised surface admittance Z_0G of a slit resonator array with subdivided neck plate and a floating poro-elastic foil in the gap, for increasing frequency f. Parameters: $R_f = 0.35$; $fcr \cdot d = 12[Hz \cdot m]$; $\rho_f = 2750[kg/m^2]$; $d_f = 0.0001[m]$; $L = 0.05[m]$; $a = 0.02[m]$; $s = 0.002[m]$; $d = 0.02[m]$; $t = 0.1[m]$; $d_1/d = 0.5$; $s_1/s = 0.45$; $\Xi = 125[Pa \cdot s/m^2]$

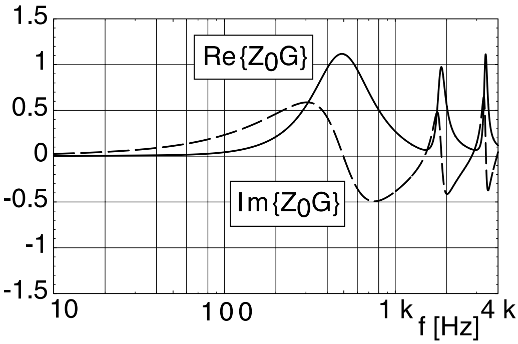

Frequency response curves of the real and imaginary parts of Z_0G for the arrangement from above

The load admittance G_1 of the back orifice of the first neck (which is needed in the second line of the chain of equations) follows as:

$$Z_0G_1 = j\,\frac{Z_0}{\omega m_{eff}}\left[\frac{1}{1-\left(\dfrac{\omega}{\omega_2}\right)^2 + j\,\dfrac{\omega m_{eff}}{Z_0}\,(Z_0G_{sv2} + 2\,\dfrac{s_2}{a}G_{y2})} - \left(1-\left(\frac{\omega}{\omega_1}\right)^2 + j\,\frac{\omega m_{eff}}{Z_0}\cdot 2\,\frac{s_1}{a}G_{y1}\right)\right]. \tag{10}$$

If different gap lengths ℓ_1, ℓ_2 are used on opposite sides of the neck, substitute

$$2\,\frac{s_i}{a}\,Z_0 G_{yi}(\ell) \to \frac{s_i}{a}\,(Z_0 G_{yi}(\ell_1) + Z_0 G_{yi}(\ell_2)); \quad i = 1,\ 2. \tag{11}$$

In the parameters of the above example are $s = s_1 + s_2$; $d = d_1 + d_2$; R_f = normalised flow resistance of the poro-elastic foil; d_f = foil thickness; ρ_f = foil material density (the foil is of aluminium); $fcr \cdot d$ = product of foil thickness and critical frequency.

H.16 Array of Slit Resonators Covered with a Foil

▸ *See also:* Mechel, Vol. II, Ch. 26 (1995)

An array of slit resonators is covered with a poro-elastic foil of effective surface mass density m_{eff} (for ease of writing also $m_{eff} \to m$). The width of the air gaps between the foil and the neck plate may be different on both sides of a neck and also the lengths of the gaps: $s = (s_1 + s_2)/2$; $L = \ell_1 + \ell_2 + a$.

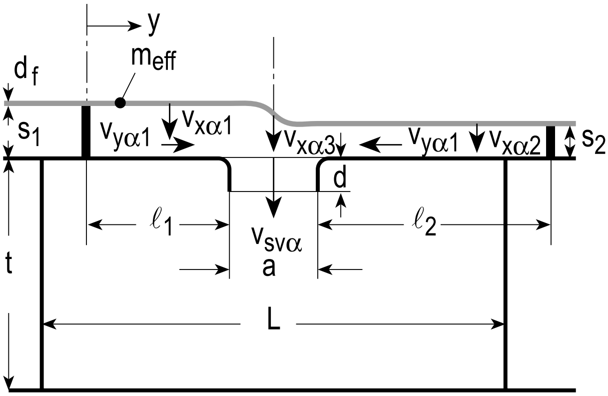

The resonator neck may be excited in three ways:

(1) via the left-hand-side foil ($\alpha = 1$);

(2) via the right-hand-side foil ($\alpha = 2$);

(3) via the foil in the orifice range ($\alpha = 3$).

A separate index $\beta = 1, 2, 3$ indicates the foil ranges (left, right, centre). The three ways of excitation can be considered as three sources. According to Helmholtz's source superposition theorem, the general state is a superposition of three states in which only one source is active and the other two are short-circuited. The following graph shows a schematic p/q-network of the arrangement with the three sources.

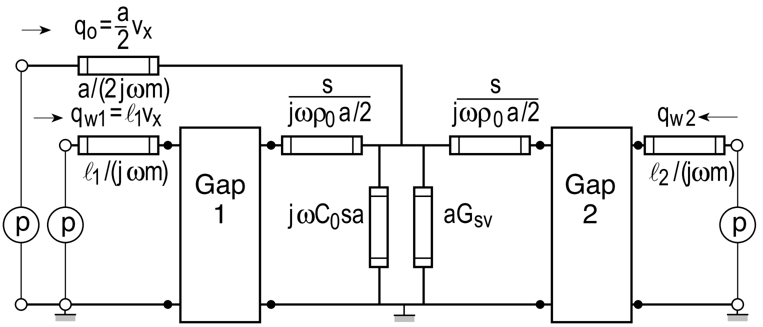

Let $\rho_{eff,\beta}$, $C_{eff,\beta}$ be the effective air density and air compressibility in a flat capillary with hard and rigid walls having lateral dimension s_β; they can be evaluated from the capillary propagation constant $\Gamma_{y\beta}$ and wave impedance $Z_{y\beta}$ (see sections on sound in capillaries in *Ch. J*, "Duct Acoustics") by:

$$\Gamma_{y\beta}^2 = -\omega^2 \rho_{eff,\beta} C_{eff,\beta} \quad ; \quad j\omega \rho_{eff,\beta} = \Gamma_{y\beta} Z_{y\beta}. \tag{1}$$

The supports of the foil in the above sketch must not be solid supports; their acoustical role can be played by positions of sound field symmetry.

The differential equations in the gaps are:

$$\begin{aligned} &-\frac{\partial v_{y\alpha\beta}}{\partial y} + \frac{v_{x\alpha\beta}}{s_\beta} = j\omega C_{eff,\beta} \cdot p_{i\alpha\beta} \ , \\ &-\frac{\partial p_{i\alpha\beta}}{\partial y} = j\omega\rho_{eff,\beta} \cdot v_{y\alpha\beta} \quad ; \quad \alpha = 1,\ 2,\ 3 \quad ; \quad \beta = 1,\ 2 \ ; \ i = 1,\ 2. \end{aligned} \tag{2}$$

They lead to the wave equations

$$\begin{aligned} &\frac{\partial^2 p_{i\alpha\beta}}{\partial y^2} + \omega^2 \rho_{eff,\beta} C_{eff,\beta} \cdot p_{i\alpha\beta} + j\omega\rho_{eff,\beta} \frac{v_{x\alpha\beta}}{s_\beta} \\ &\qquad = \frac{\partial^2 p_{i\alpha\beta}}{\partial y^2} - \Gamma_{y\beta}^2 \cdot p_{i\alpha\beta} + j\omega\rho_{eff,\beta} \frac{v_{x\alpha\beta}}{s_\beta} = 0. \end{aligned} \tag{3}$$

Or, with the Kronecker symbol $\delta_{\alpha,\beta}$:

$$\begin{aligned} &\delta_{\alpha,\beta} \cdot p - p_{i\alpha\beta} = j\omega m_{eff} \cdot v_{x\alpha\beta} \quad ; \quad v_{x\alpha\beta} = \frac{1}{j\omega m_{eff}} (\delta_{\alpha,\beta} \cdot p - p_{i\alpha\beta}) \ , \\ &\frac{\partial^2 p_{i\alpha\beta}}{\partial y^2} - \left(\Gamma_{y\beta}^2 + \frac{\rho_{eff,\beta}}{m_{eff}\, s_\beta} \right) \cdot p_{i\alpha\beta} = -\delta_{\alpha,\beta} \frac{\rho_{eff,\beta}}{m_{eff}\, s_\beta} \cdot p; \ \alpha = 1,\ 2,\ 3; \ \beta = 1,\ 2 \ ; \ i = 1,\ 2. \end{aligned} \tag{4}$$

Suitable solutions are:

$$\begin{aligned} &p_{i\alpha\beta}(y) = A_{\alpha\beta} \cosh(\Gamma_\beta y) + \delta_{\alpha,\beta} \cdot B_\beta \cdot p \quad ; \quad \alpha = 1,\ 2,\ 3 \quad ; \quad \beta = 1,\ 2\ , \\ &v_{y\alpha\beta}(y) = -\frac{\Gamma_\beta}{j\omega\rho_{eff,\beta}} A_{\alpha\beta} \sinh(\Gamma_\beta y) = -\frac{\Gamma_\beta}{\Gamma_{y\beta} Z_{y\beta}} A_{\alpha\beta} \sinh(\Gamma_\beta y) \end{aligned} \tag{5}$$

with

$$\Gamma_\beta^2 = \Gamma_{y\beta}^2 + \frac{\rho_{eff,\beta}}{s_\beta m_{eff}} = \Gamma_{y\beta}^2 + \frac{\Gamma_{y\beta} Z_{y\beta}}{j\omega s_\beta m_{eff}}$$
$$B_\beta = \frac{\rho_{eff,\beta}/s_\beta m_{eff}}{\Gamma_{y\beta}^2 + \rho_{eff,\beta}/s_\beta m_{eff}} = \frac{1}{1 + j\,\dfrac{\omega m_{eff}}{Z_0}\,\dfrac{\Gamma_{y\beta}\, s_\beta}{Z_{y\beta}/Z_0}}. \tag{6}$$

The boundary conditions of continuity in the orifice range lead to:

$$\begin{aligned}
\frac{A_{11}}{p} &= -\frac{B_1}{2}\,\frac{2s_1U_2 + WV_2}{U_1V_2 + U_2V_1} \quad ; \quad \frac{A_{12}}{p} = +\frac{B_1}{2}\,\frac{2s_1U_1 - WV_1}{U_1V_2 + U_2V_1}\,,\\
\frac{A_{21}}{p} &= +\frac{B_2}{2}\,\frac{2s_2U_2 - WV_2}{U_1V_2 + U_2V_1} \quad ; \quad \frac{A_{22}}{p} = -\frac{B_2}{2}\,\frac{2s_2U_1 + WV_1}{U_1V_2 + U_2V_1}\,,\\
\frac{A_{31}}{p} &= \frac{\cosh(\Gamma_2\ell_2)}{U_1\,\cosh(\Gamma_2\ell_2) + U_2\,\cosh(\Gamma_1\ell_1)}\,; \; \frac{A_{32}}{p} = \frac{\cosh(\Gamma_1\ell_1)}{U_1\,\cosh(\Gamma_2\ell_2) + U_2\,\cosh(\Gamma_1\ell_1)}
\end{aligned} \tag{7}$$

with

$$\begin{aligned}
s &= (s_1 + s_2)/2 \quad ; \quad \omega_0^2 = \frac{1}{m_{eff}\, s\, C_0} = \frac{\rho_0 c_0^2}{m_{eff}\, s}\,,\\
W &= 1 - \left(\frac{\omega}{\omega_0}\right)^2 + j\omega m_{eff}\, G_{sv}
\end{aligned} \tag{8a}$$

$$\begin{aligned}
U_\beta &= j\,\frac{s_\beta}{a}\,\omega m_{eff}\,\frac{\Gamma_\beta}{\Gamma_{y\beta} Z_{y\beta}}\,\sinh(\Gamma_\beta\ell_\beta) + \frac{1}{2}\,W\,\cosh(\Gamma_\beta\ell_\beta) \quad ; \quad \beta = 1,\,2\,,\\
V_\beta &= j\,\frac{s\,a}{2}\,\omega\rho_0\,\frac{\Gamma_\beta}{\Gamma_{y\beta} Z_{y\beta}}\,\sinh(\Gamma_\beta\ell_\beta) + s_\beta\,\cosh(\Gamma_\beta\ell_\beta) \quad ; \quad \beta = 1,\,2.
\end{aligned} \tag{8b}$$

The average surface admittance of the arrangement is defined as:

$$\begin{aligned}
G = \frac{1}{L}\,\frac{1}{p}\Bigg[&\int_0^{\ell_1} (v_{x11} + v_{x21} + v_{x31})\,dy + a\cdot(v_{x13} + v_{x23} + v_{x33})\\
&+ \int_0^{\ell_2} (v_{x12} + v_{x22} + v_{x32})\,dy\Bigg].
\end{aligned} \tag{9}$$

One gets with the above solutions:

$$\begin{aligned}
Z_0G = j\,\frac{Z_0}{\omega m_{eff}}\Bigg[&-1 + \frac{L_1}{L}\,B_1 + \frac{L_2}{L}\,B_2\\
&+ \left(\frac{A_{11}}{p} + \frac{A_{21}}{p} + \frac{A_{31}}{p}\right)\cdot\left[\frac{\sinh(\Gamma_1\ell_1)}{\Gamma_1\ell_1} + \frac{a}{2L}\,\cosh(\Gamma_1\ell_1)\right]\\
&+ \left(\frac{A_{12}}{p} + \frac{A_{22}}{p} + \frac{A_{32}}{p}\right)\cdot\left[\frac{\sinh(\Gamma_2\ell_2)}{\Gamma_2\ell_2} + \frac{a}{2L}\,\cosh(\Gamma_2\ell_2)\right]\Bigg].
\end{aligned} \tag{10}$$

In the *special case of symmetrical gaps*, i.e. $s_1 = s_2 = s$; $\ell_1 = \ell_2 = \ell$:

$$Z_0 G = j\,\frac{Z_0}{\omega m}\left[-1 + B + \left(\frac{A_{11}}{p} + \frac{A_{21}}{p} + \frac{A_{31}}{p}\right)\cdot\left[2\frac{\sinh(\Gamma\ell)}{\Gamma\ell} + \frac{a}{L}\cosh(\Gamma\ell)\right]\right],$$
$$\frac{A_{11}}{p} = -\frac{B}{4}\,\frac{2sU + WV}{UV} \quad;\quad \frac{A_{21}}{p} = +\frac{B}{4}\,\frac{2sU - WV}{UV} \quad;\quad \frac{A_{31}}{p} = \frac{1}{2U} \tag{11}$$

with

$$\Gamma^2 = \Gamma_y^2 + \frac{\rho_{eff}}{s\,m_{eff}} = \Gamma_y^2 + \frac{\Gamma_y Z_y}{j\omega s\,m_{eff}} \quad;\quad B = \frac{\rho_{eff}/sm_{eff}}{\Gamma_y^2 + \rho_{eff}/sm_{eff}} = \frac{1}{1 + j\,\dfrac{\omega m_{eff}}{Z_0}\,\dfrac{\Gamma_y s}{Z_y/Z_0}}, \tag{12}$$

$$W = 1 - \left(\frac{\omega}{\omega_0}\right)^2 + j\omega m_{eff}\,G_{sv},$$
$$U = j\,\frac{s}{a}\,\omega m_{eff}\,\frac{\Gamma}{\Gamma_y Z_y}\,\sinh(\Gamma\ell) + \frac{1}{2}W\cosh(\Gamma\ell), \tag{13}$$
$$V = j\,\frac{s\,a}{2}\,\omega\rho_0\,\frac{\Gamma}{\Gamma_y Z_y}\,\sinh(\Gamma\ell) + s\cdot\cosh(\Gamma\ell)$$

and $\dfrac{A_{11}}{p} + \dfrac{A_{21}}{p} + \dfrac{A_{31}}{p} = \dfrac{1 - BW}{2U}$,

so that finally in this special case:

$$\begin{aligned} Z_0 G &= j\,\frac{Z_0}{\omega m_{eff}}\left[-1 + B + (1 - BW)\frac{\dfrac{a}{L} + 2\dfrac{\tanh(\Gamma\ell)}{\Gamma\ell}}{W + 2\dfrac{\ell}{a}\left(1 + j\omega s m_{eff}\dfrac{\Gamma_y}{Z_y}\right)\dfrac{\tanh(\Gamma\ell)}{\Gamma\ell}}\right] \\ &= j\,\frac{Z_0}{\omega m_{eff}}\left[-1 + B + (1 - BW)\frac{\dfrac{a}{L} + 2\dfrac{\tanh(\Gamma\ell)}{\Gamma\ell}}{W + 2\dfrac{\ell}{a}\left(1 - \omega^2/\omega_{eff}^2\right)\dfrac{\tanh(\Gamma\ell)}{\Gamma\ell}}\right] \end{aligned} \tag{14}$$

with $\omega_{eff}^2 = 1/(m_{eff}s \cdot C_{eff})$ the square of the foil resonance (angular) frequency of the cover foil with the effective air compressibility in the gap.

► *See also:* Mechel, Vol. II, Ch. 26 (1995) for a discussion of the result and of a possible parameter non-linearity in the gaps.

H.17 Poro-elastic Foils

► *See also:* Mechel, Vol. II, Ch. 26 (1995); Mechel (2000)

Poro-elastic foils may be tight or porous, limp or elastic. Their common features are

(1) lateral homogeneity in scales which are comparable with the free bending wave length,

(2) incompressibility (at least approximate).

Thus the description below of poro-elastic foils uniformly covers materials like limp metal or resin foils, thin porous layers, clothes, gauzes, felts, wire mesh, perforated metal sheets, and elastic plates (with or without perforations). Poro-elastic foils must not be plane; they also may have the form of curved shells.

It is assumed that the foil is placed in a co-ordinate surface of a co-ordinate system in which the wave equation is separable. We apply orthogonal co-ordinates $\{x_1, x_2, x_3\}$ for a general survey and assume that the foil occupies a co-ordinate surface $\{x_1, x_2\}$ and that the co-ordinate x_3 is normal to the foil, which is at the position $x_3 = \xi$. It seems that Cremer has introduced the term *Trennimpedanz* (partition impedance) for the quantity Z_T defined by:

$$Z_T = \frac{\Delta p}{v} = \frac{p_{front}(x_1, x_2, \xi) - p_{back}(x_1, x_2, \xi)}{v(x_1, x_2)}, \tag{1}$$

where p_{front}, p_{back} are the sound pressures in front of and behind the foil, respectively, and v is the velocity of the foil which is counted positive in the direction front $\to$ back.

The boundary conditions to be applied at a foil are:

$$v_{front} = v_{back} = v \quad ; \quad p_{front} - p_{back} = Z_T \cdot v. \tag{2}$$

Begin with a *tight and limp foil*: $Z_T = j\,\omega\, m_f = j\,\omega\, \rho_f\, d_f$,

where m_f is the surface mass density of the foil, d_f the foil thickness, and ρ_f the foil material density.

First generalisation: *Porous limp foil*:

The flow resistance $\Sigma = \Xi \cdot d_f$ (Ξ = flow resistivity of the foil material) acts in parallel with the mass reactance of the foil:

$$Z_t = \frac{j\,\omega\, m_f \cdot \Sigma}{j\,\omega\, m_f + \Sigma} = j\,\omega\, m_f \frac{1}{1 + \dfrac{j\,\omega\, m_f}{\Sigma}} = j\,\omega\, m_p. \tag{3}$$

So this first generalisation is performed by the substitution:

$$m_f \to m_{eff,p} = \frac{m_f}{1 + \dfrac{j\,\omega\, m_f}{\Sigma}}. \tag{4}$$

Second generalisation: *Tight elastic foil*:

The oscillation of the foil (which indeed is a thin plate) obeys the bending wave equation

$$\left[\Delta_{x_1,x_2}\Delta_{x_1,x_2} - k_B^4\right] v = \frac{j\,\omega}{B} \cdot \Delta p, \tag{5}$$

where $\Delta_{x,y}$ is the Laplace operator in the indicated co-ordinates, k_B is the wave number of the free bending wave on the plate, B is the bending stiffness, and $\Delta p = p_{front} - p_{back}$ is the driving sound pressure difference. With

$$k_B^4 = \omega^2 \frac{m_f}{B} \quad ; \quad \frac{k_0}{k_B} = \sqrt{\frac{f}{f_{cr}}}, \tag{6}$$

where $\omega = 2\pi f$ and f_{cr} = (critical) coincidence frequency, one immediately gets:

$$Z_T = \frac{\Delta p}{v_p} = j\,\omega\,m_f \cdot \left[1 - \left(\frac{f}{f_{cr}}\right)^2 \frac{1}{k_0^4} \cdot \frac{\Delta_{x_1,x_2}\Delta_{x_1,x_2} v}{v}\right], \tag{7}$$

$$\frac{Z_T}{Z_0} = j\,k_0 \frac{m_f}{\rho_0} \cdot \left[1 - \left(\frac{f}{f_{cr}}\right)^2 \frac{1}{k_0^4} \cdot \frac{\Delta_{x_1,x_2}\Delta_{x_1,x_2} v}{v}\right] = j\,k_0 \frac{m_f}{\rho_0} \cdot \left[1 - \left(\frac{f}{f_{cr}}\right)^2 \sin^4\chi\right] \tag{8}$$

with an effective angle χ of sound incidence on the plate (see below).

Third generalisation: *Elastic foil with bending wave losses*:

Energy dissipation in the foil can be taken into account by a loss factor η introducing a complex modulus $B \to B \cdot (1 + j\eta)$. This leads to:

$$\begin{aligned} \frac{Z_T}{Z_0} &= Z_m F \cdot \left[\,(1 - F^2 \sin^4\chi) - j\,\eta\,F^2 \sin^4\chi\right] \\ &= Z_m F \cdot \left[1 - \left(\frac{f}{f_c}\right)^2 - j\,\eta\left(\frac{f}{f_c}\right)^2\right] \quad ; \quad Z_m = j\frac{\omega_{cr} m_f}{Z_0}; \quad F = \frac{f}{f_{cr}}, \end{aligned} \tag{9}$$

where Z_m is the normalised inertial impedance of the plate at the critical frequency f_{cr} and f_c is the coincidence frequency at the incidence angle χ, with $f_{cr} = f_c \cdot \sin^2\chi$.

So elasticity and bending losses of the foil can be taken into account by using an effective surface mass density:

$$m_f \to m_{eff,e} = m_f \cdot \left[1 - \left(\frac{f}{f_c}\right)^2 - j\,\eta\left(\frac{f}{f_c}\right)^2\right]. \tag{10}$$

Fourth generalisation: *Combine porosity and elasticity effects*:

$$\text{Substitute} \quad m_f \to m_{eff,p,e} = \frac{m_{eff,e}}{1 + \dfrac{j\,\omega\,m_{eff,e}}{\Sigma}}. \tag{11}$$

Cylindrical shell:

The co-ordinate system is $\{x_1, x_2, x_3\} \to \{\vartheta, z, r\}$. The value $\xi = a$ is the radius of the shell. The sound fields separate into factors (v_p = velocity of the shell)

$$p(r, \vartheta, z) = R(r) \cdot T(\vartheta) \cdot U(z) \quad ; \quad v_p(a, \vartheta, z) = A \cdot T(\vartheta) \cdot U(z). \tag{12}$$

The form of U(z) may be any of, or a linear combination of: $U(z)=\begin{cases} e^{\pm j k_z z} \\ \cos(k_z z) \\ \sin(k_z z) \end{cases}$. (13)

The shape of R(r) may be one of the cylinder functions

$$Z_n(k_r r)=\left\{J_n(k_r r)\,,\ Y_n(k_r r)\,,\ H_n^{(1)}(k_r r)\,,\ H_n^{(2)}(k_r r)\right\}. \tag{14}$$

Then $T(\vartheta)$ for fields which are periodic in ϑ is: $T(\vartheta)=\begin{cases} \cos(n\vartheta) \\ \sin(n\vartheta) \end{cases}$. (15)

The Laplace operators in cylindrical co-ordinates are:

$$\Delta=\frac{\partial^2}{\partial r^2}+\frac{1}{r}\frac{\partial}{\partial r}+\frac{1}{r^2}\frac{\partial^2}{\partial\vartheta^2}+\frac{\partial^2}{\partial z^2}\quad;\quad\Delta_{\vartheta,z}=\frac{1}{a^2}\frac{\partial^2}{\partial\vartheta^2}+\frac{\partial^2}{\partial z^2}. \tag{16}$$

The bending wave equation is satisfied with the above field factors, when the following secular equation holds:

$$k_0^2=k_z^2+k_r^2\quad;\quad 1=(k_z/k_0)^2+(k_r/k_0)^2=\sin^2\Theta+\cos^2\Theta. \tag{17}$$

The angle Θ is between the wave vector and the radius. The two-dimensional Laplace operator gives, together with the Bessel differential equation for the $Z_n^{(i)}(k_r r)$:

$$\Delta_{\vartheta,z}\,p(a,\vartheta,z)=-\left(\frac{n^2}{a^2}+k_z^2\right)\cdot p(a,\vartheta,z). \tag{18}$$

Therefore: $$\frac{\Delta_{\vartheta,z}\Delta_{\vartheta,z}v_p}{v_p}=\left(\frac{n^2}{a^2}+k_z^2\right)^2=k_0^4\left(\frac{n^2}{(k_0a)^2}+\sin^2\Theta\right)^2. \tag{19}$$

Comparing this with the form for Z_T/Z_0 leads to the effective angle χ of incidence:

$$\sin\chi=\left(\frac{n^2}{(k_0a)^2}+\sin^2\Theta\right)^{1/2}. \tag{20}$$

Spherical shell:

Spherical co-ordinate system $\{r,\vartheta,\varphi\}$ and the correspondence $\{x_1,x_2,x_3\}\to\{\vartheta,\varphi,r\}$. The factors of the field are:

$$p(r,\vartheta,\varphi)=R(r)\cdot T(\vartheta)\cdot P(\varphi)\quad;\quad v_p(a,\vartheta,z)=A\cdot T(\vartheta)\cdot P(\varphi) \tag{21}$$

with R(r) being spherical Bessel functions and $T(\vartheta)$ (associated) Legendre functions of the first and second kind:

$$R(r)=z_m(k_0r)=\left\{j_m(k_0r)\,,\ y_m(k_0r)\,,\ h_m^{(1)}(k_0r)\,,\ h_m^{(2)}(k_0r)\right\}; \tag{22}$$

$$T(\vartheta)=\begin{cases} P_m^n(\cos\vartheta) \\ Q_m^n(\cos\vartheta) \end{cases}\quad;\quad P(\varphi)=\begin{cases} P_m^n\cos(n\,\varphi) \\ Q_m^n\sin(n\,\varphi) \end{cases}. \tag{23}$$

The Laplace operators are:

$$\Delta=\frac{\partial^2}{\partial r^2}+\frac{2}{r}\frac{\partial}{\partial r}+\frac{1}{r^2}\frac{\partial^2}{\partial\vartheta^2}+\frac{1}{r^2\mathrm{tg}\,\vartheta}\frac{\partial}{\partial\vartheta}+\frac{1}{r^2\sin^2\vartheta}\frac{\partial^2}{\partial\varphi^2}, \tag{24a}$$

$$\Delta_{\vartheta,\varphi} = \frac{1}{a^2}\frac{\partial^2}{\partial\vartheta^2} + \frac{1}{a^2 \mathrm{tg}\,\vartheta}\frac{\partial}{\partial\vartheta} + \frac{1}{a^2\sin^2\vartheta}\frac{\partial^2}{\partial\varphi^2}, \tag{24b}$$

and therefore: $$\frac{\Delta_{\vartheta,z}\Delta_{\vartheta,z}v_p}{v_p} = k_0^4\left(\frac{m(m+1)}{(k_0a)^2}\right)^2 \tag{25}$$

with the effective angle χ of incidence given by:

$$\sin\chi = \left(\frac{m(m+1)}{(k_0a)^2}\right)^{1/2}. \tag{26}$$

Because of $P_m^n(\cos\vartheta) \equiv 0;\ n > m$, the angle of incidence is $\chi = 0$ for the "breathing sphere" $m = n = 0$, which is plausible.

See Mechel, Acta Acustica, 86 (2000) for elliptic-cylindrical and hyperbolic-cylindrical shells.

Partition impedance of membranes:

Membranes get their bending stiffness from the tension in their plane (only plane membranes in the (x, y) plane; the method could also be applied to blown-up balloons). The inhomogeneous wave equation of a membrane is:

$$\left(\Delta + k_m^2\right) v_m = \frac{j\omega}{T}\left(p_{front} - p_{back}\right) \quad ; \quad k_m = \omega\sqrt{M/T} \tag{27}$$

with the surface mass density M and the tension T of the membrane. The partition impedance follows immediately:

$$Z_T = \frac{p_{front} - p_{back}}{v_m} = \frac{T}{j\omega}\left(\frac{\Delta v_m}{v_m} + k_m^2\right) = \frac{jT}{\omega}\left(k_{mx}^2 + k_{my}^2 - k_m^2\right) \tag{28}$$

for a pattern of the membrane velocity: $v_m(x,y) = A \cdot e^{\pm j k_{mx} x} \cdot e^{\pm j k_{my} y}$. (29)

H.18 Foil Resonator

► *See also:* Mechel, Vol. II, Ch. 26 (1995)

A foil resonator consists of a foil having a (effective) surface mass density m_f at a distance t to a hard wall; the interspace may be filled with air or (partially) with a porous material.

The surface impedance Z for normal sound incidence is:

$$\frac{Z}{Z_0} = j k_0 t \frac{m_f}{\rho_0 t} + \begin{cases} -j\cot(k_0 t) & ; \quad \text{air} \\ \dfrac{Z_{an}}{\tanh(\Gamma_{an} k_0 t)} & ; \quad \text{completely porous material} \end{cases} \tag{1}$$

with $\Gamma_{an} = \Gamma_a/k_0$, $Z_{an} = Z_a/Z_0$ the normalised characteristic values of the porous material.

The (angular) resonance frequency with air in the volume is, under condition $k_0 t \ll 1$:

$$\omega_0 = c_0\sqrt{\rho_0/(m_f\, t)} \quad ; \quad f_0 \approx 600/\sqrt{m_f\, t} \ \ (f_0 \text{ in Hz};\ m \text{ in kg/m}^2;\ t \text{ in cm}). \tag{2}$$

If $k_0 t \ll 1$ does not hold, the resonance equation is (for the *n*th resonance):

$$\frac{\omega_n t}{c_0} \cdot \tan \frac{\omega_n t}{c_0} = \frac{\rho_0 t}{m_f}. \tag{3}$$

An approximation for the lowest resonance solution is:

$$\left(\frac{\omega_0 t}{c_0}\right)^2 = \frac{105 + 45\,(\rho_0 t/m_f) - \sqrt{11025 + 5250\,(\rho_0 t/m_f) + 1605\,(\rho_0 t/m_f)^2}}{20 + 2\,(\rho_0 t/m_f)}. \tag{4}$$

For oblique sound incidence with the polar angle of incidence Θ, substitute $Z_0 \to Z_0/\cos\Theta$; $k_0 \to k_0 \cdot \cos\Theta$. As long as $k_0 t \cdot \cos\Theta \ll 1$, the resonance changes to $\omega_0 \to \omega_0/\cos\Theta$.

For oblique incidence on a foil resonator with porous material in the volume:

$$\frac{Z}{Z_0} = j\,k_0 t \frac{m_f}{\rho_0 t} + \frac{\Gamma_{an} Z_{an}}{\sqrt{\Gamma_{an}^2 + \sin^2\Theta} \cdot \tanh\left(k_0 t \sqrt{\Gamma_{an}^2 + \sin^2\Theta}\right)}. \tag{5}$$

The lowest three resonances $\omega_0, \omega_1, \omega_2$ (with air in the volume) can be read from the following nomograph. Enter the nomograph on its vertical axis with the value m of the foil surface mass density; proceed horizontally to the line for the distance t; proceed vertically to one of the (thick) lines for $\omega_0, \omega_1, \omega_2$ and from there horizontally to the line for the value of m; then vertically to the horizontal axis, where you can read the resonance frequency f_0 (or f_1, f_2). (The example in the nomograph is for $m = 0.5[\mathrm{kg/m^2}]$; $t = 2[\mathrm{cm}]$; giving $f_0 = 700[\mathrm{Hz}]$.)

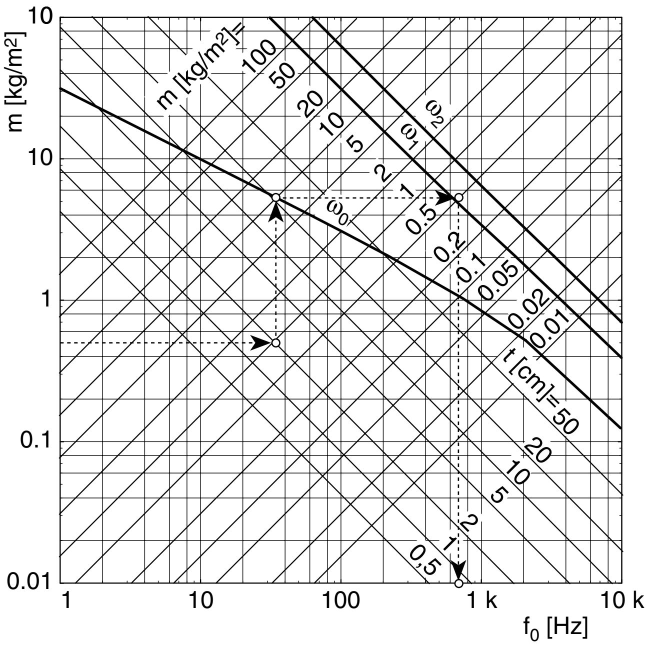

H.19 Ring Resonator

Ring resonators are used, for example, in mufflers and in low-frequency silencer sections, e.g. in gas turbine run-up and test cells.

The aim of this section is to evaluate the orifice input admittance G. The input orifice may be covered with a poro-elastic foil (Sect. H.17) with a partition impedance Z_s (normalised). The normalised admittance G then is:

$$G = \frac{G_v}{1 + Z_s G_v}, \tag{1}$$

where G_v is the (normalised) input admittance of the ring-shaped neck. A porous absorber layer in zone IV ($r_s \le r \le r_a$) is supposed to be made locally reacting by partitions.

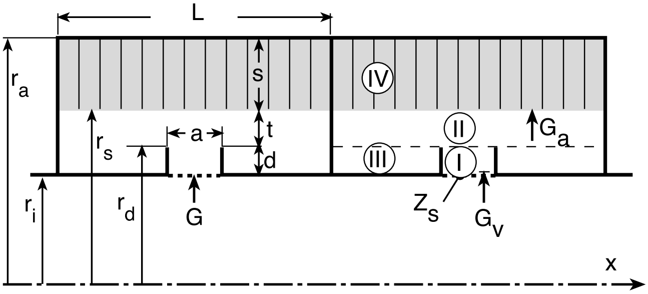

Corresponding to the low-frequency application, only the fundamental cylindrical mode is supposed to propagate in the field zones.

Field formulations in the zones (with Bessel, Neumann, and Hankel functions):

Zone I:

$$\begin{aligned} p_I &= a_0 \cdot H_0^{(2)}(k_0 r) + b_0 \cdot H_0^{(1)}(k_0 r) \\ &= (a_0 + b_0) \cdot J_0(k_0 r) + j \cdot (a_0 - b_0) \cdot Y_0(k_0 r)\ , \\ Z_0 v_{rI} &= -j \cdot (a_0 + b_0) \cdot J_1(k_0 r) + (a_0 - b_0) \cdot Y_1(k_0 r)\ . \end{aligned} \tag{2}$$

Zone II:

$$\begin{aligned} p_{II} &= c_0 \cdot J_0(k_0 r) + d_0 \cdot Y_0(k_0 r)\ , \\ Z_0 v_{rII} &= -j \cdot [c_0 \cdot J_1(k_0 r) + d_0 \cdot Y_1(k_0 r)]\ . \end{aligned} \tag{3}$$

Zone III:

$$\begin{aligned} p_{III} &= e_0 \cdot J_0(k_0 r) + f_0 \cdot Y_0(k_0 r)\ , \\ Z_0 v_{rIII} &= -j \cdot [e_0 \cdot J_1(k_0 r) + f_0 \cdot Y_1(k_0 r)]\ . \end{aligned} \tag{4}$$

Zone IV:

$$\begin{aligned} p_{IV} &= g_0 \cdot J_0(-j\,\Gamma_{an} r) + h_0 \cdot Y_0(-j\,\Gamma_{an} r)\ , \\ Z_0 v_{rIV} &= \frac{j}{Z_{an}} \left[g_0 \cdot J_1(-j\,\Gamma_{an} r) + h_0 \cdot Y_1(-j\,\Gamma_{an} r)\right]\ . \end{aligned} \tag{5}$$

with Γ_{an}, Z_{an} the normalised characteristic values of the porous material.

The radial input admittance (normalised) G_a of the absorber layer (zone IV) is:

$$G_a = \frac{j}{\Gamma_{an}} \frac{J_1(j\,\Gamma_{an}k_0r_s)\cdot Y_1(j\,\Gamma_{an}k_0r_a) - J_1(j\,\Gamma_{an}k_0r_a)\cdot Y_1(j\,\Gamma_{an}k_0r_s)}{J_0(j\,\Gamma_{an}k_0r_s)\cdot Y_1(j\,\Gamma_{an}k_0r_a) - J_1(j\,\Gamma_{an}k_0r_a)\cdot Y_0(j\,\Gamma_{an}k_0r_s)}. \tag{6}$$

Boundary conditions:

The interior neck orifice is additionally loaded with the mass impedance $Z_m = j \cdot k_0 a \cdot \Delta\ell_i/a$ of the interior orifice end correction.

$$\begin{aligned} &r = r_s: \\ &-j\,[c_0\cdot J_1(k_0r_s) + d_0\cdot Y_1(k_0r_s)] \overset{!}{=} G_a\cdot[c_0\cdot J_0(k_0r_s) + d_0\cdot Y_0(k_0r_s)] \end{aligned} \tag{7}$$

$r = r_d;\,\mathrm{I}-\mathrm{II}$:

velocity:

$$\begin{aligned} &-j\,[c_0\cdot J_1(k_0r_d) + d_0\cdot Y_1(k_0r_d)] \overset{!}{=} \\ &\quad \frac{a}{L}\left[-j\,(a_0+b_0)\cdot J_1(k_0r_d) + (a_0-b_0)\cdot Y_1(k_0r_d)\right] \\ &\quad -j\left(1-\frac{a}{L}\right)[e_0\cdot J_1(k_0r_d) + f_0\cdot Y_1(k_0r_d)] \end{aligned} \tag{8}$$

pressure:

$$\begin{aligned} &(a_0+b_0)\cdot J_0(k_0r_d) + j\,(a_0-b_0)\cdot Y_0(k_0r_d) \\ &-Z_m\cdot\left[-j\,(a_0+b_0)\cdot J_1(k_0r_d) + (a_0-b_0)\cdot Y_1(k_0r_d)\right] \overset{!}{=} c_0\cdot J_0(k_0r_d) + d_0\cdot Y_0(k_0r_d) \end{aligned}$$

$r = r_d;\,\mathrm{II}-\mathrm{III}$:

$$\begin{aligned} &\text{pressure:} \\ &e_0\cdot J_0(k_0r_d) + f_0\cdot Y_0(k_0r_d) \overset{!}{=} c_0\cdot J_0(k_0r_d) + d_0\cdot Y_0(k_0r_d) \end{aligned} \tag{9}$$

$$\begin{aligned} &r = r_i: \\ &e_0\cdot J_1(k_0r_i) + f_0\cdot Y_1(k_0r_i) \overset{!}{=} 0. \end{aligned} \tag{10}$$

Setting the arbitrary amplitude $a_0 = 1$, the neck input admittance is:

$$G_v = -j\,\frac{(1+b_0)\cdot J_1(k_0r_i) + j\,(1-b_0)\cdot Y_1(k_0r_i)}{(1+b_0)\cdot J_0(k_0r_i) + j\,(1-b_0)\cdot Y_0(k_0r_i)}. \tag{11}$$

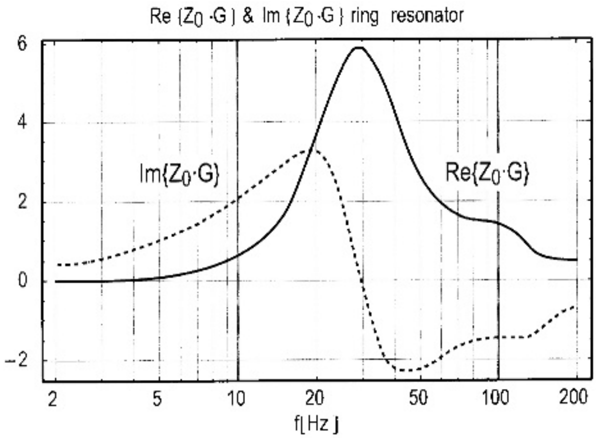

Example of Re$\{Z_0G\}$, Im$\{Z_0G\}$ of a low-tuned ring resonator for a turbine test cell; with input parameters for computation as listed.

(*Duct*)
$ri[m] = 3.$
$ra[m] = 4.9$
(*Cell*)
$L[m] = 1.0$
$a[m] = 0.25$
$d[m] = 0.2$
$t[m] = 0.2$
$s[m] = 1.5$
(*Absorber*)
$s[m] = 1.5$
$\Xi[Pas/m^2] = 500$

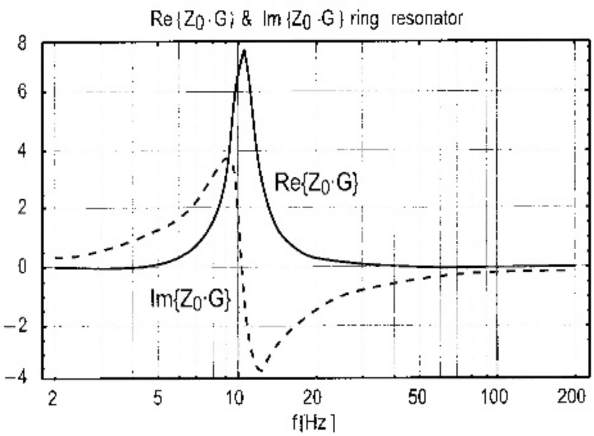

Ring resonator as above, but the necks additionally covered with a tight aluminium foil, $d_f = 1$ mm thick

So one must solve the boundary condition equations for $b_0 =: -N/D$ with

$$
\begin{aligned}
N = {} & \\
& \Big\{ -J_i(k_0 r_i)\ \big(G_a J_0(k_0 r_s) + j\, J_1(k_0 r_s)\big)\ \Big(J_1(k_0 r_i)\, Y_0(k_0 r_d) - J_0(k_0 r_d)\, Y_1(k_0 r_i)\Big) \\
& \quad \cdot \Big(J_1(k_0 r_s)\, Y_0(k_0 r_d) - J_0(k_0 r_d)\, Y_1(k_0 r_s)\Big)\ \Big(-j\, H_0^{(1)}(k_0 r_d) + Z_m H_1^{(1)}(k_0 r_d)\Big) \\
& \quad + \Big[G_a\ \Big(J_0(k_0 r_d)\, Y_0(k_0 r_s) - J_0(k_0 r_s)\, Y_0(k_0 r_d)\Big) + j\ \Big(J_0(k_0 r_d)\, Y_1(k_0 r_s) - J_1(k_0 r_s)\, Y_0(k_0 r_d)\Big)\Big] \qquad (12) \\
& \quad \cdot \Big[-j\, a/L \cdot J_0(k_0 r_d)\, J_1(k_0 r_i)\, H_1^{(1)}(k_0 r_d)\ \Big(J_1(k_0 r_i)\, Y_0(k_0 r_d) - J_0(k_0 r_d)\, Y_1(k_0 r_i)\Big) \\
& \qquad - J_1(k_0 r_i)\ \Big(J_1(k_0 r_i)\ \big(J_1(k_0 r_s)\, Y_0(k_0 r_d) + (a/L - 1)\, J_0(k_0 r_d)\, Y_1(k_0 r_d)\big)\Big) \\
& \quad - J_0(k_0 r_d)\, Y_1(k_0 r_i)\ \Big(J_1(k_0 r_s) + (a/L - 1)\, J_1(k_0 r_d)\Big)\Big) \cdot\ \Big(-j\, H_0^{(1)}(k_0 r_d) + Z_m H_1^{(1)}(k_0 r_d)\Big)\Big]\Big\}
\end{aligned}
$$

$$
\begin{aligned}
D = {} & \\
& \Big\{ J_1(k_0 r_i)\ \Big(G_a J_0(k_0 r_s) + j\, J_1(k_0 r_s)\Big)\ \Big(J_1(k_0 r_i)\, Y_0(k_0 r_d) - J_0(k_0 r_d)\, Y_1(k_0 r_i)\Big) \\
& \quad \cdot \Big(J_1(k_0 r_s)\, Y_0(k_0 r_d) - J_0(k_0 r_d)\, Y_1(k_0 r_s)\Big)\ \Big(j\, H_0^{(2)}(k_0 r_d) - Z_m H_1^{(2)}(k_0 r_d)\Big) \\
& \quad + \Big[G_a\ \Big(J_0(k_0 r_d)\, Y_0(k_0 r_s) - J_0(k_0 r_s)\, Y_0(k_0 r_d)\Big) - j\ \Big(J_1(k_0 r_s)\, Y_0(k_0 r_d) - J_0(k_0 r_d)\, Y_1(k_0 r_s)\Big)\Big] \qquad (13) \\
& \quad \cdot \Big[-j\, a/L \cdot J_0(k_0 r_d)\, J_1(k_0 r_i)\, H_1^{(2)}(k_0 r_d)\ \Big(J_1(k_0 r_i)\, Y_0(k_0 r_d) - J_0(k_0 r_d)\, Y_1(k_0 r_i)\Big) \\
& \qquad + J_1(k_0 r_i)\ \Big(J_1(k_0 r_i)\ \Big(J_1(k_0 r_s)\, Y_0(k_0 r_d) + (a/L - 1)\, J_0(k_0 r_d)\, Y_1(k_0 r_d)\Big) \\
& \qquad - J_0(k_0 r_d)\, Y_1(k_0 r_i)\ \Big(J_1(k_0 r_s) + (a/L - 1)\, J_1(k_0 r_d)\Big)\Big) \cdot\ \Big(j\, H_0^{(2)}(k_0 r_d) - Z_m H_1^{(2)}(k_0 r_d)\Big)\Big]\Big\}\,.
\end{aligned}
$$

H.20 Wide-Angle Absorber, Scattered Far Field

► *See also:* Mechel, Vol. III, Ch. 5 (1998); Mechel, Acustica 81 (1995); Schroeder/Gerlach (1977)

The focus of this section originally was conceived as wide-angle diffusers, Schroeder & Gerlach (1977), but the unavoidable losses make the discussion here applicable to effective absorbers. In principle, "diffuser" and "absorber" are contradictions in se. This section is more concerned with the "diffuser", in that it describes mainly the scattered far field (see next *Sect. H.21* for other field ranges).

The focus of our discussion here is on 1-D or 2-D arrays of $\lambda/4$-resonators. The depth t_k of the resonators varies in one of two possible pseudo-random manners (see below). Mostly, the arrangement is composed of groups of resonators, and the pseudo-random variation of t_k is within the group; then the object has a periodic structure. Three indices will be used: k for the number of a resonator in the group, m for the group and n for the resonator within the arrangement.

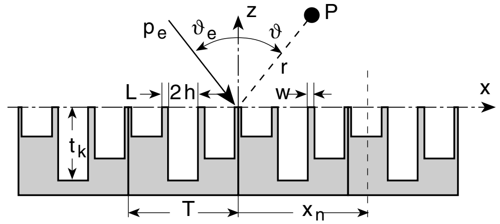

k=	0	1	N-1	0	1	N-1	0	1	N-1	0	1	N-1	QRD
	1	2	N-1	1	2	N-1	1	2	N-1	1	2	N-1	PRD

m= -M/2 | -1 | 0 | M/2–1

n= –M/2·N .... -1 0 1 .... M/2·N–1 QRD
–M/2·(N–1) .... -1 0 1 .... M/2·(N–1)–1 PRD

1-D array

The "classical" arrangements are as follows (N = prime number):

QRD: *quadratic residue diffuser*

$$\textit{1-D}: \quad t_k = \frac{\pi\, c_0 \ \ \mathrm{mod}\,(k^2, N)}{N\, \omega_r} \quad ; \quad k = 0, 1, \ldots, N-1 \tag{1}$$

$$\textit{2-D}: \quad t_{k,\ell} = \frac{\pi\, c_0 \ \ \mathrm{mod}\,(k^2 + \ell^2, N)}{N\, \omega_r} \quad ; \quad k, \ell = 0, 1, \ldots, N-1 \tag{2}$$

with $\omega_r = 2\pi f_r$ the "working (angular) frequency" and mod(a, b) = "modulo function" the remainder of a/b.

PRD: *primitive root diffuser*

$$\textit{1-D}: \quad t_k = \frac{\pi\, c_0 \ \ \mathrm{mod}\,(\rho^k, N)}{N\, \omega_r} \quad ; \quad k = 1, \ldots, N-1 \tag{3}$$

with ρ the "primitive root" of N. ($\mathrm{mod}(\rho^k, N)$ produces the numbers 1, 2, . . ., N − 1 in irregular sequence, if k = 1, 2, . . ., N − 1).

The needed Helmholtz numbers for 1-D diffusers are:

$$k_0 t_k = \frac{f}{f_r} \cdot \begin{cases} \dfrac{\pi}{N}\ \mathrm{mod}\,(k^2, N) \quad ; \quad k = 0, 1, \ldots, N-1; \quad \text{QRD} \\[2ex] \dfrac{\pi}{N}\ \mathrm{mod}\,(\rho^k, N) \quad ; \quad k = \ 1, \ldots, N-1; \quad \text{PRD.} \end{cases} \tag{4}$$

Cell centre co-ordinates are:

$$\text{QRD: } x_n = x_{k,m} = \left(n + \frac{1}{2}\right) L = mT + \left(k + \frac{1}{2}\right) L; \begin{cases} n = -MN/2, \ldots, +MN/2 - 1 \\ m = -M/2, \ldots, +M/2 - 1 \\ k = 0, \ldots, N-1 \end{cases} \tag{5}$$

$$\text{PRD: } x_n = x_{k,m} = \left(n + \frac{1}{2}\right) L = mT + \left(k - \frac{1}{2}\right) L; \begin{cases} n = -M(N-1)/2, \ldots, \\ \qquad + M(N-1)/2 - 1 \\ m = -M/2, \ldots, +M/2 - 1 \\ k = 1, \ldots, N-1. \end{cases}$$

The input admittance (normalised) $G(x_k)$ of a chamber is:

$$G(x_k) = \frac{\tanh(\Gamma_{an} k_0 t_k)}{Z_{an}}, \tag{6}$$

where Γ_{an}, Z_{an} are the normalised propagation constant and wave impedance in the cell; the fundamental mode values in capillaries are used if viscous and thermal losses are taken into account (see sections on capillaries in *Ch. J*, "Duct Acoustics").

Scattered far field for 2-D diffuser:

The scattered far field p_s for a 2-D diffuser can always be factorised:

$$p_s(r, \vartheta, \varphi) = P_i \cdot \Phi_s(\vartheta_e, \varphi_e | \vartheta, \varphi) \cdot \frac{e^{-jk_0 r}}{k_0 r}. \tag{7}$$

The angular distribution Φ_s is evaluated from:

$$\Phi_s(\vartheta_e, \varphi_e | \vartheta, \varphi) = \frac{-j\, k_0^2 \cos\vartheta_e}{2\pi\,(\cos\vartheta_e + \langle G \rangle)} \iint_A G(x, y) \cdot e^{-j\,(\mu_x x + \mu_y y)}\, dx\, dy \tag{8}$$

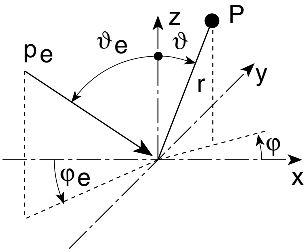

$$\text{with} \quad \begin{aligned} \mu_x &= k_0(\sin\vartheta_e \cos\varphi_e - \sin\vartheta \cos\varphi)\ , \\ \mu_y &= k_0(\sin\vartheta_e \sin\varphi_e - \sin\vartheta \sin\varphi). \end{aligned} \tag{9}$$

If the surface $A = (MT)^2$ of the arrangement has the homogeneous, averaged admittance $\langle G \rangle$, then:

$$\Phi_s = \frac{-j\, k_0^2 \cos\vartheta_e \cdot < G >}{2\pi\,(\cos\vartheta_e + < G >)} (MT)^2 \frac{\sin\,(\mu_x MT/2)}{\mu_x MT/2} \frac{\sin\,(\mu_y MT/2)}{\mu_y MT/2}. \tag{10}$$

For the 2-D QRD with cell centre co-ordinates:

$$\begin{aligned} x_m = x_{k,m_g} &= \left(m + \frac{1}{2}\right) L = m_g T + \left(k + \frac{1}{2}\right) L; \left\{ \begin{array}{l} m = -MN/2, \ldots, +MN/2 \\ m_g = -M/2, \ldots, +M/2 - 1 \\ k = 0, \ldots, N-1\ , \end{array} \right. \\ y_n = x_{\ell,n_g} &= \left(n + \frac{1}{2}\right) L = n_g T + \left(\ell + \frac{1}{2}\right) L; \left\{ \begin{array}{l} n = -MN/2, \ldots, +MN/2 \\ n_g = -M/2, \ldots, +M/2 - 1 \\ \ell = 0, \ldots, N-1. \end{array} \right. \end{aligned} \tag{11}$$

(m_g, n_g = group indices ; k, ℓ = cell incices), the scattered far field distribution is:

$$\Phi_s = \frac{-j\,(k_0 h)^2\ \cos\vartheta_e}{\pi\,(\cos\vartheta_e + <G>)} \cdot \frac{\sin\ \mu_x h}{\mu_x h} \cdot \frac{\sin\ \mu_y h}{\mu_y h} \cdot e^{-j\,(\mu_x+\mu_y)\,L/2}$$
$$\cdot \sum_{m_g,\,n_g} e^{-j\,(\mu_x m_g + \mu_y n_g)\,T} \cdot \sum_{k,\,\ell} G(k,\ \ell)\, e^{-j\,(\mu_x k + \mu_y \ell)\,L}. \tag{12}$$

The difference of the QRD, as compared with a surface A of equal size and same average admittance $\langle G\rangle$, is mainly produced by the factor of the last sum.
In the following examples of $|\Phi_s|$ the cell orifices may contain a normalised flow resistance R (e.g. a wire mesh; see parameter list). The QRD with N = 11 is exceptional in that it shows a strong backscattering.

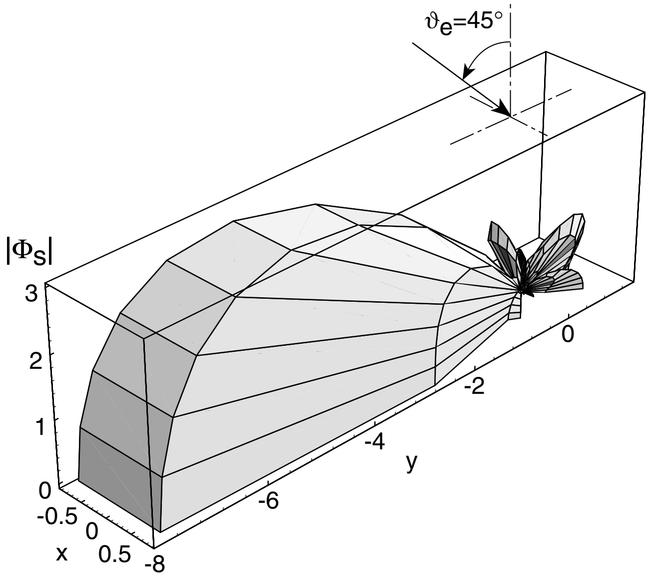

Scattered far field directivity of a QRD with N = 11.
Input parameters: $f = 285[\mathrm{Hz}]$; $f_r = 285[\mathrm{Hz}]$; $\vartheta_e = 45^\circ$; $\varphi_e = 90^\circ$; $N = 11$; $M = 4$; $h = 0.03[\mathrm{m}]$; $w = 0.003[\mathrm{m}]$; $R = 0$; $\Delta\vartheta = 6^\circ$; $\Delta\varphi = 12^\circ -$

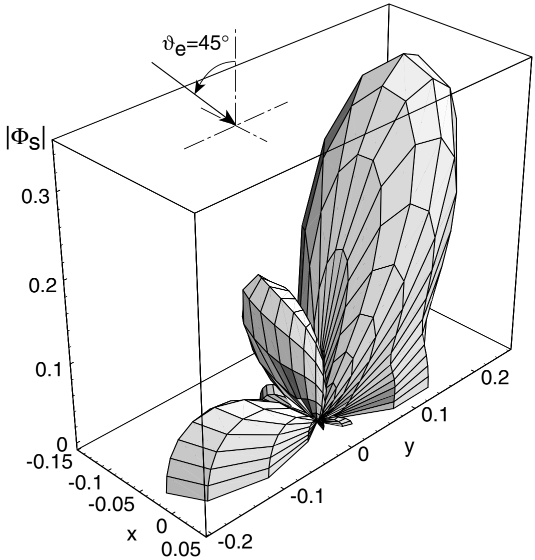

Angular distribution $|\Phi_s|$ of scattered far field with $M = 4$.
Input parameters: $f = 285[Hz]$; $f_r = 285[Hz]$; $\vartheta_e = 45°$; $\varphi_e = 90°$; $N = 7$; $M = 4$; $h = 0.03[m]$; $w = 0.003[m]$; $R = 0$; $\Delta\vartheta = 6°$; $\Delta\varphi = 12°$–

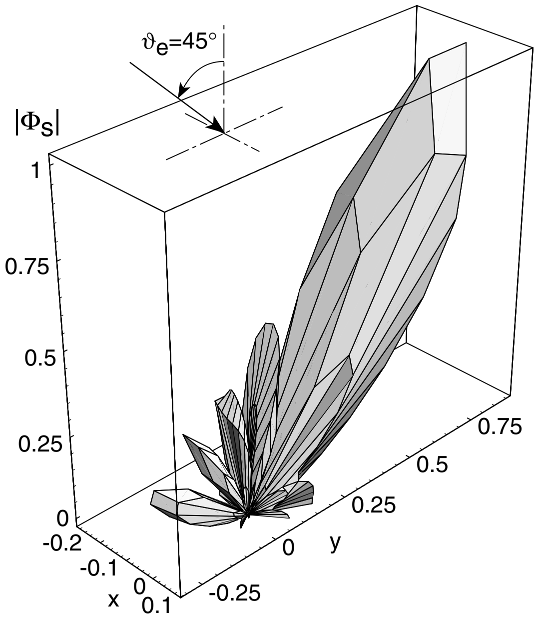

Angular distribution $|\Phi_s|$ of scattered far field with $M = 8$.
Input parameters: $f = 285[Hz]$; $f_r = 285[Hz]$; $\vartheta_e = 45°$; $\varphi_e = 90°$; $N = 7$; $M = 8$; $h = 0.03[m]$; $w = 0.003[m]$; $R = 0$; $\Delta\vartheta = 6°$; $\Delta\varphi = 12°$–

Scattered far field for 1-D diffuser: ($\varphi_e = 0$)

Scattered far field:

$$p_s(r,\ \vartheta,\ \varphi) = -P_i \sqrt{\frac{j}{2\pi}} \cdot \Phi_s(\vartheta_e|\vartheta) \cdot \frac{e^{-jk_0 r}}{\sqrt{k_0 r}}. \tag{13}$$

Directivity function (A = width of diffuser):

$$\Phi_s(\vartheta_e|\vartheta) = \int_{-k_0 A/2}^{+k_0 A/2} G(x)\ \frac{p(x,0)}{P_i}\ e^{jk_0 x\ \sin\vartheta}\ d(k_0 x) \tag{14}$$

with sound pressure at the surface and surface admittance G(x):

$$\begin{aligned}\frac{p(x,0)}{P_i} = {} & 2\,e^{-jk_0 x\ \sin\vartheta_e} - \frac{\cos\vartheta_e}{\cos\vartheta_e + \langle G\rangle} \\ & e^{-jk_0 x\ \sin\vartheta_e} \int_{-k_0 A/2}^{+k_0 A/2} G(x')\ H_0^{(2)}(k_0|x-x'|)\ e^{-jk_0 (x'-x)\ \sin\vartheta_e}\ d(k_0 x').\end{aligned} \tag{15}$$

So Φ_s has the form:

$$\begin{aligned}\Phi_s(\vartheta_e|\vartheta) = {} & 2\int_{-k_0 A/2}^{+k_0 A/2} G(x)\ e^{jk_0 x\,(\sin\vartheta - \sin\vartheta_e)}\ d(k_0 x) \\ & - \frac{\cos\vartheta_e}{\cos\vartheta_e + <G>} \cdot \iint_{-k_0 A/2}^{+k_0 A/2} G(x)\,G(y)\ e^{jk_0 (x\ \sin\vartheta - y\,\sin\vartheta_e)} \\ & \cdot H_0^{(2)}(k_0|x-y|)\ d(k_0 x)\ d(k_0 y) \\ := {} & I_1 - \frac{\cos\vartheta_e}{\cos\vartheta_e + \langle G\rangle} \cdot I_2.\end{aligned} \tag{16}$$

The first integral I_1 is for a QRD (for a PRD: summation $k = 1, \ldots, N-1$, and change sign in the exponent of the last factor in the third line below):

$$\begin{aligned}I_1 &= 4\,k_0 h\,\frac{\sin\left(k_0 h\,(\sin\vartheta - \sin\vartheta_e)\right)}{k_0 h\,(\sin\vartheta - \sin\vartheta_e)} \sum_n G(x_n)\,e^{jk_0 x_n\,(\sin\vartheta - \sin\vartheta_e)} \\ &= 4\,k_0 h\,\frac{\sin\left(k_0 h\,(\sin\vartheta - \sin\vartheta_e)\right)}{k_0 h\,(\sin\vartheta - \sin\vartheta_e)}\, e^{j\,k_0 L/2\cdot(\sin\vartheta - \sin\vartheta_e)} \\ &\quad \cdot \sum_{m=-M/2}^{M/2-1} e^{j\,m k_0 T\,(\sin\vartheta - \sin\vartheta_e)} \sum_{k=0}^{N-1} G(x_k)\,e^{j\,k\,k_0 L\,(\sin\vartheta - \sin\vartheta_e)}.\end{aligned} \tag{17}$$

The second integral I_2 is

$$\begin{aligned}I_2 &= \sum_{n,n'} G(x_n) G(x_{n'}) \cdot e^{j\,k_0 (x_n\,\sin\vartheta - x_{n'}\,\sin\vartheta_e)} \cdot I_{n,n'}\ , \\ I_{n,n'} &:= \iint_{-k_0 h}^{k_0 h} e^{j\,(x\,\sin\vartheta - y\,\sin\vartheta_e)} \cdot H_0^{(2)}(|n-n'|\,k_0 L + x - y)\ dx\ dy.\end{aligned} \tag{18}$$

See Mechel, Vol. III, Ch. 5 (1998) for the integration of $I_{n,n}$.

H.21 Wide-Angle Absorber, Near Field and Absorption

▸ *See also:* Mechel, Vol. III, Ch. 5 (1998); Mechel, Acustica 81 (1995)

The focus of this section is the same as in the previous *Sect. H.20*. This section is mainly concerned with the field analysis near the absorber (diffuser) and its absorption. The parts of this section are:

- 1-D absorber:
  - exterior field without losses; in the cells fundamental capillary mode;
  - exterior field without losses, in the cells higher capillary modes;
  - exterior field with losses;
- 2-D absorber.

A plane wave p_e is incident with a polar angle ϑ_e.

1-D absorber:

The absorber is composed of cell groups with width $T = N \cdot L$ (for QRD) or $T = (N-1) \cdot L$ (for PRD). The cell raster is $L = 2h + w$; $2h$ = cell width; w = thickness of walls between cells. The absorber is treated as a periodic structure with period length T.

Fundamental capillary mode in the cells:

Field in front of the absorber:

$$p(x,z) = p_e(x,z) + p_s(x,z) \quad ; \quad \begin{aligned} p_e(x,z) &= P_e \cdot e^{j(-xk_x + z\,k_z)}\,, \\ p_s(x,z) &= \sum_{n=-\infty}^{+\infty} A_n \cdot e^{-\gamma_n z} \cdot e^{-j\beta_n x} \end{aligned} \tag{1}$$

$$\text{with} \quad \begin{aligned} &k_x = k_0 \sin\vartheta_e \quad ; \; k_z = k_0 \cos\vartheta_e; \\ &\beta_n = \beta_0 + n\frac{2\pi}{T} \quad ; \; \frac{\gamma_n}{k_0} = \sqrt{(\sin\vartheta_e + n\cdot\lambda_0/T)^2 - 1}; \; \gamma_0 = j\,k_z = j\,k_0 \cos\vartheta_e. \end{aligned} \tag{2}$$

Index range of radiating space harmonics (the other harmonics are surface waves):

$$-\frac{T}{\lambda_0}(1+\sin\vartheta_e) \le n_s \le \frac{T}{\lambda_0}(1-\sin\vartheta_e). \tag{3}$$

At the surface:

$$p(x,0) = \left[P_e + A_0 + \sum_{n\neq 0} A_n \cdot e^{-jn\frac{2\pi}{T}x} \right] e^{-j\,k_x x}\,, \tag{4}$$

$$-Z_0 v_z(x,0) = \left[(P_e - A_0)\cos\vartheta_e + j\sum_{n\neq 0} A_n \frac{\gamma_n}{k_0} \cdot e^{-jn\frac{2\pi}{T}x} \right] e^{-j\,k_x x}. \tag{5}$$

Boundary condition:

$$(P_e - A_0)\cos\vartheta_e + j\sum_{n\neq 0} A_n \frac{\gamma_n}{k_0} \cdot e^{-jn\frac{2\pi}{T}x} = G(x) \cdot \left[P_e + A_0 + \sum_{n\neq 0} A_n \cdot e^{-jn\frac{2\pi}{T}x} \right] \tag{6}$$

or, with the Fourier analysis of $G(x)$:

$$G(x) = \sum_{n=-\infty}^{+\infty} g_n \cdot e^{-jn\frac{2\pi}{T}x} \quad ; \quad g_n = \frac{1}{T}\int_0^T G(x) \cdot e^{+jn\frac{2\pi}{T}x}\,dx. \tag{7}$$

System of equations for the A_n ($\delta_{m,n}$ = Kronecker symbol):

$$\sum_{n=-n_{hi}}^{+n_{hi}} A_n \cdot \left[g_{-m-n} - j\,\delta_{m,-n}\frac{\gamma_n}{k_0} \right] = P_e\,(\delta_{m,0}\cos\vartheta_e - g_{-m}) \quad ; \quad m = -n_{hi}, \ldots, +n_{hi}\,. \tag{8}$$

With the admittance profile $\quad G(x_k) = \dfrac{\tanh(\Gamma_{an}\,k_0 t_k)}{Z_{an}}$ (9)

in the *k*th cell with $\quad k_0 t_k = \dfrac{f}{f_r}\,\dfrac{\pi}{N} \cdot \begin{cases} \mathrm{mod}(k^2,\ N) & ; \quad \mathrm{QRD} \\ \mathrm{mod}(\rho^k,\ N) & ; \quad \mathrm{PRD} \end{cases}\,,$ (10)

where Γ_{an}, Z_{an} are the normalised capillary propagation constant and wave impedance.

The Fourier components are:

$$\begin{aligned} g_n &= \frac{2h}{T}\sum_{k=0}^{N-1} G(x_k)\,e^{-jn\pi(2k+1)/N}\,\frac{\sin(2n\pi\,h/T)}{2n\pi\,h/T} \quad ; \quad \mathrm{QRD}\,, \\ g_n &= \frac{2h}{T}\sum_{k=1}^{N-1} G(x_k)\,e^{-jn\pi(2k-1)/(N-1)}\,\frac{\sin(2n\pi\,h/T)}{2n\pi\,h/T} \quad ; \quad \mathrm{PRD}. \end{aligned} \tag{11}$$

The absorption coefficient $\alpha(\vartheta_e)$ is:

$$\alpha(\vartheta_e) = 1 - \left|\frac{A_0}{P_e}\right|^2 - \frac{1}{\cos\vartheta_e}\sum_{n_s \neq 0}\left|\frac{A_{n_s}}{P_e}\right|^2 \sqrt{1-(\sin\vartheta_e + n_s\,\lambda_0/T)^2}, \tag{12}$$

where the summation index n_s spans the range of radiating space harmonics, but not $n_s = 0$. The second term $|A_0/P_e|^2$ represents the geometrical reflection $|r_g|^2$; therefore the third term represents the non-geometrical reflection $|r_s|^2$ by scattering.

The following diagram shows $\alpha(\vartheta_e)$ over f; first, without losses in the exterior space taken into account (thick, full line), second, the exterior losses considered by the substitution $k_0 \to k_\rho$, where k_ρ is the free field wave number of viscous and heat-conducting air (thin, dashed line). This substitution surely under-estimates by far the real losses; however, the strong modification of $\alpha(\vartheta_e)$ by the substitution indicates the sensitivity to losses.

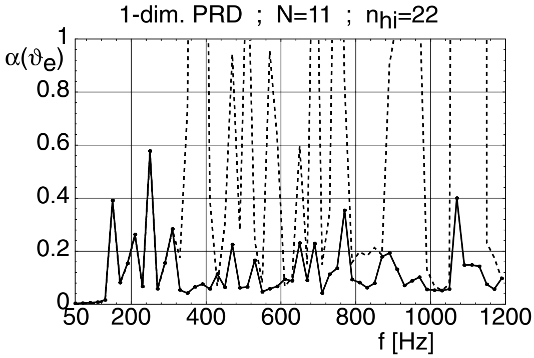

Absorption coefficient $\alpha(\vartheta_e)$ of a 1-D PRD; solid: no losses in exterior space; dashed: with free field wave number k_ρ of lossy air used in the exterior space. Input parameters: $f_r = 285[\mathrm{Hz}]; \vartheta_e = 45°; h = 0.03[\mathrm{m}]; w = 0.003[\mathrm{m}]; R = 0; n_{hi} = 22; \Delta f = 20[\mathrm{Hz}]$

This result suggests that with a small (normalised) additional flow resistance R in the orifices (e.g. by a wire mesh) a good absorber could be realised.

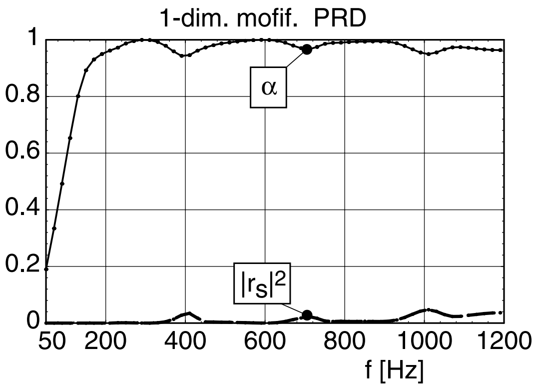

A 1-D PRD as above, but with an additional flow resistance R=0.4 in the cell orifices. Input parameters: $f_r = 285[\mathrm{Hz}]; \vartheta_e = 45°; h = 0.03[\mathrm{m}]; w = 0.003[\mathrm{m}]; R = 0.4; N = 15; n_{hi} = 30$

The dependence of this high absorption on the polar angle ϑ_e of sound incidence is depicted in the next 3-D graph of $\alpha(f, \vartheta_e)$ over frequency f and angle of incidence ϑ_e.

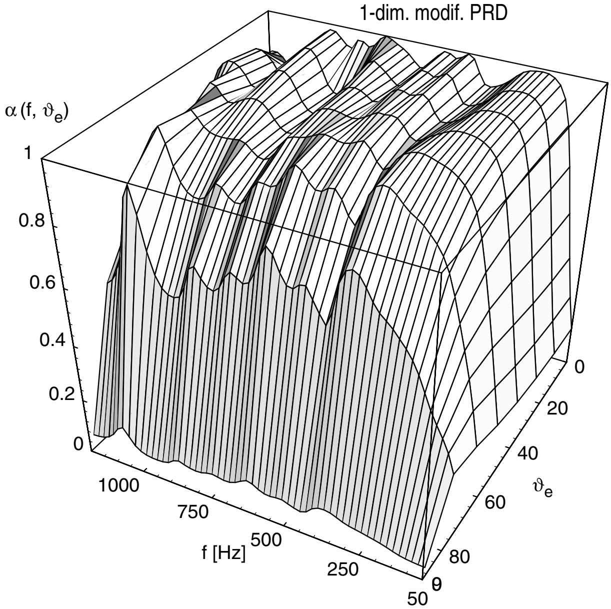

Absorption coefficient $\alpha(\vartheta_e)$ of the 1-D PRD from above, plotted over f and ϑ_e
Input parameters: $f_r = 285[\mathrm{Hz}]$; $\vartheta_e = 0 - 90°$; $h = 0.03[\mathrm{m}]$; $w = 0.003[\mathrm{m}]$; $R = 0.4$; $N = 15$; $n_{hi} = 22$

Losses and higher modes in the cells of a 1-D absorber:

Assume density waves of lossy air in the exterior space, i.e. with a free field wave number $k_\rho \approx k_0$, and assume capillary wave modes in the cells. The field formulation in the k-th cell is:

$$p_k(x, z) = e^{-j\beta_0 x_k} \sum_{n=0}^{\infty} B_{k,n} \cdot \cosh(\Gamma_n(z - t_k)) \cdot q_n(x - x_k) \tag{13}$$

with $\beta_0 = k_\rho \cdot \sin\vartheta_e$ and the mode profiles

$$q_n(x - x_k) = \begin{cases} \cos(\varepsilon_n(x - x_k)) & ; \quad n = n_e \\ \sin(\varepsilon_n(x - x_k)) & ; \quad n = n_o \end{cases} \tag{14}$$

for the symmetrical even modes ($n_e = 0, 2, 4\ldots$) and the anti-symmetrical odd modes ($n_o = 1, 3, 5\ldots$). The characteristic equation for the $\varepsilon_n = \varepsilon_{\rho n}$ of *symmetrical modes* is:

$$\begin{aligned}&[(\varepsilon_\rho h)^2 - (k_\rho h)^2] \left(\frac{\Theta_\rho}{\Theta_\alpha} - 1\right) \frac{\tan\sqrt{(\varepsilon_\rho h)^2 - (k_\rho h)^2 + (k_\nu h)^2}}{\sqrt{\ldots}} + \varepsilon_\rho h \cdot \tan \varepsilon_\rho h \\ &\qquad - \frac{\Theta_\rho}{\Theta_\alpha} \sqrt{(\varepsilon_\rho h)^2 - (k_\rho h)^2 + (k_\alpha h)^2} \cdot \tan\sqrt{\ldots} = 0,\end{aligned} \tag{15}$$

where $\sqrt{\ldots}$ denotes the nearest root and

$$\frac{\Theta_\rho}{\Theta_\alpha}=\frac{(k_\rho h)^2}{(k_\alpha h)^2}\;\frac{1-\kappa\,(k_\alpha h)^2/(k_{\alpha 0}h)^2}{1-\kappa\,(k_\rho h)^2/(k_{\alpha 0}h)^2} \tag{16}$$

with the free field wave numbers

$$(k_0h)^2=\left(\frac{\omega h}{c_0}\right)^2;\,(k_\nu h)^2=-j\,\frac{\omega}{\nu}\,h^2;\,(k_{\alpha 0}h)^2=\kappa\,\mathrm{Pr}\cdot(k_\nu h)^2\;,$$

$$\left.\begin{matrix}(k_\rho h)^2\\ \\ (k_\alpha h)^2\end{matrix}\right\}=\frac{\left[\dfrac{1}{(k_0h)^2}+\dfrac{4}{3\,(k_\nu h)^2}+\dfrac{\kappa}{(k_{\alpha 0}h)^2}\right]\mp\sqrt{[\ldots]^2-2\cdot\{\ldots\}}}{\left\{\dfrac{2\kappa}{(k_{\alpha 0}h)^2}\left(\dfrac{1}{\kappa(k_0h)^2}+\dfrac{4}{3\,(k_\nu h)^2}\right)\right\}}, \tag{17}$$

where $[\ldots]$ and $\{\ldots\}$ under the root repeat the corresponding expressions from outside the root. The characteristic equation for the $\varepsilon_n=\varepsilon_{\rho n}$ of *anti-symmetrical modes* is obtained by the substitutions $\cos\rightarrow\sin$; $\sin\rightarrow-\cos$; $\tan\rightarrow-\cot$. Start values for the numerical solution of the characteristic equation are, for even modes, $\varepsilon_0h=\varepsilon_\rho h$; $\varepsilon_{n>0}h=n\pi/2$ and, for odd modes, $\varepsilon_{n>0}h=n\pi/2$.

The field in the exterior space is formulated as:

$$p(x,z)=p_e(x,z)+p_s(x,z)\quad;\quad\begin{aligned}p_e(x,z)&=P_e\cdot e^{j\,(-xk_x+z\,k_z)}\;,\\ p_s(x,z)&=\sum_{n=-\infty}^{+\infty}A_n\cdot e^{-\gamma_n z}\cdot e^{-j\beta_n x},\end{aligned} \tag{18}$$

where p_s is periodic in x with a period length T, and with

$$k_x=k_0\;\sin\vartheta_e\quad;\quad k_z=k_0\;\cos\vartheta_e\;;$$

$$\beta_n=\beta_0+n\frac{2\pi}{T};\quad\frac{\gamma_n}{k_0}=\sqrt{(\sin\vartheta_e+n\cdot\lambda_0/T)^2-1};\quad\gamma_0=j\,k_z=j\,k_0\;\cos\vartheta_e. \tag{19}$$

The boundary conditions at the surface give a linear system of equations for the amplitudes A_n of the reflected space harmonics:

$$\begin{aligned}&\sum_{n=-n_{hi}}^{+n_{hi}}A_n\left[\frac{T}{h}\,\delta_{m,n}\left[j\,\delta_{m,0}\;\cos\vartheta_e+(1-\delta_{m,0})\,\frac{\gamma_m}{k_0}\right]\right.\\ &\left.-\circ\sum_{k}^{N-1}e^{j\,(m-n)\,2\pi\,x_k/T}\sum_{i=0}^{i_{hi}}(-1)^i\,\frac{\Gamma_i}{k_\rho}\;\tanh(\Gamma_i t_k)\,\frac{S_{m,i}\cdot S_{n,i}}{Q_i}\right]\\ &=\left[j\,\frac{T}{h}\,\delta_{m,0}\;\cos\vartheta_e+\circ\sum_{k}^{N-1}e^{j\,m\,2\pi\,x_k/T}\sum_{i=0}^{i_{hi}}(-1)^i\,\frac{\Gamma_i}{k_\rho}\;\tanh(\Gamma_i t_k)\,\frac{S_{m,i}\cdot S_{0,i}}{Q_i}\right]\cdot P_e,\end{aligned} \tag{20}$$

where $\delta_{m,n}$ is the Kronecker symbol and the circle o at $\circ\sum$ indicates that cells with depth $t_k=0$ (which exist for a QRD) are excluded from the summation. The amplitudes $B_{k,n}$ follow, with a set of solutions A_n, from:

$$B_{k,m}=\frac{(P_e+A_0)\,R_{0,m}+\sum\limits_{n\neq 0}A_n\,e^{-jn\,2\pi\,x_k/T}\,R_{n,m}}{Q_m\;\cosh(\Gamma_m t_k)}. \tag{21}$$

These equations use mode norms and coupling coefficients:

$$Q_n := \frac{1}{h}\int_{-h}^{+h} q_n^2(y)\,dy = \begin{cases} 1+\dfrac{\sin 2\varepsilon_n h}{2\varepsilon_n h}\,; & n=n_e=0,\,2,\dots \\[2ex] 1-\dfrac{\sin 2\varepsilon_n h}{2\varepsilon_n h}\,; & n=n_o=1,\,3,\dots \end{cases} \tag{22}$$

$$S_{m,n} := \frac{1}{h}\int_{-h}^{+h} e^{j\beta_m y}\cdot\begin{Bmatrix}\cos(\varepsilon_n y)\\ \sin(\varepsilon_n y)\end{Bmatrix} dy;\quad \begin{Bmatrix} n=n_e \\ n=n_o\end{Bmatrix}\quad;\quad m=0,\,\pm1,\,\pm2,\dots$$

$$= \frac{1}{h\,(\beta_m^2-\varepsilon_n^2)}\left[\,(\beta_m+\varepsilon_n)\,\sin((\beta_m-\varepsilon_n)h)+(\beta_m-\varepsilon_n)\,\sin((\beta_m+\varepsilon_n)h)\,\right];\; n=n_e \tag{23}$$

$$= \frac{1}{h\,(\beta_m^2-\varepsilon_n^2)}\left[\,(\beta_m+\varepsilon_n)\,\sin((\beta_m-\varepsilon_n)h)-(\beta_m-\varepsilon_n)\,\sin((\beta_m+\varepsilon_n)h)\,\right];\; n=n_o$$

$$R_{m,n} := \frac{1}{h}\int_{-h}^{+h} e^{-j\beta_m y}\cdot\begin{Bmatrix}\cos(\varepsilon_n y)\\ \sin(\varepsilon_n y)\end{Bmatrix} dy\quad;\quad \begin{Bmatrix} n=n_e \\ n=n_o\end{Bmatrix}\quad;\quad m=0,\,\pm1,\,\pm2,\dots \tag{24}$$

$$= \begin{cases} S_{m,n_e} & ;\quad n=n_e \\[2ex] -S_{m,n_o} & ;\quad n=n_o\,. \end{cases}$$

Limit values for $\beta_m \to \pm\varepsilon_n$ are: $S_{m,n_e} \to Q_{n_e}$; $\quad S_{m,n_o} \to \pm j\; Q_{n_o}$. (25)

See Mechel, Vol. III, Ch. 5 (1998) for field evaluation with 2-D absorbers.

H.22 Tight Panel Absorber, Rigorous Solution

► *See also:* Mechel (2001); Mechel (1997)

A tight, long, elastic panel is simply supported at its borders at $x = \pm c$. Its thickness is d, the plate material density ρ_p, the elastic parameter for bending $f_{cr}d$, with the critical frequency f_{cr}, and the bending loss factor is η. The panel covers a back volume of depth t. The characteristic propagation constant and wave impedance in the back volume are Γ_a, Z_a (thus the back volume may be filled with air, i.e. $\Gamma_a \to j\cdot k_0$; $Z_a \to Z_0$, if t is not too small, or Γ_a, Z_a from a flat capillary for small t, or Γ_a, Z_a from porous materials if the back volume is filled with such material). The front side of the arrangement is flush with a hard baffle wall. A plane wave p_e is incident (normal to the z axis) with a polar angle Θ.

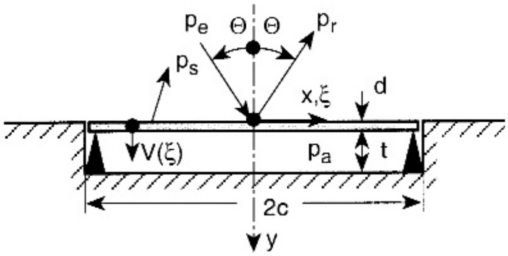

Field formulation in front of the absorber:

$$p(x,y) = p_e(x,y) + p_r(x,y) + p_s(x,y) \tag{1}$$

with p_r the reflected wave after reflection at a hard plane $y = 0$ and p_s the scattered wave.

$$\begin{aligned} &p_e(x,y) = P_e \cdot e^{-j\,k_x x} \cdot e^{-j\,k_y y} \quad ; \quad p_r(x,y) = P_e \cdot e^{-j\,k_x x} \cdot e^{+j\,k_y y}\ ; \\ &k_x = k_0\ \sin\Theta \quad ; \quad k_y = k_0\ \cos\Theta . \end{aligned} \tag{2}$$

Field p_a in the back volume, with the wave and impulse equations:

$$\left(\Delta - \Gamma_a^2\right)\ p_a = 0 \quad ; \quad v_a = \frac{-1}{\Gamma_a Z_a}\,\mathrm{grad}\, p_a \tag{3}$$

as the sum of volume modes:

$$p_a(x,y) = \sum_{k\geq 0} a_k \cdot p_{ak}(x) \cdot \cos\left(\kappa_k (y-t)\right)\ , \tag{4}$$

$$\kappa_k c = j\sqrt{(\Gamma_a c)^2 + \gamma_k^2}\ ,$$

$$p_{ak}(\xi) = \begin{cases} \cos\left(k\pi\xi/2\right) = \cos(\gamma_k \xi) \quad ; \quad k = 0,\ 2,\ 4, \ldots \\ \sin\left(k\pi\xi/2\right) = \sin(\gamma_k \xi) \quad ; \quad k = 1,\ 3,\ 5, \ldots \end{cases} \quad ; \quad \gamma_k = k\pi/2\ , \tag{5}$$

$$v_{ay}(\xi, y=0) = \frac{-1}{\Gamma_a Z_a} \sum_{k\geq 0} a_k \kappa_k \cdot p_{ak}(\xi) \cdot \sin\ (\kappa_k t). \tag{6}$$

Plate vibration velocity $V(x)$, or $V(\xi)$ with $\xi = x/c$:

$$\begin{aligned} &V(\xi) \ = \sum_{n\geq 1} V_n \cdot v_n(\xi)\ , \\ &v_n(x) = \begin{cases} \cos\left(n\pi\xi/2\right) = \cos(\gamma_n \xi) \quad ; \quad n = 1,\ 3,\ 5, \ldots \\ \sin\left(n\pi\xi/2\right) = \sin(\gamma_n \xi) \quad ; \quad n = 2,\ 4,\ 6, \ldots \end{cases} \quad ; \quad \gamma_n = n\pi/2. \end{aligned} \tag{7}$$

The feature of $p_s(x,0) = p_s(\xi)$ to have a finite normal particle velocity $v_{sy}(x,0)$ in $-c \leq x \leq +c$ and zero normal velocity outside suggests the use of elliptic-hyperbolic cylinder co-ordinates (ρ, ϑ) for the formulation of that component field. These co-ordinates follow from the Cartesian co-ordinates (x, y) by the transformation

$$x = c \cdot \cosh\rho \cdot \cos\vartheta \quad ; \quad y \ = c \cdot \sinh\ \rho \cdot \sin\vartheta. \tag{8}$$

$x = \pm c$ are the positions of the common foci of the ellipses and hyperbolic branches.

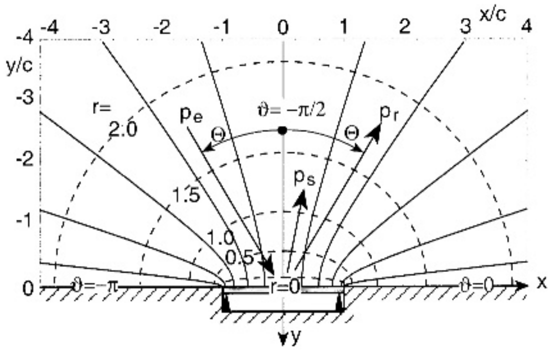

At $\rho = 0$:
$\xi = x/c = \cos\vartheta$

$$v_\rho \xrightarrow[\rho\to 0]{} -v_y$$
$$v_\vartheta \xrightarrow[\rho\to 0]{} v_x$$

$$\operatorname{grad} p \xrightarrow[\rho\to 0]{} \frac{1}{c\ \sin\vartheta}\left[\frac{\partial p}{\partial \rho}\vec{n}_\rho + \frac{\partial p}{\partial \vartheta}\vec{n}_\vartheta\right]. \tag{9}$$

The wave equation in these co-ordinates is written as follows:

$$\frac{\partial^2 p}{\partial \rho^2} + \frac{\partial^2 p}{\partial \vartheta^2} + (k_0 c)^2\left(\cosh^2\rho - \cos^2\vartheta\right)\cdot p(\rho,\vartheta) = 0. \tag{10}$$

It separates for $p(\rho,\vartheta) = U(\vartheta)\cdot W(\rho)$ into the two Mathieu differential equations:

$$\begin{aligned} &\frac{d^2U(z)}{dz^2} + \left(b - 4q\cos^2 z\right)\cdot U(z) \quad = 0 \\ &\frac{d^2W(z)}{dz^2} - \left(b - 4q\cosh^2 z\right)\cdot W(z) = 0 \end{aligned} \tag{11}$$

with $q = (k_0c)^2/4$ and b a separation constant. Solutions are the Mathieu functions (see Mechel (1997) for these functions). The sum $p_e + p_r$ can be expanded in Mathieu functions $ce_m(\vartheta)$, $Jc_m(\rho)$:

$$p_e(\rho,\ \vartheta) + p_r(\rho,\ \vartheta) = 4P_e\sum_{m=0}^{\infty}(-j)^m ce_m(\alpha)\cdot Jc_m(\rho)\cdot ce_m(\vartheta). \tag{12}$$

A formulation of p_s which has the mentioned features for each term is:

$$\begin{aligned} &p_s(\rho,\ \vartheta) = 4\sum_{m=0}^{\infty} D_m(-j)^m ce_m(\alpha)\cdot Hc_m^{(2)}(\rho)\cdot ce_m(\vartheta) \\ &\alpha = \pi/2 - \Theta \quad ; \quad q = (k_0c)^2/4 \end{aligned} \tag{13}$$

The $ce_m(\vartheta)$ are “azimuthal Mathieu functions” which are even in ϑ at $\vartheta = 0$, and the $Hc_m^{(2)}(\rho) = Jc_m(\rho) - j\cdot Yc_m(\rho)$ are associated “radial Mathieu functions”, or “Mathieu-Hankel functions” of the second kind, which represent outward propagating waves and satisfy Sommerfeld's far field condition. They are composed by the "Mathieu-Bessel" function $Jc_m(\rho)$ and the "Mathieu-Neumann" function $Yc_m(\rho)$ like the cylindrical "Hankel functions" of the 2nd kind. The Mathieu functions depend on the parameter q. Note for later use that $ce_m(\vartheta)$, $Jc_m(\rho)$, $Yc_m(\rho)$ are real functions and $Jc'_m(0) = 0$, $Hc'^{(2)}_m(0) = -j \cdot Yc'_m(0)$ (where the primes indicate derivatives with respect to ρ). It will be important for later evaluations that the $ce_m(\vartheta)$ are generated as a Fourier series*)

$$ce_m(\vartheta) = \sum_{s=0}^{+\infty} A_{2s+p} \cdot \cos\left((2s+p)\vartheta\right) \quad ; \quad m = 2r + p \quad ; \quad \begin{cases} r = 0,\ 1,\ 2,\ \ldots \\ p = 0,\ 1 \end{cases} , \tag{14}$$

so the real Fourier coefficients A_{2s+p} are delivered by the computing program which generates the Mathieu function.

The plate vibration modes $v_n(\xi)$, the back volume modes $p_{ak}(\xi)$ and the Mathieu functions $ce_m(\vartheta)$ are normal functions in the range of the plate with norms:

$$\begin{aligned} & N_{pn} = \int_{-1}^{1} v_n^2(\xi)\ d\xi = 1 \quad ; \quad N_{ak} = \int_{-1}^{1} p_{ak}^2(\xi)\ d\xi = \begin{cases} 2\ ; \ k = 0 \\ 1\ ; \ k > 0 \end{cases} , \\ & N_{sm} = \int_{-\pi}^{0} ce_m^2(\vartheta)\ d\vartheta = \int_{0}^{\pi} ce_m^2(\vartheta)\ d\vartheta = \frac{\pi}{2} \end{aligned} \tag{15}$$

The remaining boundary conditions to be satisfied are:

$$\begin{aligned} & v_{sy}(\xi) = V(\xi)\ , \\ & v_{ay}(\xi) = V(\xi)\ , \\ & p_e(\xi) + p_r(\xi) + p_s(\xi) - p_a(\xi) = \sum_{n\geq 1} V_n Z_{Tn} \cdot v_n(\xi), \end{aligned} \tag{16}$$

where, in the last condition, Z_{Tn} are modal partition impedances of the panel:

$$\frac{Z_{Tn}}{Z_0} = 2\pi Z_m F \left[\eta F^2 \left(\frac{\gamma_n}{k_0 c}\right)^4 + j\left(1 - F^2\left(\frac{\gamma_n}{k_0 c}\right)^4\right)\right] \quad ; \quad F = \frac{f}{f_{cr}} \quad ; \quad Z_m = \frac{f_{cr} d}{Z_0} \rho_p . \tag{17}$$

The last condition assumes that the left-hand side is expanded in plate modes $v_n(\xi)$ and that the condition holds term-wise.

Multiplication of the first condition with $\sin\vartheta \cdot ce_m(\vartheta)$ and integration with respect to ϑ over $(-\pi, 0)$ gives:

$$D_m = \frac{-k_0 c}{2\pi(-j)^m} \frac{1}{ce_m(\alpha) \cdot Yc'_m(0)} \sum_{n\geq 1} Z_0 V_n \cdot Q_{m,n} . \tag{18}$$

Multiplication of the second condition with $p_{ak}(\xi)$ and integration over $-1 \leq \xi \leq +1$ gives:

$$a_k = \frac{-\Gamma_a Z_a}{\kappa_k \cdot N_{ak} \cdot \sin(\kappa_k t)} \sum_{n\geq 1} V_n \cdot S_{k,n} \quad ; \quad k \geq 0. \tag{19}$$

*) See Preface to the 2nd edition.

Multiplication of the last condition with $v_n(\xi)$ and integration over $-1 \le \xi \le +1$ gives:

$$\begin{aligned} & N_{pn}\frac{Z_{Tn}}{Z_0}\cdot Z_0V_n \\ & = 4\sum_{m\ge 0}(-j)^m ce_m(\alpha)\cdot Q_{m,n}\cdot\left[P_e Jc_m(0)+D_m Hc_m^{(2)}(0)\right]-\sum_{k\ge 0}a_k\cdot S_{k,n}\cdot\cos(\kappa_k t)\,, \end{aligned} \tag{20}$$

and after insertion of D_m, a_k the linear system of equations for Z_0V_n ($\nu = 1, 2, 3, \ldots$):

$$\begin{aligned} & \sum_{n\ge 1} Z_0V_n \\ & \cdot\left\{\delta_{n,\nu}N_{p\nu}-\frac{k_0cZ_0}{Z_{T\nu}}\left[\frac{2j}{\pi}\sum_{m\ge 0}\frac{Hc_m^{(2)}(0)}{Hc_m'^{(2)}(0)}\cdot Q_{m,\nu}Q_{m,n}+\frac{\Gamma_aZ_a}{k_0Z_0}\sum_{k\ge 0}\frac{S_{k,\nu}\cdot S_{k,n}/N_{ak}}{\kappa_kc\cdot\tan(\kappa_kt)}\right]\right\} \\ & = 4P_e\frac{Z_0}{Z_{T\nu}}\sum_{m\ge 0}(-j)^m ce_m(\alpha)\cdot Q_{m,\nu}\cdot Jc_m(0) \end{aligned} \tag{21}$$

with the Kronecker symbol $\delta_{n,\nu}$. After its solution, the amplitudes D_m, a_k follow from above.

These equations use the following mode-coupling coefficients:

$$\begin{aligned} S_{k,n} &:= \int_{-1}^{+1} p_{ak}(\xi)\cdot v_n(\xi)\,d\xi\,, \\ p_{ak}(\xi) &= \begin{cases}\cos(k\pi\xi/2)=\cos(\gamma_k\xi) & ;\quad k=0,2,4,\ldots \\ \sin(k\pi\xi/2)=\sin(\gamma_k\xi) & ;\quad k=1,3,5,\ldots\end{cases}\quad ;\ \gamma_k = k\pi/2\,, \\ v_n(\xi) &= \begin{cases}\cos(n\pi\xi/2)=\cos(\gamma_n\xi) & ;\quad n=1,3,5,\ldots \\ \sin(n\pi\xi/2)=\sin(\gamma_n\xi) & ;\quad n=2,4,6,\ldots\end{cases}\quad ;\ \gamma_n = n\pi/2 \end{aligned} \tag{22}$$

with the values

$$S_{k,n} = \begin{cases} 0 & ;\quad k_e \ \&\ n_e \\ 0 & ;\quad k_o \ \&\ n_o \\ \dfrac{2}{\pi}\left(\dfrac{(-1)^{(k_o-n_e-1)/2}}{k_o-n_e}+\dfrac{(-1)^{(k_o+n_e-1)/2}}{k_o+n_e}\right) & ;\quad k_o \ \&\ n_e \\ \dfrac{2}{\pi}\left(\dfrac{(-1)^{(k_e-n_o-1)/2}}{k_e-n_o}-\dfrac{(-1)^{(k_e+n_o-1)/2}}{k_e+n_o}\right) & ;\quad k_e \ \&\ n_o \end{cases} \tag{23}$$

and the coupling coefficients

$$Q_{m,n} := \int_{-1}^{+1} ce_m(\arccos\xi)\cdot v_n(\xi)\,d\xi = \int_0^{\pi} \sin\vartheta\cdot ce_m(\vartheta)\cdot v_n(\cos\vartheta)\,d\vartheta\,,$$

$$v_n(\xi) = \begin{cases} \cos\left(n\pi\xi/2\right) = \cos(\gamma_n\xi) & ; \quad n = 1, 3, 5, \dots \\ \sin\left(n\pi\xi/2\right) = \sin(\gamma_n\xi) & ; \quad n = 2, 4, 6, \dots \end{cases} \quad ; \quad \gamma_n = n\pi/2\,, \tag{24}$$

$$ce_m(\vartheta) = \sum_{s=0}^{+\infty} A_{2s+p}\cdot\cos\left((2s+p)\vartheta\right) \quad ; \quad m = 2r+p \quad ; \quad \begin{cases} r = 0, 1, 2, \dots \\ p = 0, 1 \end{cases}$$

with zero values if both m and n are even or odd, and for different parities of m, n:

$$\begin{aligned} Q_{2r,n} = &\sqrt{\frac{2\pi}{\gamma_n}}\sum_{s\ge 0} A_{2s}\left[J_{1/2}(\gamma_n) + (1-\delta_{0,s})\sum_{i=1}^{s}(-1)^i\frac{i!}{(2i)!}\left(\frac{2}{\gamma_n}\right)^i\right. \\ &\left.\cdot J_{i+1/2}(\gamma_n)\prod_{k=0}^{i-1}\left(4s^2-4k^2\right)\right]\,, \end{aligned} \tag{25}$$

$$\begin{aligned} Q_{2r+1,n} = &\sqrt{\frac{2\pi}{\gamma_n}}\sum_{s\ge 0} A_{2s+1}\left[J_{3/2}(\gamma_n) + (1-\delta_{0,s})\sum_{i=1}^{s}(-1)^i\frac{i!}{(2i)!}\right. \\ &\left.\cdot\prod_{k=1}^{i}\left((2s+1)^2-(2k-1)^2\right)\left(\frac{2}{\gamma_n}\right)^i\cdot J_{i+3/2}(\gamma_n)\right] \end{aligned}$$

with Bessel functions of half-integer orders $J_{i+1/2}(z)$.

The sound absorption coefficient $\alpha(\Theta) = \Pi_a/\Pi_e$ is evaluated with the effective incident power Π_e (per unit panel length):

$$\Pi_e = \frac{c\cdot\cos\Theta}{Z_0}|P_e|^2, \tag{26}$$

and the absorbed effective sound power:

$$\begin{aligned} \Pi_a &= \frac{c}{2}\mathrm{Re}\left\{\int_{-1}^{+1}(p_e+p_r+p_s)\cdot v_{sy}^*\,d\xi\right\} \\ &= \frac{-4c\pi}{k_0 c\, Z_0}\sum_{m\ge 0} ce_m^2(\alpha)\cdot Yc_m'(0)\cdot\mathrm{Re}\left\{\left(P_e\cdot Jc_m(0) + D_m\cdot Hc_m^{(2)}(0)\right)\cdot D_m^*\right\}. \end{aligned} \tag{27}$$

Special case: back volume is locally reacting

i.e. its input impedance (at $y = 0$) is $Z_b = Z_a\cdot\coth(\Gamma_a t)$. (28)

The boundary conditions then become:

$$\begin{aligned} p_e(\xi) + p_r(\xi) + p_s(\xi) &= \sum_{n\ge 1} V_n(Z_{Tn}+Z_b)\cdot v_n(\xi)\,, \\ v_{sy}(\xi) &= \sum_{n\ge 1} V_n\cdot v_n(\xi). \end{aligned} \tag{29}$$

The system of equations for the plate mode amplitudes Z_0V_n will be ($\nu = 1, 2, 3, \ldots$):

$$\sum_{n\geq 1} Z_0V_n \cdot \left[\delta_{n,\nu} - \frac{2j\,k_0c}{\pi}\,\frac{Z_0}{Z_{T\nu}+Z_b} \sum_{m\geq 0} Q_{m,\nu}\cdot Q_{m,n}\cdot \frac{Hc_m^{(2)}(0)}{Hc_m'^{(2)}(0)} \right]$$
$$= 4P_e \frac{Z_0}{Z_{T\nu}+Z_b} \sum_{m\geq 0} (-j)^m ce_m(\alpha)\cdot Jc_m(0)\cdot Q_{m,\nu}. \qquad (30)$$

The amplitudes D_m of the scattered field are evaluated as above, as is the absorption coefficient. An alternative form for the sound absorption coefficient in this special case is:

$$\Pi_a = \frac{c}{2}\int_{-1}^{+1} \mathrm{Re}\left\{ \sum_{n\geq 1} V_n(Z_{Tn}+Z_b)\cdot v_n(\xi)\cdot \sum_{n\geq 1} V_n^*\cdot v_n(\xi) \right\}\, d\xi$$
$$= \frac{c}{2Z_0} \sum_{n\geq 1} N_{pn}\mathrm{Re}\left\{ \frac{Z_{Tn}+Z_b}{Z_0} \right\}\cdot |Z_0V_n|^2\,, \qquad (31)$$
$$\alpha(\Theta) = \frac{1}{2\,\cos\Theta} \sum_{n\geq 1} \mathrm{Re}\left\{ \frac{Z_{Tn}+Z_b}{Z_0} \right\}\cdot |Z_0V_n/P_e|^2\,.$$

The numerical examples for a plywood panel absorber use as constant parameters $d = 6\,\mathrm{mm}$, $\rho_p = 700\,\mathrm{kg/m^3}$, $f_{cr}d = 20\,\mathrm{Hz}\cdot\mathrm{m}$, $\eta = 0.02$; the back volume with depth $t = 10$ cm is filled with glass fibre material having a flow resistivity $\Xi = 2500\ \mathrm{Pa}\cdot\mathrm{s/m^2}$. The angle of sound incidence is $\Theta = 45°$. The used upper limits for the modes are $n_{hi} = 10$; $k_{hi} = m_{hi} = 8$. The plots of $\alpha(\Theta)$ over the frequency f also contain (as dashed curves, for orientation) the absorption coefficient for an infinite panel.

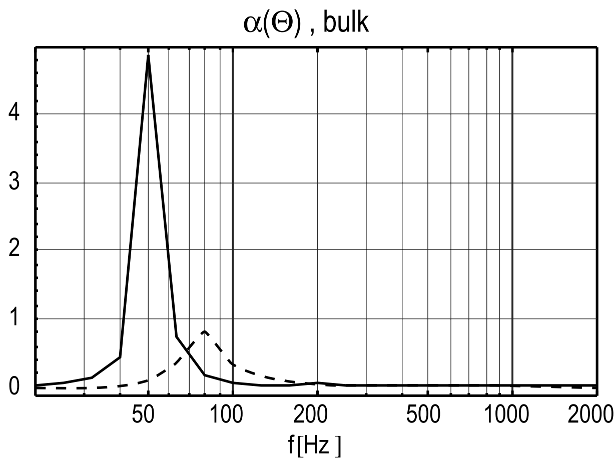

Sound absorption coefficient $\alpha(\Theta)$ for $\Theta = 45°$ of a plywood panel absorber with $c = 0.2$ m; modal analysis: solid line; infinite panel: dashed line. Input parameters: $c = 0.2$[m]; $d = 0.006$[m]; $t = 0.1$[m]; $\rho_p = 700[\mathrm{kg/m^3}]$; $\eta = 0.02$; $Z_r/Z_0 = 0$; $\Xi = 2500[\mathrm{Pa}\cdot\mathrm{s/m^2}]$; $n_{hi} = 10$; $m_{hi} = 8$; $k_{hi} = 8$

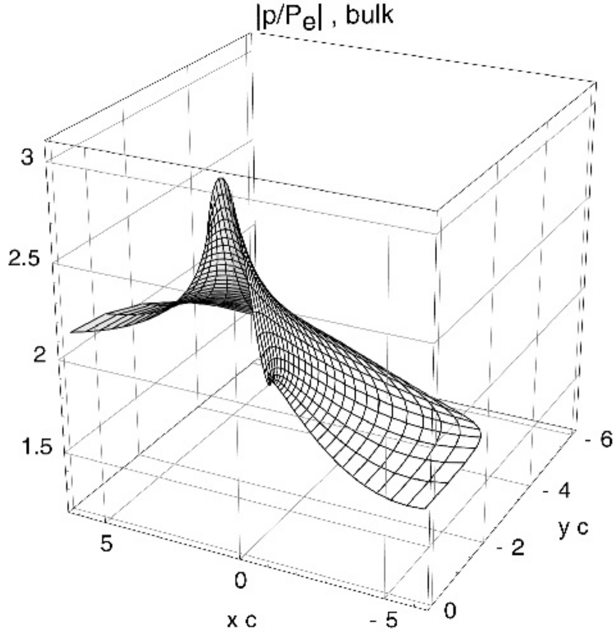

Magnitude of the sound pressure field for the above absorber, at $f = 50$ Hz; sound incidence is from the side of negative x/c values

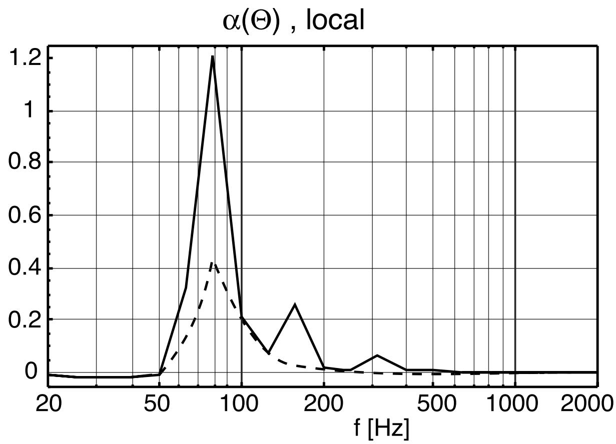

Sound absorption coefficient $\alpha(\Theta)$ for $\Theta = 45^\circ$ of a plywood panel absorber with $c = 0.5$ m and locally reacting back volume; modal analysis: solid line; infinite panel: dashed line. Input parameters: $c = 0.5[\mathrm{m}]$; $d = 0.006[\mathrm{m}]$; $t = 0.1[\mathrm{m}]$; $\rho_p = 700[\mathrm{kg/m^3}]$; $\eta = 0.02$; $Z_{r}/Z_0 = 0$; $\Xi = 2500[\mathrm{Pa \cdot s/m^2}]$; $n_{hi} = 10$; $m_{hi} = 8$; $k_{hi} = 8$

H.23 Tight Panel Absorber, Approximations

► *See also:* Mechel (2001)

The focus and symbols of this section are as in the previous *Sect. H.22.* This section describes approximations which avoid the evaluation of Mathieu functions.

The principal step in such approximations is the subdivision of the boundary value problem in two subtasks. The first subtask finds the plate mode amplitudes with the assumption that $p_s(\xi)$ can be neglected compared to $p_e(\xi)+p_r(\xi)$. This sum is supposed to be the driving force on the front side for the plate motion. The assumption is plausible if the surface impedance of the plate is not too small (i.e. outside resonances). The second step then evaluates the absorbed power with the plate mode amplitudes V_n found in the first step.

If the back volume is supposed to be bulk reacting (i.e. possible sound propagation parallel to the plate) the boundary conditions of the first subtask are:

$$\begin{aligned} &p_e(\xi)+p_r(\xi)-p_a(\xi)=2P_e\cdot e^{-j\,k_x c\,\xi}-p_a(\xi)=\sum_{n\geq 1} V_n Z_{Tn}\cdot v_n(\xi)\;, \\ &v_{ay}(\xi)=\sum_{n\geq 1} V_n\cdot v_n(\xi), \end{aligned} \tag{1}$$

where in the first equation the left-hand side is supposed to be expanded in plate modes $v_n(\xi)$ so that modal plate partition impedances Z_{Tn} (*Sect. H.22*) can be applied. It should be noticed that this equation describes the excitation of the plate by a distributed force without radiation load on the side of excitation. Multiplication of the first equation with $v_\nu(\xi)(\nu=1,2,3,\dots)$ and integration over $-1\leq\xi\leq+1$ yields the equations:

$$V_\nu Z_{T\nu} N_{p\nu}=2P_e\cdot R_\nu-\sum_{k\geq 0} a_k\cdot S_{k,\nu}\cdot\cos\,(\kappa_k t) \tag{2}$$

with the mode coupling coefficients $S_{k,n}$ from the previous section, and the new coefficients:

$$R_n:=\int_{-1}^{+1} e^{-j\,k_x c\,\xi}\cdot v_n(\xi)\,d\xi=\begin{cases}\dfrac{4n\pi\,(-1)^n\cos(k_x c)}{(n\pi)^2-4\,(k_x c)^2} & ;\quad n=\text{odd}\\[2ex] \dfrac{-4j\,n\pi\,(-1)^{n/2}\sin(k_x c)}{(n\pi)^2-4\,(k_x c)^2} & ;\quad n=\text{even}\end{cases}\;. \tag{3}$$

Insertion of the back volume mode amplitudes a_k which follow from the second boundary conditions as in the previous *Sect. 22*:

$$a_k=\frac{-\Gamma_a Z_a}{\kappa_k\cdot N_{ak}\cdot\sin\,(\kappa_k t)}\sum_{n\geq 1} V_n\cdot S_{k,n}\quad;\quad k\geq 0 \tag{4}$$

gives the following system of equations to be solved for V_n if the back volume is bulk reacting:

$$\sum_{n\geq 1} V_n\cdot\left[\delta_{n,\nu}\cdot N_{p\nu}-\frac{\Gamma_a Z_a}{Z_{T\nu}}\sum_{k\geq 0}\frac{S_{k,n}\cdot S_{k,\nu}\cdot\cot\,(\kappa_k t)}{\kappa_k\cdot N_{ak}}\right]=2P_e\cdot\frac{R_\nu}{Z_{T\nu}} \tag{5}$$

($\delta_{n,\nu}$ is the Kronecker symbol).

If the back volume is locally reacting, the only remaining boundary condition becomes:

$$p_e(\xi) + p_r(\xi) = \sum_{n\geq 1} V_n(Z_{Tn} + Z_b) \cdot v_n(\xi). \tag{6}$$

Multiplication and integration as before gives the explicit expressions for V_n:

$$V_n = \frac{2P_e \cdot R_n}{(Z_{Tn} + Z_b)\, N_{pn}}. \tag{7}$$

The second subtask determines the absorbed sound power, assuming that the plate velocity $V(\xi)$, expanded in $V_n \cdot v_n(\xi)$, is a given oscillation (i.e. again without consideration of a possible back reaction of radiation on the oscillation).

In a first variant of this step one applies the product $(p_e(\xi) + p_r(\xi)) \cdot V^*(\xi)$ for the evaluation of the power which $(p_e(\xi) + p_r(\xi))$ feeds into the plate. Thus one makes the same error twice, because $(p_e(\xi) + p_r(\xi))$ is not the true exciting pressure:

$$\Pi_{a1} = \frac{c}{2}\int_{-1}^{+1} \mathrm{Re}\left\{ (p_e(\xi) + p_r(\xi)) \cdot \sum_{n\geq 1} V_n^* \cdot v_n(\xi) \right\} d\xi = P_e \cdot\ c \sum_{n\geq 1} \mathrm{Re}\left\{V_n^* \cdot R_n\right\}. \tag{8}$$

In a second variant one takes into account the sound pressure radiated by the plate with the given velocity profile $V(\xi)$ in a baffle wall. We write p_s for the radiated sound ($V(\xi)$ is counted positive in the direction oriented into the plate; thus the plate in fact is a sink for the energy of p_s). The absorbed power is given by the integral over $\big(p_e(\xi) + p_r(\xi)\big) \cdot V^*(\xi) + p_s(\xi) \cdot V^*(\xi)$. The first term gives the power contribution Π_{a1}; the second term is the absorbed effective power Π_{as} due to p_s. This can be obtained by (see Heckl (1977)):

$$\begin{aligned}\Pi_{as} &= \frac{c}{2}\int_{-1}^{+1} \mathrm{Re}\left\{p_s(\xi) \cdot V^*(\xi)\right\}\, d\xi = \frac{k_0 Z_0}{4\pi}\int_{-k_0}^{k_0} \frac{|\hat{v}(k_1)|^2}{\sqrt{k_0^2 - k_1^2}}\, dk_1 \\ &= \frac{k_0 Z_0}{4\pi}\int_{-\pi/2}^{\pi/2} |\hat{v}(k_0 \cos\psi)|^2\, d\psi,\end{aligned} \tag{9}$$

where $\hat{v}(k_1)$ is the wave number spectrum of $V(x)$, which follows by a Fourier transform ($L = 2c$ is the plate width):

$$\hat{v}(k_1) = \int_{-\infty}^{+\infty} V(x) \cdot e^{-j\,k_1 x}\, dx = \int_{L} V(x) \cdot e^{-j\,k_1 x}\, dx = c\int_{-1}^{+1} V(\xi) \cdot e^{-j\,k_1 c\cdot\xi}\, d\xi, \tag{10}$$

and the back transformation;

$$V(x) = \frac{1}{2\pi}\int_{-\infty}^{+\infty} \hat{v}(k_1) \cdot e^{+j\,k_1 x}\, dk_1. \tag{11}$$

In the present application $V(\xi)$ is the sum of terms $V_n \cdot v_n(\xi)$. The wave number spectrum $\hat{v}_n(k_1)$ of $v_n(\xi)$ is:

$$\hat{v}_n(k_1) = c\int_{-1}^{+1} e^{-j\,k_1 c\,\xi} \cdot v_n(\xi)\, d\xi = \begin{cases} c\dfrac{4n\pi\,(-1)^n \cos(k_1 c)}{(n\pi)^2 - 4\,(k_1 c)^2} & ;\quad n = \text{odd} \\ c\dfrac{-4j\,n\pi\,(-1)^{n/2} \sin(k_1 c)}{(n\pi)^2 - 4\,(k_1 c)^2} & ;\quad n = \text{even} \end{cases}, \tag{12}$$

and the contribution to the absorbed power becomes:

$$\Pi_{as} = \frac{k_0 Z_0}{4\pi} \int_{-\pi/2}^{\pi/2} \left| \sum_{n\ge 1} V_n \cdot \hat{v}_n(k_0\ \cos\ \psi) \right|^2 d\psi. \tag{13}$$

The integral must be evaluated numerically.

A third variant of the second subtask completes the absorbed intensity to $(p_e(\xi) + p_r(\xi) + p_s(\xi)) \cdot V^*(\xi)$ but does not worry about possible scattering at the border lines between plate and baffle wall. The scattered field p_s is expanded in plate modes

$$p_s(x, y) = \sum_{n\ge 1} d_n \cdot v_n(x) \cdot f_n(y). \tag{14}$$

A plausible form for $f_n(y)$ representing outgoing waves is $f_n(y) = \exp(j\varepsilon_n y)$; the terms satisfy the wave equation and Sommerfeld's condition if $(\varepsilon_n c)^2 = (k_0 c)^2 - \gamma_n^2$; $\mathrm{Im}\{\varepsilon_n\} \le 0$. From $v_{sy}(\xi) = V(\xi)$ one gets:

$$d_n = -\frac{k_0}{\varepsilon_n} Z_0 V_n. \tag{15}$$

The absorbed power is:

$$\begin{aligned} \Pi_a &= \frac{c}{2}\int_{-1}^{+1} \mathrm{Re}\left\{ \left(p_e(\xi) + p_r(\xi) + p_s(\xi)\right) \cdot \sum_{n\ge 1} V_n^* \cdot v_n(\xi) \right\} d\xi = \Pi_{a1} + \Pi_{as}\ , \\ \Pi_{as} &= \frac{c}{2}\int_{-1}^{+1} \mathrm{Re}\left\{ \sum_{n\ge 1} d_n \cdot v_n(\xi) \cdot \sum_{n\ge 1} V_n^* \cdot v_n(\xi) \right\} d\xi \\ &= \frac{-c}{2Z_0} \sum_{n\ge 1} \mathrm{Re}\left\{ \frac{k_0}{\varepsilon_n} \right\} \cdot N_{pn} \cdot |Z_0 V_n|^2. \end{aligned} \tag{16}$$

The approximation results are acceptable, except in or near plate resonances.

A very simple approximation, serving more for orientation than as approximation, assumes the plate to be infinitely wide ($L \to \infty$). Then the absorption coefficient $\alpha(\Theta)$ follows from the reflection factor R as $\alpha(\Theta) = 1 - |R|^2$ with

$$R = \frac{(Z_T + Z_b) \cdot \cos\Theta - Z_0}{(Z_T + Z_b) \cdot \cos\Theta + Z_0}, \tag{17}$$

where Z_T is the plate partition impedance of an infinite panel:

$$\frac{Z_T}{Z_0} = 2\pi Z_m F\left[\eta F^2 \sin^4\Theta + j\left(1 - F^2\sin^4\Theta\right)\right] \quad ; \quad F = \frac{f}{f_{cr}} \quad ; \quad Z_m = \frac{f_{cr}d}{Z_0}\rho_p, \tag{18}$$

and Z_b is the input impedance of the back volume, which is given, for a locally reacting volume, by:

$$Z_b = Z_a \cdot \coth(\Gamma_a t); \tag{19}$$

and for a bulk reacting volume by:

$$\begin{aligned} &\frac{Z_b}{Z_0} = \frac{\Gamma_{an} Z_{an}}{\Gamma_{an}\cos\theta_1}\cdot\coth(k_0 t\,\Gamma_{an}\cos\theta_1) \quad ; \quad \Gamma_{an} = \Gamma_a/k_0 \quad ; \quad Z_{an} = Z_a/Z_0 \\ &\Gamma_{an}\cos\theta_1 = \sqrt{\Gamma_{an}^2 + \sin^2\Theta}. \end{aligned} \tag{20}$$

H.24 Porous Panel Absorber, Rigorous Solution

▸ *See also:* Mechel (2001)

The object here is like the absorber in *Sect. H.22*, except now the panel is supposed to be perforated with a porosity σ. Field formulations and symbols will be taken from there.

A tight, long, elastic panel is simply supported at its borders at $x = \pm c$. Its thickness is d, the plate material density ρ_p, the elastic parameter for bending $f_{cr}d$, with the critical frequency f_{cr}, the bending loss factor is η. The panel covers a back volume of depth t. The characteristic propagation constant and wave impedance in the back volume are Γ_a, Z_a (thus the back volume may be filled with air, i.e. $\Gamma_a \to j\cdot k_0$; $Z_a \to Z_0$ if t is not too small, or Γ_a, Z_a from a flat capillary for small t, or Γ_a, Z_a from porous materials if the back volume is filled with such material). The front side of the arrangement is flush with a hard baffle wall. A plane wave p_e is incident (normal to the z axis) with a polar angle Θ.

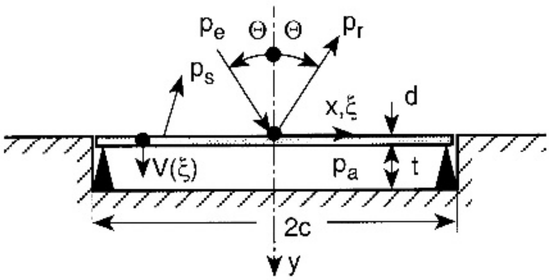

To make the perforation tractable in the analysis, it is supposed that a "micro-structured" perforation is applied. This means that the diameter of the perforations and their distances are small compared with both the sound wave length and the panel width. We further suppose a homogeneous distribution of the perforation over the panel (possibly except narrow border areas).

One first has to fix how the acoustic qualities of the perforation and of the perforated panel have to be defined. The perforation changes the mechanical parameters, effective plate material density ρ_p and bending modulus B of the plate:

$$\rho_p \to \rho_p(1-\sigma) \quad ; \quad B \to B \cdot (1-\sqrt{\sigma}) \quad ; \quad f_{cr}d \to f_{cr}d\sqrt{\frac{1-\sigma}{1-\sqrt{\sigma}}}. \tag{1}$$

The indicated change in B is for nearly square holes and perforation raster; more sophisticated relations can be derived for other geometries. The symbol Z_T will be used for the partition impedance of an equivalent tight plate, evaluated with these parameters and defined by $\Delta p = Z_T \cdot v_p$, where v_p is the velocity of this tight panel. The pores are characterised with an impedance $Z_r = Z_r' + j \cdot Z_r''$ determined by $\Delta p = Z_r \cdot v_r$, where Δp is the pressure difference driving the average velocity v_r through the perforated plate at rest. Preferably one determines Z_r' experimentally (because the technical roughness of hole walls and the effect of rounding of the hole corners are difficult to describe analytically; an exception could be straight, very fine holes for which the real part Z_r' also can be determined precisely from the theory of capillaries), and the imaginary part Z_r'' by evaluation from:

$$\frac{Z_r''}{Z_0} = \frac{k_0 a}{\sigma}\left(\frac{d}{a} + \frac{\Delta\ell_e}{a} + \frac{\Delta\ell_i}{a}\right), \tag{2}$$

where a is any representative hole dimension (mostly its radius) and $\Delta\ell_e, \Delta\ell_i$ are the exterior and interior end corrections, respectively, where the important distinction should be made for the interior end correction whether the interior orifice ends in air or on a porous material.

Z_r can be realised either by the friction force and end corrections of the pores themselves and/or by the impedance of thin porous sheets (e.g. a fine wire mesh) covering the perforation orifice. In the latter case it must be distinguished whether the sheet is force-locking with the plate or not.

The assumption of the micro-structure of the perforation implies that the sound pressure distributions along the panel surfaces do not have significant ripples by the perforation pattern. The formulations of the component fields therefore remain as in *Sect. H.22*. For the determination of the unknown amplitudes a_k, D_m, V_n one needs three boundary conditions as in *Sect. H.22*, but now modified for the parallel volume flow through the panel and the pores.

The sketch indicates, in a representative area element S, the distribution of the velocities on the plate and the holes.

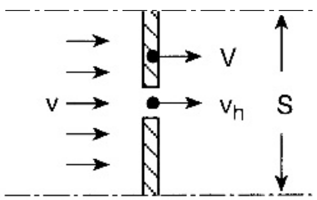

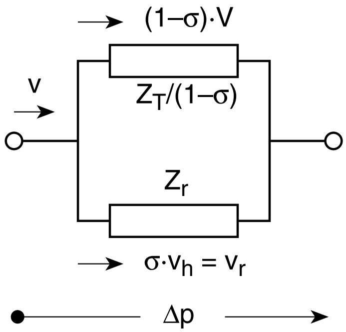

The average velocity is:

$$\begin{aligned} v &= (1-\sigma)\cdot V + \sigma \cdot v_h \\ &= (1-\sigma)\cdot V + v_r \\ &= (1-\sigma)\cdot V + \Delta p/Z_r . \end{aligned} \tag{3}$$

The second sketch shows the equivalent network for the perforated panel.

The effective impedance is:

$$Z_{eff} = \frac{Z_r \cdot Z_T/(1-\sigma)}{Z_r \cdot Z_T + (1-\sigma)}, \tag{4}$$

and the first boundary condition becomes:

$$\Delta p = Z_{eff} \cdot v = \frac{Z_r \cdot Z_T/(1-\sigma)}{Z_r + Z_T/(1-\sigma)} \left[(1-\sigma)\cdot V + \Delta p/Z_r\right], \tag{5}$$

or with a transformation, if $\sigma \neq 1$:

$$\Delta p \frac{Z_r}{Z_r + Z_T/(1-\sigma)} = \frac{Z_r \cdot Z_T}{Z_r + Z_T/(1-\sigma)} \cdot V. \tag{6}$$

This corresponds to the boundary condition with tight plates in *Sect. H.22* if we use the effective plate partition impedance:

$$Z_{Teff} = \frac{Z_r \cdot Z_T}{Z_r + Z_T/(1-\sigma)}. \tag{7}$$

In these relations $\Delta p = p_e + p_r + p_s - p_a.$ (8)

The other boundary conditions of matching velocities become:

$$v = (1-\sigma)\cdot V + \Delta p/Z_r \stackrel{!}{=} \left\{ \begin{array}{l} v_{sy} \\ v_{ay} \end{array} \right. . \tag{9}$$

Up to now it was tacitly assumed that the friction force on the plate could be neglected compared to the driving force from Δp. This assumption is plausible if the holes of the perforation are sufficiently wide (say a few millimetres) and the porosity is not too high. But for large porosity values with narrow pores or with a force-locking, vibrating wire mesh, the friction exerts an additional force ΔF_r on the panel if the relative velocity $v_h - V \neq 0$. The driving force on the panel in a section S becomes:

$$\Delta F = \Delta F_p + \Delta F_r = Z_T \cdot V\, S_p + \sigma Z_r' \cdot (v_h - V)\, S_h, \tag{10}$$

or, after division with the plate area S_p:

$$\begin{aligned}\Delta p &= \left[Z_T + Z_r' \frac{\sigma}{1-\sigma} \left(\frac{v_r}{V} - \sigma \right) \right] \cdot V \\ &= \left[Z_T + Z_r' \frac{\sigma}{1-\sigma} \left(\frac{\Delta p/Z_r}{\Delta p/Z_T} - \sigma \right) \right] \cdot V \\ &= \left[Z_T + Z_r' \frac{\sigma}{1-\sigma} \left(\frac{Z_T}{Z_r} - \sigma \right) \right] \cdot V.\end{aligned} \tag{11}$$

The expression in the last brackets replaces Z_T in the above equations if friction force coupling must be taken into account.

After these preparations one has the following boundary conditions:

$$\Delta p = \sum_{n \geq 1} Z_{Teff\,n} \cdot V_n \cdot v_n(\xi)\,, \tag{12}$$

$$v_{sy} = (1-\sigma) \cdot V + \Delta p/Z_r\,, \tag{13}$$

$$v_{ay} = (1-\sigma) \cdot V + \Delta p/Z_r. \tag{14}$$

Combination of the first equation with the second or third gives:

$$v_{sy} = \sum_{n \geq 1} V_n \cdot v_n(\xi) \left[(1-\sigma) + \frac{Z_{Teff\,n}}{Z_r} \right], \tag{15}$$

$$v_{ay} = \sum_{n \geq 1} V_n \cdot v_n(\xi) \left[(1-\sigma) + \frac{Z_{Teff\,n}}{Z_r} \right]. \tag{16}$$

Multiplication of eq. (15) with $\sin\vartheta \cdot ce_m(\vartheta)$ and integration over $0 \leq \vartheta \leq \pi$, and multiplication of the eq. (16) with $p_{ak}(\xi)$ and integration over $-1 \leq \xi \leq +1$ using from Sect. H.22:

$$v_{sy}(\rho = 0,\ \vartheta) = \frac{-4}{k_0 c\, Z_0 \sin\vartheta} \sum_{m \geq 0} D_m (-j)^m ce_m(\alpha) \cdot Yc_m'(0) \cdot ce_m(\vartheta), \tag{17}$$

$$v_{ay}(\xi, y = 0) = \frac{-1}{\Gamma_a Z_a} \sum_{k \geq 0} a_k \kappa_k \cdot p_{ak}(\xi) \cdot \sin\,(\kappa_k t) \tag{18}$$

gives, respectively:

$$\frac{-2\pi}{k_0 c} (-j)^m ce_m(\alpha) \cdot Yc_m'(0) \cdot D_m = \sum_{n \geq 1} Z_0 V_n \cdot Q_{m,n} \left[(1-\sigma) + \frac{Z_{Teff\,n}}{Z_r} \right], \tag{19}$$

$$\frac{-N_{ak}}{\Gamma_a Z_a/Z_0}\kappa_k \cdot \sin(\kappa_k t) \cdot a_k = \sum_{n\geq 1} Z_0 V_n \cdot S_{k,n}\left[(1-\sigma)+\frac{Z_{Teff\,n}}{Z_r}\right]. \tag{20}$$

With $\Delta p = p_e + p_r + p_s - p_a$ inserted into the boundary (12) condition and multiplication with $v_\nu(\xi)(\nu \geq 1)$, integration over $-1 \leq \xi \leq +1$ leads, with D_m, a_k inserted from (19), (20) above, to the key system of equations for Z_0V_n (an overbar over impedances indicates normalisation with Z_0):

$$\begin{aligned}&\sum_{n\geq 1} Z_0 V_n \\ &\cdot\Bigg[\delta_{n,\nu}N_{p\nu} + \frac{2k_0c}{\pi}\left(\frac{(1-\sigma)}{\overline{Z}_{Teff\,\nu}}+\frac{1}{\overline{Z}_r}\right)\sum_{m\geq 0}(-j)^m ce_m(\alpha)\frac{Hc_m^{(2)}(0)}{Yc'_m(0)} \cdot Q_{m,\nu} \cdot Q_{m,n} \\ &\quad -\Gamma_a\overline{Z}_a\left(\frac{(1-\sigma)}{\overline{Z}_{Teff\,\nu}}+\frac{1}{\overline{Z}_r}\right)\sum_{k\geq 0}\frac{\cot(\kappa_k t)}{\kappa_k \cdot N_{ak}} \cdot S_{k,\nu} \cdot S_{k,n}\Bigg] \\ &= \frac{4P_e}{\overline{Z}_{Teff\,\nu}}\sum_{m\geq 0}(-j)^m ce_m(\alpha) \cdot Jc_m(0) \cdot Q_{m,\nu}.\end{aligned} \tag{21}$$

If one compares this system with the corresponding system of equations in Sect. H.22 for tight panels, one sees the transition due to the perforation:

$$\frac{1}{\overline{Z}_{T\nu}} \rightarrow \left(\frac{(1-\sigma)}{\overline{Z}_{Teff\,\nu}}+\frac{1}{\overline{Z}_r}\right). \tag{22}$$

The amplitudes D_m, a_k follow from (19), (20) with the solutions Z_0V_n as:

$$\begin{aligned}D_m &= -\frac{k_0c}{2\pi(-j)^m ce_m(\alpha) \cdot Yc'_m(0)}\sum_{n\geq 1} Z_0V_n \cdot Q_{m,n}\left[(1-\sigma)+\frac{Z_{Teff\,n}}{Z_r}\right], \\ a_k &= -\frac{\Gamma_a Z_a/Z_0}{N_{ak}\kappa_k \cdot \sin(\kappa_k t)}\sum_{n\geq 1} Z_0V_n \cdot S_{k,n}\left[(1-\sigma)+\frac{Z_{Teff\,n}}{Z_r}\right].\end{aligned} \tag{23}$$

The numerical examples are for a plywood panel absorber with $d = 6$ mm, $\rho_p = 700$ kg/m^3, $f_{cr}d = 20$ Hz $\cdot$ m, $\eta = 0.02$ and a porosity $\sigma = 0.2$; the panel width is $L = 2c = 0.4$ m; the back volume with $t = 10$ cm is filled with glass fibres with $\Xi = 2500$ Pa $\cdot$ s/m^2. Sound incidence is under $\Theta = 45°$. The impedance of the pores is set to a fixed value $Z_r = 10 \cdot Z_0$. The first diagram is evaluated without friction force coupling, the second diagram with friction force coupling. Both diagrams show as dashed curves the absorption coefficients for an infinite porous panel with otherwise identical parameters.

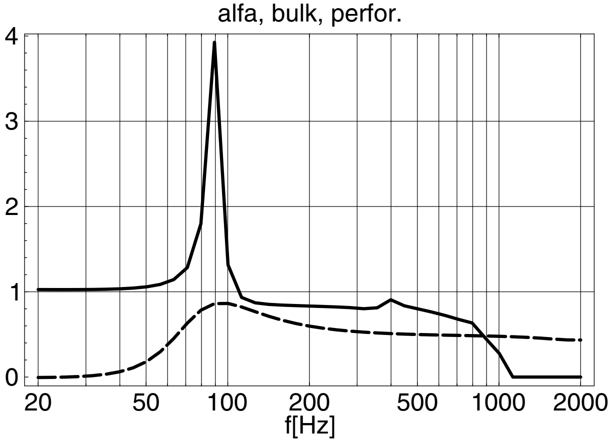

Sound absorption coefficient $\alpha(\Theta)$ for a porous plywood panel absorber without friction coupling. Solid line: finite-size panel; dashed line: infinite panel.
Input parameters: $\Theta = 45^\circ$; $c = 0.2$ [m]; $\sigma = 0.2$; $d = 0.006$ [m]; $t = 0.1$ [m]; $\rho_p = 700$ [kg/m^2]; $f_{cr}d = 20$ [Hz $\cdot$ m]; $\eta = 0.02$; $\Xi = 2500$ [Pa $\cdot$ s/m^2]; $Z_r/Z_0 = 10$

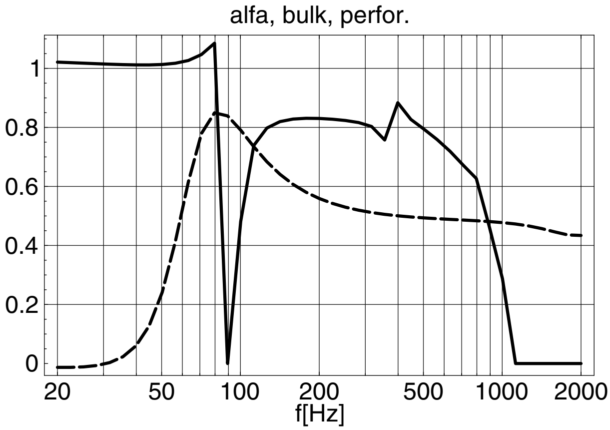

Sound absorption coefficient $\alpha(\Theta)$ for a porous plywood panel absorber as above, but with friction coupling. Solid line: finite-size panel; dashed line: infinite panel

The difference in α with or without friction coupling is rather high in the displayed examples because of the rather high value of $Z_r = 10 \cdot Z_0$; it decreases with decreasing flow resistance of Z_r.

References

Heckl, M.: Abstrahlung von ebenen Schallquellen. Acustica **37**, 155–166 (1977)

Mechel, F.P.: he wide-angle diffuser – a wide-angle absorber? Acustica **81**, 379–401 (1995)

Mechel, F.P.: Schallabsorber, Vol. II, Ch. 10: Sound in capillaries. Hirzel, Stuttgart (1995)

Mechel, F.P.: Schallabsorber, Vol. II, Ch. 18: Plates with slits and resonators with slit plates, without losses. Hirzel, Stuttgart (1995)

Mechel, F.P.: Schallabsorber, Vol. II, Ch. 19: Slit plates and slit plate resonators with viscous and caloric losses. Hirzel, Stuttgart (1995)

Mechel, F.P.: Schallabsorber, Vol. II, Ch. 21: Perforated plates (circular holes), and resonators with perforated plate. Hirzel, Stuttgart (1995)

Mechel, F.P.: Schallabsorber, Vol. II, Ch. 23: Slit plates and perforated plates on absorber layers. Hirzel, Stuttgart (1995)

Mechel, F.P.: Schallabsorber, Vol. II, Ch. 24: Helmholtz resonator with additional losses. Hirzel, Stuttgart (1995)

Mechel, F.P.: Schallabsorber, Vol. II, Ch. 26: Foil absorbers Hirzel, Stuttgart (1995)

Mechel, F.P.: Mathieu Functions; Formulas, Generation, Use. Hirzel, Stuttgart (1997)

Mechel, F.P.: Schallabsorber, Vol. III, Ch. 5: Wide-angle diffusors. Hirzel, Stuttgart (1998)

Mechel, F.P.: About the partition impedance of plates, shells, membranes. Acta Acustica **86**, 1054–1058 (2000)

Mechel, F.P.: Panel absorber. J. Sound Vibr. **248**, 43–70 (2001)

Schroeder, M.R., Gerlach, R.E.: Diffuse sound reflection surfaces. 9th ICA, Madrid, paper D8 (1977)